Tellus B
Chemical and Physical Meteorology

Treatment of Key Aerosol and Cloud Processes in Earth System Models – Recommendations from the FORCeS Project

ORIGINAL RESEARCH PAPER

In honour of the memory of Prof. Astrid Kiendler-Scharr and her contributions to atmospheric science

ILONA RIIPINEN**
SINI TALVINEN**
ANOUCK CHASSAING
PARASKEVI GEORGAKAKI
XINYANG LI
CARLOS PÉREZ GARCÍA-PANDO
TOMMI BERGMAN
SNEHITHA M. KOMMULA
ULRIKE PROSKE
ANGELOS GKOUVOUSIS
ALEXANDRA P. TSIMPIDI
MARIOS CHATZIPARASCHOS
ALMUTH NEUBERGER
VLASSIS A. KARYDIS
SILVIA M. CALDERÓN
SAMI ROMAKKANIEMI
DANIEL G. PARTRIDGE
THÉODORE KHADIR
LUBNA DADA
TWAN VAN NOIJE
STEFANO DECESARI
ØYVIND SELAND
PAUL ZIEGER
FRIDA BENDER
KEN CARSLAW
JAN CERMAK
MONTSERRAT COSTA-SURÓS
MARIA GONÇALVES AGEITOS
YVETTE GRAMLICH
OVE W. HAUGVALDSTAD
EEMELI HOLOPAINEN
CORINNA HOOSE
ORIOL JORBA
STYLIANOS KAKAVAS
MARIA KANAKIDOU
HARRI KOKKOLA
RADOVAN KREJCI
THOMAS KÜHN
MARKKU KULMALA
PHILIPPE LE SAGER
RISTO MAKKONEN
STELLA E. I. MANAVI
THOMAS F. MENTEL
ALEXANDROS MILOUSIS
STELIOS MYRIOKEFALITAKIS
ATHANASIOS NENES
TUOMO NIEMINEN
SPYROS N. PANDIS
DAVID PATOULIAS
TUUKKA PETÄJÄ
JOHANNES QUAAS
LEIGHTON REGAYRE
SUSANNE M. C. SCHOLZ
MICHAEL SCHULZ
KSAKOUSTI SKYLLAKOU
RUBEN SOUSSE

STOCKHOLM UNIVERSITY PRESS

CORRESPONDING AUTHORS:
Ilona Riipinen
Department of Environmental Science, Stockholm University, Stockholm, Sweden; Bolin Centre for Climate Research, Stockholm University, Stockholm, Sweden
Ilona.riipinen@aces.su.se

Sini Talvinen
Department of Environmental Science, Stockholm University, Stockholm, Sweden; Bolin Centre for Climate Research, Stockholm University, Stockholm, Sweden; Now at Department of Technical physics, University of Eastern Finland, Kuopio, Finland
sini.talvinen@uef.fi

KEYWORDS:
aerosol–cloud interactions; earth system models; aerosol and cloud processes; anthropogenic aerosols; climate forcing

TO CITE THIS ARTICLE:
Riipinen, I., Talvinen, S., Chassaing, A., Georgakaki, P., Li, X., García-Pando, C.P., Bergman, T., Kommula, S.M., Proske, U., Gkouvousis, A., Tsimpidi, A.P., Chatziparaschos, M.,

PHILIP STIER
ANNELE VIRTANEN
MANU ANNA THOMAS
KLAUS WYSER
JULIE T. VILLINGER
ANNICA M. L. EKMAN

*Author affiliations can be found in the back matter of this article

**These authors contributed equally to this work

Neuberger, A., Karydis, V.A., Calderón, S.M., Romakkaniemi, S., Partridge, D.G., Khadir, T., Dada, L., van Noije, T., Decesari, S., Seland, Ø., Zieger, P., Bender, F., Carslaw, K., Cermak, J., Costa-Surós, M., (JIŰ<⁉Q@N Ageitos, M., Gramlich, Y., Haugvaldstad, O.W., Holopainen, E., Hoose, C., Jorba, O., Kakavas, S., Kanakidou, M., Kokkola, H., Krejci, R., Kühn, T., Kulmala, M., Le Sager, P., Makkonen, R., Manavi, S.E.I., Mentel, T.F., Milousis, A., Myriokefalitakis, S., Nenes, A., Nieminen, T., Pandis, S.N., Patoulias, D., Petäjä, T., Quaas, J., Regayre, L., Scholz, S.M.C., Schulz, M., Skyllakou, K., Sousse, R., Stier, P., Thomas, M.A., Villinger, J.T., Virtanen, A., Wyser, K. and Ekman, A.M.L. 2026. Treatment of Key Aerosol and Cloud Processes in Earth System Models – Recommendations from the FORCeS Project. *Tellus B: Chemical and Physical Meteorology,* 78(1): 1–66. DOI: https://doi.org/10.16993/tellusb.1883

ABSTRACT

Uncertainty in estimations of the net contribution of anthropogenic aerosol particles, particularly of aerosol-cloud interactions (ACIs) to the Earth's radiation budget, limits our ability to understand past and project future climate change. Earth System Models (ESMs) are among the key tools for assessing the magnitude and impacts of changes in various forcing agents on the global climate system. Hence, improving aerosol and cloud descriptions in ESMs is an important way forward to increase the confidence in estimates of climate impacts of aerosol perturbations in the past, present and future. In the framework of the FORCeS project, experimental and theoretical approaches were combined to bridge the current key gaps in the fundamental understanding of essential aerosol and cloud processes and their descriptions in selected European ESMs. Regarding aerosol types and processes, we focused on organic aerosol, particulate nitrate, absorbing aerosols, and ultrafine aerosol sources including new particle formation and growth. In terms of cloud processes, we targeted cloud droplet activation, hydrometeor growth and evaporation, ice formation and multiplication as well as aerosol processing and scavenging by clouds. The selection was made based on the identified knowledge gaps in the scientific understanding of these processes and/or their current representation in ESMs, as well as a novel perturbed parameter ensemble approach to detecting potential structural deficiencies in an ESM. Here, we review the state-of-the-art, outline our approach for arriving at recommendations for improving the representation of key aerosol and cloud processes within ESMs, and then provide such recommendations applicable in models operating at the Earth system scale. The limitations of the recommendations, applicability, as well as alternative approaches and future research directions are discussed. Overall, the findings highlight the need for continuous efforts towards smart ways for representing the aerosol number size distribution as well as consistent representations of key parameters (e.g., liquid water content and cloud droplet number concentration). Furthermore, we provide guidance for future ESM evaluation emphasising, in particular, the need for exploring the consistency of key parameters, process-based (as opposed to parameter-based), and the complementarity of in-situ and remote-sensed measurements for model evaluation.

1 INTRODUCTION

FORCeS (Constrained aerosol forcing for improved climate projections, https://forces-project.eu/, last accessed: 3rd January 2025) was a 23-partner European project that aimed to better understand and reduce the uncertainty in anthropogenic aerosol radiative forcing. Anthropogenic aerosols exert a net cooling effect on climate through aerosol-radiation interactions (ARI, also referred to as the aerosol direct effect) and aerosol-cloud interactions (ACI, also referred to as the aerosol indirect effect) particularly by acting as cloud condensation nuclei (CCN) or ice nucleating particles (INPs) and influencing the properties of clouds. Increases in anthropogenic aerosols since pre-industrial times have led to a cooling effect, described by the effective radiative forcing (ERF), estimated to be between −1.7 and −0.4 W m^{-2} (when calculated as a difference between 1750 and 2019, Szopa *et al.*, 2021). Natural aerosols have also changed since pre-industrial times, either affected by anthropogenic impacts (e.g. land use change), changes in climate, or a combination thereof. However, pre-industrial aerosol emissions remain uncertain (e.g. Carslaw *et al.*, 2013; Mahowald *et al.*, 2024). For instance, atmospheric dust loading has increased by approximately 55 ± 30% producing an ERF of −0.07 ± 0.18 W m^{-2} (Kok *et al.*, 2023). Changes in aerosols have partly masked the warming effect of greenhouse gases (Bauer *et al.*, 2022; Forster *et al.*, 2021; Quaas *et al.*, 2022; Salvi, Ceppi and Gregory, 2022; Szopa *et al.*, 2021). Uncertainty in ERF also arises from the complexity of simulating the relevant atmospheric processes within Earth System Models (ESMs), especially related to ACI (e.g. Jia *et al.*, 2021; Kahn *et al.*, 2023; Regayre *et al.*, 2018), hindering our understanding of past and future climate (Knutti, Rugenstein and Hegerl, 2017; Stevens *et al.*, 2016). In ESMs, most of the aerosol processes need to be parametrised—due to the computational cost—rather than resolved by equations based on physical principles. This poses a central problem as nonlinear processes occurring at scales that are unresolvable by ESMs are represented by average quantities within the model grid-box. To improve estimates of aerosol ERF, improved and observationally constrained descriptions of the key processes involving aerosols and clouds are therefore required. These descriptions should naturally be as simple as possible in the context of the available computational resources. The aerosol and trace gas processes within the scope of FORCeS (Figure 1) include the descriptions of organic aerosols, particulate nitrate, absorbing aerosols (including dust, black carbon and brown carbon) and ultrafine aerosol microphysics. FORCeS also targeted key cloud microphysical processes such as cloud droplet activation, hydrometeor growth, and hydrometeor dynamics, ice nucleation and secondary

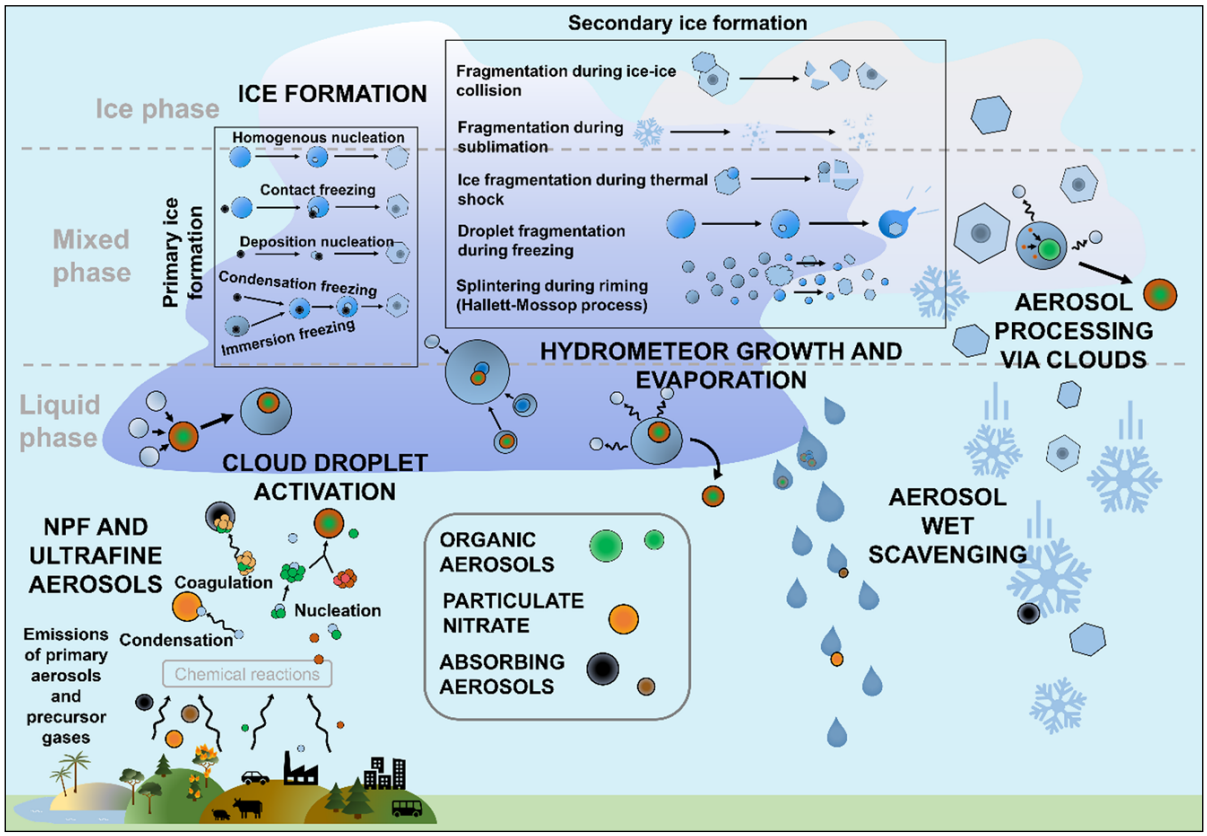

Figure 1 Visualisation of the aerosol and cloud processes targeted within FORCeS, including organic aerosol, particulate nitrate, absorbing aerosols, ultrafine aerosols and new particle formation (NPF), as well as cloud droplet activation, hydrometeor growth and evaporation, ice formation and aerosol processing and scavenging by clouds.

ice formation, and aerosol processing and scavenging by clouds. The targeted processes were selected based on an expert assessment of scientific knowledge gaps and past systematic investigations of the expected sensitivity of the ESM predictions to these processes (Carslaw *et al.*, 2013; Kulmala *et al.*, 2011). The choice of processes was therefore based on a combination of different perspectives including: 1) past systematic assessments of model sensitivities (see e.g. Carslaw *et al.* (2013); 2) identifying areas with considerable accumulated process understanding that had not made its way to ESMs; 3) processes that were perceived potentially important but missing from current ESMs (and therefore part of the structural model errors and not included in sensitivity assessments conducted to date); 4) feasibility of making substantial progress during the four-year lifetime of the FORCeS project (see Sect. 2 and Figure 2 for more details on the process). The processes covered and model developments recommended within FORCeS therefore represent a mix where the relative weight of these different perspective varies – ranging from potentially incremental to certainly significant and from highly ambitious to certainly feasible. Below we provide some essential background information on these key processes and give a short overview on how they are typically described in ESMs.

1.1 ORGANIC AEROSOLS

At least half of the sub-micrometre particle mass is comprised of organic compounds (17–92%, (Tsimpidi *et al.*, 2025), which underlines the importance of accounting for organic aerosols (OA) in estimates of aerosol ERF (e.g. Shrivastava *et al.*, 2017). However, despite the expansion in our understanding of OA processes during the last decade, models still struggle to reproduce the observed OA concentrations in certain areas (Ciarelli *et al.*, 2016; Mao *et al.*, 2018; Tsimpidi *et al.*, 2016). First, uncertainties in emission inventories arise from the treatment of semivolatile (often called condensable) compounds at the emission source (Denier van der Gon *et al.*, 2015; Simpson *et al.*, 2020). Second, simulation of the production and evolution of atmospheric secondary organic aerosol (SOA) is challenging due to the complexity of the associated compounds, chemical reactions and microphysics (Shiraiwa *et al.*, 2017). The descriptions of OA in ESMs can be improved through better accounting for e.g. the volatility distribution of the SOA species and their precursors. Furthermore, important feedbacks driven by climate impacts on the sources and sinks of OA are poorly constrained (Blichner *et al.*, 2024; Tsigaridis *et al.*, 2014; Yli-Juuti *et al.*, 2021).

Organic aerosols have natural (e.g. biosphere, wildfires, sea spray) as well as anthropogenic (e.g. agriculture and various combustion processes) sources. A large fraction of the total atmospheric OA is secondary (Griffin *et al.*, 1999; Kroll and Seinfeld, 2008), whose description requires knowledge about the emissions and concentrations of atmospheric volatile (VOCs) and intermediate volatility organic compounds (IVOCs), their oxidation within the atmosphere, and the volatility of the oxidation products – the latter determining the partitioning of various species between the gas- and condensed phases. Similarly, the primary organic aerosol (POA) components interact dynamically with the gas phase through condensation and evaporation upon transport and transformation in the atmosphere (Robinson *et al.*, 2007). Consequently, the compounds contributing to atmospheric OA are often described using the volatility basis set (VBS) that approximates the complex mixture via surrogate species binned according to their effective saturation concentrations (Donahue *et al.*, 2006, 2011).

Currently, the VBS framework is used to interpret laboratory experiments (Dada *et al.*, 2023a; Stolzenburg *et al.*, 2018; Tröstl *et al.*, 2016) – for instance, to describe particle growth in field measurements (Mohr *et al.*, 2019; Wang *et al.*, 2024) – and it has been implemented in models with varying degrees of resolution (Farina *et al.*, 2010; Irfan *et al.*, 2024; Jiang *et al.*, 2019; Liu *et al.*, 2021; Tsimpidi *et al.*, 2010, 2014). Within the atmosphere, OA components interact with each other, water (e.g. Carlton and Turpin, 2013; Fan *et al.*, 2021; Voliotis *et al.*, 2022) and other chemical species present in the particles (e.g. sulfates, nitrates, BC and crustal material (Li *et al.*, 2021b; McFiggans *et al.*, 2019; Zheng *et al.*, 2020b). These interactions naturally add another dimension of complexity in understanding the evolution and impacts of OA.

The sources, properties and atmospheric evolution of the compounds present in atmospheric OA are important for the prediction of aerosol-cloud-climate interactions within ESMs (Kostenidou *et al.*, 2018). Besides influencing the overall particulate matter (PM) loadings and the optical properties of the atmosphere (Zhu *et al.*, 2023), the concentration and properties of OA components influence the aerosol number size distribution (He *et al.*, 2021b; Zaveri *et al.*, 2014) and hence the number of available CCN and INPs (Kuwata *et al.*, 2013; Zheng *et al.*, 2020a). Specifically, the representation of volatility is important for determining the ability of the organic species to contribute to new particle formation (NPF, see also Sect. 1.4) and nanoparticle growth (Riipinen *et al.*, 2011, 2012; Stolzenburg *et al.*, 2023). The aforementioned effects impact the quantification of the contribution of natural vs. anthropogenic aerosol influence on climate (e.g. Carslaw *et al.*, 2013), including climate impacts of land-use change (e.g. Barati *et al.*, 2023), or climate feedbacks involving forest-derived aerosols (e.g. Thornhill *et al.*, 2021). Finally, the interactions of OA with atmospheric water are important for simulating the influence of aerosol perturbations on cloud microphysics and radiation directly, but also for the removal of OA

from the atmosphere by wet scavenging (Hodzic *et al.*, 2020; Holopainen *et al.*, 2020).

The advances in our understanding of the processes related to OA during the last decades have not been fully exploited to advance the representation of the corresponding processes in ESMs. The simulation of SOA is challenging due to the multiple surrogate species that are required to represent the broad spectrum of chemical compounds relevant for OA (Curtius *et al.*, 2024; Dada *et al.*, 2023a; Ehn *et al.*, 2014; He *et al.*, 2021a; Pozzer *et al.*, 2022; Shen *et al.*, 2022, 2024; Wu *et al.*, 2021). The ability of large-scale models and ESMs to reproduce the observed OA concentrations is highly variable (Kanakidou *et al.*, 2005; Shrivastava *et al.*, 2017; Sporre *et al.*, 2020). In general, ESMs divide OA into primary and secondary, i.e. POA and SOA. However, the simulated sources, number of used surrogate compounds, chemical processing and assumed volatilitity distributions for the organic species vary widely among models. In some ESMs, SOA formation from anthropogenic sources is not explicitly represented; instead, the organic mass is emitted directly as primary particles, bypassing the intermediate oxidation and condensation processes. Also the treatment of the volatility of the OA components ranges from assuming entirely non-volatile and nonreactive OA to the description of OA with two volatility classes (e.g. Bergman *et al.*, 2022). More advanced VBS representations with varying number of volatility bins are also available (Holopainen *et al.*, 2022; Irfan *et al.*, 2024) but rarely applied in fully coupled ESMs.

The global emissions of biogenic VOCs are usually described within ESMs using models that link land-use, terrestrial biota and environmental parameters. The Model of Emissions of Gases and Aerosols from Nature (MEGAN, Guenther *et al.*, 2012) is an example of an emission model that is commonly used, and based on empirically driven emission factors for various land-use types. Another example is LPJ-GUESS which is a process-based dynamic vegetation and biogeochemistry model (Döscher *et al.*, 2022 and references therein). VOC oxidation by OH and ozone is generally described by simplified chemical reaction schemes assuming, for example, constant SOA yields (Henze and Seinfeld, 2006; Hodzic *et al.*, 2016; Tsigaridis *et al.*, 2014). VOC oxidation by the nitrate radical is at present generally not accounted for in ESMs, with some exceptions, despite the potential large sensitivity of SOA formation from biomass burning emissions to this oxidation pathway (Kodros *et al.*, 2020). Overall, ESMs still exhibit large uncertainty and systematic biases in terms of the coupling between temperature, VOC emissions, OA and cloud properties (Blichner *et al.*, 2024). Furthermore, factors other than temperature such as CO_2 concentration or stress due to drought or insect outbreaks, can also have a significant impact on VOC emissions (e.g. Faiola and Taipale, 2020; Holopainen *et al.*, 2022; Holopainen and Gershenzon, 2010; Midzi *et al.*, 2022), thus affecting the concentration of SOA and further aerosol radiative forcing (Bergström *et al.*, 2014; Mentel *et al.*, 2013). These, however, are rarely considered in the basic versions of ESMs.

1.2 PARTICULATE NITRATE

Inorganic ions such as sulfate (SO_4^{2-}), ammonium (NH_4^+) and nitrate (NO_3^-) are major components of the atmospheric PM (Seinfeld and Pandis, 2016), and therefore have significant effects on ARI and ACI – not least due to their interactions with water (Burgos *et al.*, 2020). Sulfate has received a lot of attention as probably the most important anthropogenic aerosol component during the industrial period (Ackerley *et al.*, 2009; Nordling *et al.*, 2021). The importance of understanding the sources, transport, atmospheric processing and effects of particulate nitrate has however become apparent in the recent years, given the decline in sulfate emissions and its links to land-use change and agricultural policies (Bauer *et al.*, 2007; Xu and Penner, 2012). Ammonium nitrate is an important aerosol component in regions with intensive agriculture and traffic, such as China, western United States and western Europe (e.g. Highwood *et al.*, 2012; Morgan *et al.*, 2010) and its relevance is expected to increase in the future (Hoesly *et al.*, 2018). Ammonium nitrate is also a key player in the atmospheric acid-base chemistry, which also has important implications for air quality and the deposition of nutrients (Baker *et al.*, 2021; Kakavas and Pandis, 2021; Karydis *et al.*, 2021; Nenes *et al.*, 2021). Global ammonia emissions from agriculture are estimated to increase by 20–105% between 2000 and 2100 (van Vuuren *et al.*, 2011). The conversion of gas-phase nitric acid to particle-phase nitrate is driven by ammonia, dust and salt minerals, influencing aerosol pH (Fenter *et al.*, 1995; Karydis *et al.*, 2016, 2021; Krueger *et al.*, 2004; Milousis *et al.*, 2024). Furthermore, the formation and properties of various organic nitrates have been the focus of research efforts in the past years (Bardakov *et al.*, 2024; Graham *et al.*, 2023).

Models still show significant spread in their estimates of nitrate levels. For example, the AeroCom phase III experiment (Bian *et al.*, 2017) showed an average NO_3^- burden of 0.63 Tg among participating models, with an intermodal standard deviation of 0.56 Tg (nearly 90% of the mean), and extremes differing by a factor of 13. In an effort to balance precision and computational efficiency in the simulation of nitrate, a range of intermediate approaches have been proposed (Soussé Villa *et al.*, 2025). One method involves simplifying the dynamic mass transfer equations to a first-order irreversible uptake process, which neglects the re-evaporation of absorbed species back into the gas phase (e.g. Fairlie *et al.*, 2010).

Another approach is a hybrid strategy that applies thermodynamic equilibrium to fine (accumulation) modes or bins (Karydis *et al.*, 2011), while using first

order irreversible uptake (Hauglustaine, Balkanski and Schulz, 2014; Hodzic, Bessagnet and Vautard, 2006) or dynamic mass transfer (Capaldo, Pilinis and Pandis, 2000; Trump *et al.*, 2015) for the coarse ones. A third option is to calculate equilibrium concentrations separately for fine and coarse particles, by first limiting the gas-phase material that can condense to each size bin or mode assuming diffusion limited condensation (Vignati *et al.*, 2004) and then redistributing the mass between the gas and the aerosol phase, assuming instant thermodynamic equilibrium between the two phases (Karydis *et al.*, 2016; Pringle *et al.*, 2010). Although aerosol thermodynamic models are commonplace in regional chemical transport models, they are often absent in many ESMs, partly due to their computational cost. For example, versions of ECHAM (Roeckner *et al.*, 2006; Tegen *et al.*, 2019) do not simulate aerosol thermodynamics, and in NorESM1-M, using CAM4-Oslo, nitrate and its climate effects are not included (Kirkevåg *et al.*, 2013). The CMIP6 (Coupled Model Intercomparison Project Phase 6, Eyring *et al.*, 2016) version of EC-Earth3-AerChem (Sect. 2.1.1), on the other hand, employes the thermodynamic gas–particle partitioning model EQSAM (Metzger *et al.*, 2002) to determine the partitioning of NH_3/NH_4^+ and HNO_3/NO_3^-, but applies this only for accumulation mode aerosols. ESMs typically assume a globally uniform dust composition, and organic nitrates are usually not explicitly simulated.

1.3 ABSORBING AEROSOL: BLACK CARBON, MINERAL DUST AND BROWN CARBON

The absorbing aerosol fraction comprises of black carbon (BC), dust aerosols and brown carbon (BrC) (Andreae and Gelencsér, 2006; Liu *et al.*, 2015). A recent review estimated the fraction of absorbing aerosol optical depth to be 57%, 30% and 10% due to BC, dust and OA, respectively (Sand *et al.*, 2021). Brown *et al.* (2021) showed that most climate models overestimate the absorption of radiation by aerosols from biomass burning. Recently, Zhong *et al.* (2023) also showed that climate model uncertainties in ERF can be reduced significantly by constraining biomass burning aerosols using observations and satellite data.

Eventually, the total absorption is derived from the sum of its components (see Figure 1 in Sand *et al.*, 2021). The mixing state of aerosol also impacts the properties of absorbing aerosol (Kelesidis *et al.*, 2022). An earlier study by Stier *et al.* (2007), however, found that the ESM absorbtion results are even more sensitive to the uncertainties in the imaginary index than to the mixing rules in their model setup. The absorption of mineral dust and carbonaceous aerosol is in general poorly characterised, which significantly contributes to uncertainty in the ARI (Bellouin *et al.*, 2020; Bond *et al.*, 2013; Kok *et al.*, 2023; Regayre *et al.*, 2023). Current ESMs treat BC and dust explicitly, but the absorbing fraction of OA is still unaccounted for, or represented with a simplistic approach as a very weakly absorbing aerosol (Hess, Koepke and Schult, 1998). The latter is therefore missing from the current IPCC estimates of radiative forcing. Better treatment of BrC could reduce the gap between results from ESMs and observations of aerosol absorption (Feng, Ramanathan and Kotamarthi, 2013; Jo *et al.*, 2016).

Dust is emitted from the Earth's surface through wind erosion processes. It consists of a mixture of minerals determined by the composition of the parent soil. These minerals have distinct physico-chemical properties (crystal structure, chemical composition), are often preferentially emitted in different aerosol sizes, and behave differently when exposed to radiation and clouds. For instance, iron oxides, hematite and goethite, dominate the absorption in the short wave (SW) range (e.g. Di Biagio *et al.*, 2019; Engelbrecht *et al.*, 2016; Moosmüller *et al.*, 2012), while clays (e.g. kaolinite, illite, smectite) and coarse minerals, such as quartz or calcite, present the highest absorption features in the longwave (LW) range (Di Biagio *et al.*, 2014, 2017). Dust is also estimated to be the most important INP in the global atmosphere, with K-feldspars and quartz likely being the most efficient sources of INPs relative to other minerals (Atkinson *et al.*, 2013; Harrison *et al.*, 2019; Zimmermann *et al.*, 2008, see also Sect. 1.7) In addition, dust particles undergo chemical aging in the atmosphere, reacting with acids (such as sulfuric, nitric, or hydrochloric acid) or acquiring coatings of organic compounds (Goodman *et al.*, 2001). The uptake rates of such compounds on dust are increased by the presence of calcite and other alkaline components (Kakavas and Pandis, 2021; Krueger *et al.*, 2004). As a result of these coatings, dust absorption and hygroscopicity are modified (Milousis *et al.*, 2025b; Usher *et al.*, 2003).

Current ESMs typically assume that dust is a single species, neglecting the known regional variations in the mineralogical composition of its sources (Claquin *et al.*, 1999; Green *et al.*, 2023; Journet, Balkanski and Harrison, 2014). The explicit representation of certain key minerals in ESMs is more limited by our incomplete understanding of global soil composition and the associated size-resolved airborne mineralogy and optical properties than by computational constraints (Gonçalves Ageitos *et al.*, 2023). In practice, this is translated into climate models specifying globally uniform imaginary parts of the dust refractive index, uptake rates and INP efficiencies. Furthermore, most ESMs underestimate the coarse and super-coarse dust fractions (Kok *et al.*, 2021). Also, dust asphericity, which is neglected in most models, is estimated to enhance the dust mass extinction in the visible radiation by up to ~40% (Kok *et al.*, 2017), which may be important for models to simultaneously match observations of optical depth and surface concentration (Kok *et al.*, 2021). Currently, ESMs are often calibrated to

achieve a global mean dust optical depth (DOD) of 0.03 ± 0.01 (Ridley *et al.*, 2016). However, relying on this single constraint on the dust cycle leaves dust direct forcing efficiency underdetermined and thus makes room for a large range of plausible assumptions about mineral composition, size distribution, asphericity, and scattering among models. Consequently the CMIP6 ESMs diverged substantially in their dust direct forcing efficiency (Haugvaldstad *et al.*, 2025). LW scattering of radiation by particles and molecules in the atmosphere is another effect that is typically neglected in models because absorption is the dominant process and including scattering would significantly increase computational costs. This omission leads to an underestimation of the LW radiative effects, particularly for coarse and super-coarse dust particles (Drugé *et al.*, 2025; Kok *et al.*, 2025). Finally, models are unable to simulate the increase in dust burden since the start of the industrial age as observed in dust sedimentary archives (Kok *et al.*, 2023). The historical forcing by dust is therefore currently unaccounted for in estimates of ERF and climate sensitivity.

BrC has recently attracted enough attention to start being explicitly incorporated in global models (Zhang *et al.*, 2020). To account for this additional aerosol absorption, most models simply include a small imaginary part to the refractive index of the organic aerosol (Tsigaridis and Kanakidou, 2018), implying that BrC is a constant fraction of OA worldwide. However, it is known that incomplete biomass burning and biofuel combustion, as well as secondary organic aerosol from the oxidation of aromatics, produce BrC with different proportions to organic aerosol (Basnet *et al.*, 2024; Laskin, Laskin and Nizkorodov, 2015; Zhang *et al.*, 2020). Furthermore, there are sources of OA that do not emit or produce measurable amounts of BrC. Variability in the absorption characteristics of BrC is attributed to emission sources and the molecular composition of BrC. Saleh (2020) categorised OA and the corresponding BrC based on their absorbing properties from very weakly (imaginary refractive index at 550 nm below 10^{-3}) to strongly absorbing (imaginary refractive index above 0.1). Such large variability can be explained by the different fuels and combustion conditions resulting in BrC production. Navarro-Barboza *et al.* (2025) highlight the potential contribution of sources other than biomass burning or biofuel—including shipping and traffic emissions—to observed BrC absorption.

The atmospheric behaviour of BrC suggests the existence of two different primary BrC aerosol types, reactive and inert. Reactive BrC loses its absorbing properties by photobleaching (photolysis and reaction with OH) with an e-folding time of about 11 h during daytime (k = 3.4 × 10^{-5} s^{-1}, Skyllakou *et al.*, 2024; Wong *et al.*, 2019). The inert type of BrC (estimated to be 6–10% of biomass-burning BrC, Forrister *et al.*, 2015; Wong *et al.*, 2019; Zhang *et al.*, 2020) is removed from the atmosphere by deposition only. The presence of BrC also has implications on the photochemistry near the surface due to its nature to absorb at UV wavelengths (Mok *et al.*, 2016). However, wildfire emissions may include "dark" BrC, which can also absorb in the visible light spectrum (Chakrabarty *et al.*, 2023).

Most ESMs consider both internally and externally mixed aerosol, and typically apply the Maxwell-Garnett mixing rule for BC and dust present in mixtures (Sand *et al.*, 2021). BC, released from various sources involving incomplete combustion (Rönkkö *et al.*, 2023; Xu *et al.*, 2021a), is currently considered in most ESMs and is estimated to exert a net warming impact on climate during the industrial period (e.g. Bond *et al.*, 2013). Its total climate effect, however, is still uncertain due to uncertainties in the mixing state and cloud interactions of BC-containing particles. Current ESMs estimate the BC loadings within a order of magnitude (see e.g. Frey *et al.*, 2021) but the agreement depends on the mass absorption coefficients (MACs) assumed when interpreting the data. For example, Sand *et al.* (2021) found large differences between the MAC values in ESMs, ranging from 3.1 to 17.7 $m^2 g^{-1}$ at 500 nm. Additional error sources are related to, for example, the coating and atmospheric ageing and scavenging of BC as well as the exact wavelength dependent function that describes the imaginary part of the refractive index or MAC.

1.4 ULTRAFINE AEROSOL AND NEW PARTICLE FORMATION

Atmospheric aerosol number concentrations are dominated by ultrafine (d_p < 100 nm, Kwon, Ryu and Carlsten, 2020) particles (UFP). A large fraction of these particles are secondary, originating from NPF driven by atmospheric vapours (Kulmala, 2003; McMurry *et al.*, 2000)—either in-situ in the atmosphere (e.g. Cai *et al.*, 2024; Zhao *et al.*, 2024) or upon emission from e.g. mobile sources (e.g. Kittelson *et al.*, 2022). In NPF, vapour molecules collide and form small stable molecular clusters, which can then further grow by coagulation and condensation reaching sizes relevant (>20 nm and larger) for cloud formation (e.g. Dada *et al.*, 2017, 2020; Kirkby *et al.*, 2011, 2016, 2023; Kulmala *et al.*, 2004, 2022; Lehtipalo *et al.*, 2018; Wang *et al.*, 2020; Williamson *et al.*, 2019). Much progress has been made in recent decades to understand various processes and vapours leading to atmospheric NPF and their overall contribution to UFP and CCN numbers (e.g. Dada *et al.*, 2023a; Dunne *et al.*, 2016; Kirkby *et al.*, 2023; Stolzenburg *et al.*, 2023; Wang *et al.*, 2023). NPF and the further condensation growth of the formed particles to sizes where they can contribute to ARI and ACI are complex processes that involve various atmospheric species such as sulfuric acid, ammonia, organics, iodic acid, etc.,—depending on location and atmospheric conditions (e.g. Baccarini *et al.*, 2020; Kerminen *et al.*, 2018; Zheng et al., 2020).

Coagulation, which is strongly dependent on particle size and concentration, also plays a major role in modifying UFP concentrations, aerosol number size distributions and, hence, CCN levels.

Particle formation driven by sulfuric acid is probably the best documented NPF process, but it is well-known that various other species such as organic compounds, basic compounds such as ammonia and amines (Dada *et al.*, 2023b; Yan *et al.*, 2021), iodic acid (He *et al.*, 2021a), nitric acid (Wang *et al.*, 2020), water as well as atmospheric ions (Enghoff and Svensmark, 2008; Kirkby *et al.*, 2011; Nieminen *et al.*, 2011) can participate in NPF depending on the environment in question (e.g. Zhao *et al.*, 2024). Long-term observations from the boreal forest in Hyytiälä show a decline in the NPF frequency and intensity over the past 25 years (Li *et al.*, 2024c), potentially driven by the decrease in sulfuric acid following the decline of sulfur dioxide (SO_2) from European sources. Meanwhile, less intense NPF events driven by highly oxidated organic molecules (HOM) from forest emissions have become more frequent (Kulmala *et al.*, 2022). Also, laboratory studies such as the CLOUD experiment (see Kirkby *et al.*, 2023 and Sect S4.1) and experiments in the SAPHIR chamber (Sect. S4.2) have investigated various systems relevant to atmospheric NPF. For instance, the presence of isoprene has been found to suppress nucleation from monoterpene oxidation products (Heinritzi *et al.*, 2020; Kiendler-Scharr *et al.*, 2009). The addition of sesquiterpenes in minute amounts, however, restores the NPF potential (Dada *et al.*, 2023a). NOx has been found to suppress NPF from monoterpenes (Dada *et al.*, 2023a; Wildt *et al.*, 2014; Yan *et al.*, 2020), but increase the potential for isoprene-driven NPF at high altitudes (Bardakov *et al.*, 2024; Zhao *et al.*, 2020). Iodic acid can trigger NPF in the absence of any other vapour (He *et al.*, 2021a) by forming iodous acid which acts as a stabilising base. In the presence of sulfuric acid, nucleation is further enhanced (He *et al.*, 2023). Nitric acid and ammonia were also found capable of rapidly growing the freshly formed particles and contributing to NPF in polluted conditions and high altitudes (Wang *et al.*, 2020, 2022). The oxidation products of anthropogenic organic vapours such as naphthalene, 1,2,4-trimethylbenzene and toluene have also been found to increase the formation rates compared with pure acid-base nucleation (Xiao *et al.*, 2021).

The description of UFP in ESMs eventually boils down to the representation of particle number size distributions (PNSDs), the particle source functions associated with the aforementioned NPF mechanisms into the smallest particle size classes, and the rest of the aerosol dynamics (coagulation, condensation/evaporation). Currently, most climate models that treat aerosol particles use either a modal representation of the size distribution (as e.g. EC-Earth3-AerChem, Sect. 2.1.1) or sectional approaches (as e.g. ECHAM-SALSA, Sect. 2.1.3). The number and assumed properties of modes and definitions of the sectional bins can differ between the models. For example, M7 in EC-Earth3-AerChem has seven modes whereas GLOMAP in UKESM1 utilises five modes (Sect. S1.1).

Parametrisations of NPF in the form of NPF rates and growth rates vary considerably in ESMs. For example, in the ECHAM models, three processes are considered; neutral and charged nucleation of sulfuric acid and water and nucleation of organic compounds and sulfuric acid via cluster activation. The neutral and charged nucleation of sulfuric acid (H_2SO_4) is based on thermochemical parameters presented in Kazil *et al.* (2010) and formation rates are then interpolated as presented in Kazil and Lovejoy (2007). Cluster activation follows Kulmala, Lehtinen and Laaksonen (2006) and Sihto *et al.* (2006). In UKESM1, on the other hand, NPF from the binary homogeneous nucleation of sulfuric acid and water follows Vehkamäki *et al.* (2002), occurring mainly in the free troposphere. Organically mediated nucleation of new particles in the boundary layer (Metzger *et al.*, 2010) is available but is not used in the release version (Mulcahy *et al.*, 2020).

Both modelling studies and observational data also highlight NPF as an important source of CCN (Gordon *et al.*, 2017; Merikanto *et al.*, 2009; Sihto *et al.*, 2011; Westervelt *et al.*, 2014; Zhang *et al.*, 2023), and for example, in boreal forest environments, increases of up to 110% in CCN due to NPF have been observed (Sihto *et al.*, 2011). However, in their regional-scale modelling study, Patoulias *et al.* (2024) showed that—unlike many previous studies have assumed (as the ones listed above)—the formation of new nanoparticles can, under certain conditions, reduce the concentrations of CCN. This effect is due to the distribution of condensable vapours to a larger number of (smaller) particles, and therefore limits the growth of the Aitken mode particles to sizes where they can activate as CCN.

1.5 CLOUD DROPLET ACTIVATION

Activation of atmospheric aerosol particles into cloud droplets is of fundamental importance for aerosol effects on clouds and climate (Albrecht, 1989), as changes in cloud droplet number concentrations (CDNCs) affect cloud albedo (Twomey, 1974). A change in the CDNC can be followed by changes in cloud liquid water path (LWP), precipitation formation and cloud lifetime, because cloud microphysical processes can also be altered. These processes include cloud droplet and ice crystal growth and evaporation, entrainment and mixing, ice nucleation, secondary ice formation, and aerosol processing and scavenging (Carslaw, 2022; McCrystall *et al.*, 2021; Tapiador *et al.*, 2019). Changes in these processes, in turn, imply potential adjustments of cloud dynamics and aerosol particle concentrations. Cloud adjustments have been shown to either amplify or dampen the first-order impacts of aerosol particles as

CCN (Chen *et al.*, 2014; Glassmeier and Lohmann, 2016; Gryspeerdt, Quaas and Bellouin, 2016; Gryspeerdt, Goran and Smith 2021; Quaas *et al.*, 2024). The mechanisms involved in the adjustments vary between cloud types, and are particularly poorly understood especially for ice and mixed-phase clouds (Lohmann, 2017). For example, due to the simplified treatments of droplet size distributions and cloud dynamics in general, ESMs tend to produce too much warm precipitation with too little variability (Jing, Suzuki and Michibata, 2019; Martinez-Villalobos, Neelin and Pendergrass, 2022; Suzuki *et al.*, 2015). Another major uncertainty that has persisted in models are the radiative biases in temperature over Southern Oceans (see e.g. Fiddes *et al.*, 2024).

In terms of fundamental thermodynamics, cloud droplet activation of dry aerosol particles at a given water vapour supersaturation in thermodynamic equilibrium is accurately described by the Köhler theory (Köhler, 1936)—if the size, chemical composition and the associated condensed-phase thermodynamics and phase-separation are known. From a microphysical perspective, the aerosol population may affect the CDNC either through a change in the chemical composition or a perturbation of the particle number size distribution in which the latter generally has the largest impact for typical atmospheric conditions (Dusek *et al.*, 2006; Karydis *et al.*, 2012; Lowe *et al.*, 2019; Partridge *et al.*, 2012). The chemical composition, however, is indicative of the relevant aerosol sources and their processing in the atmosphere, which, in turn, dictate the properties of the aerosol particle size distribution. At the scale of an air parcel, Twomey, (1959) showed that the CDNC can be described as a logarithmic function of the number concentration of aerosols active as CCN (N_{CCN}) at 1% supersaturation. If we assume that changes in CDNC are driven by changes in the N_{CCN} as $ACI_{CDNC} = \partial \ln CDNC / \partial \ln N_{CCN}$ (Feingold *et al.*, 2001), ACI_{CDNC} could, in principle, be derived from in-situ observations, provided that the number of aerosols active as CCN at the relevant supersaturation is known. In practice, this is a challenging task, as a large fraction of CCN are too small to interact with visible light and their concentrations can vary considerably with altitude and in different environments. It is often assumed that N_{CCN} is equal to some proxy, for example, the total number of aerosol particles larger than the smallest detectable diameter, the aerosol optical depth (Oreopoulos, Cho and Lee, 2020; Shinozuka *et al.*, 2015), the number of aerosols larger than a certain size (e.g. Yli-Juuti *et al.*, 2021), the CCN concentration measured at a given constant supersaturation (e.g. Hudson *et al.*, 2015) or the total amount of aerosol sulfate (McCoy *et al.*, 2017). However, even if ACI_{CDNC} can be derived from in-situ measurements conducted under similar environmental conditions, the values can vary substantially depending on, for example, the aerosol size distribution, cloud liquid water path and updraft velocity (and hence the range of ambient levels of supersaturation). It is currently unclear whether the spread in ACI_{CDNC} obtained from satellite observations (see also S5.1) has a physical basis or if it is a result of methodological issues (e.g. Bellouin *et al.*, 2020; Quaas *et al.*, 2020).

A cloud response to changes in aerosol concentrations on a local scale may be buffered on the macro-scale and thus become less prominent when analysed from a climate-scale perspective. This scaling issue becomes pertinent when comparing values of ACI_{CDNC} from large-scale models with in-situ observations, and merits the use of global-scale remote sensing data for model evaluation. However, there are several issues with deriving ACI_{CDNC} from remote sensing. These are described in more detail in, for example, Quaas *et al.* (2020) but include: (a) uncertainties in determining N_{CCN}, (b) non-simultaneous observations of aerosol and cloud properties as they cannot be derived simultaneously in the same column, (c) general uncertainties in CDNC retrievals together with the fact that CDNC is derived indirectly from satellite retrievals at cloud top and not at cloud base where most of the aerosols are activated as CCN, and (d) the derivation of CDNC through assuming adiabatic and non-precipitating conditions. Previous comparisons of ACI_{CDNC} between large-scale models and satellite data indicate that the CDNC appears to be more sensitive to changes in aerosols in models as can be derived from satellite observations (Bender, Engström and Karlsson, 2016; Malavelle *et al.*, 2017; Quaas *et al.*, 2009; Saponaro *et al.*, 2020). It is not fully understood whether this discrepancy is caused mainly by retrieval issues, differences in sampling of meteorological conditions or different temporal and spatial variability. Connecting all the relevant scales (Figure 2, Dunne *et al.*, 2014; Fanourgakis *et al.*, 2019; Kokkola *et al.*, 2025) is necessary to resolve the remaining issues related to understanding how perturbations in atmospheric aerosol loadings are reflected in CDNC.

In practice, most present ESMs describe cloud droplet activation using physically-based parameterisations of maximum supersaturation (S_{max}) in adiabatically ascending air parcels. Various parameterisations of this process, typically applied for large scale/stratiform clouds, are available and can be used (see e.g. Ghan *et al.*, 2011 and references therein). These schemes take information about the PNSD, aerosol chemical composition and some information about parametrised sub-grid scale updraft velocities within the given gridbox as inputs. They calculate the number of activated droplets (N_{act}) by using the estimated S_{max} and Köhler theory to obtain the number of aerosol particles having a diameter greater than the smallest activated diameter (Abdul-Razzak, Ghan and Rivera-Carpio, 1998; Abdul-Razzak and Ghan, 2000). The most commonly employed droplet activation parametrisation schemes in GCMs (general circulation models), and subsequently

in ESMs, fall into two categories. One group comprises of parametrisations following (Abdul-Razzak, Ghan and Rivera-Carpio, 1998; Abdul-Razzak and Ghan, 2000), which are based on detailed comparisons with cloud parcel models. In contrast, a more complex class involves iterative "population splitting" approaches, such as that developed by Fountoukis and Nenes (2005). Schemes based on empirical relationships between CDNC, aerosol number concentration and updraughts are also available (Lin and Leaitch, 1997). Besides the activation itself, the way that the parametrisations of updraft velocities–which are expected to be highly variable within the scale of a typical ESM gridbox–have important impacts on the CDNC predicted by a given ESM.

1.6 CLOUD MICROPHYSICAL PROCESSES BEYOND ACTIVATION

Rapid adjustments contribute to the effective radiative forcing due to ACI (Forster *et al.*, 2021; Szopa *et al.*, 2021). However, their effects and magnitude are uncertain (e.g. Bellouin *et al.*, 2020). While the principal effect of anthropogenic aerosols is to enhance the CDNC through cloud droplet activation (e.g. Quaas *et al.*, 2020), the adjustments are mainly due to cloud sink processes. Clouds may dissipate due to precipitation; in which case the condensation and coagulation growth of cloud hydrometeors are the microphysical processes of relevance. Precipitating clouds are thought to respond to CDNC enhancements by an increase in lifetime due to a slowdown of their precipitation formation rate (e.g. Gryspeerdt *et al.*, 2019). This translates into increases in cloud horizontal extent (cloud fraction) as well as in vertical extent or cloud LWP. However, an increase in aerosols in non-precipitating clouds can also cause enhanced evaporation through turbulent mixing with surrounding dry air and result in a decrease in LWP and cloud fraction (Ackerman *et al.*, 2004; Bulatovic *et al.*, 2019; Wood, 2012) with a strength that varies with boundary layer depth (Possner *et al.*, 2020).

In general, cloud droplets form at the cloud base and grow initially through condensation within the rising air parcel (Howell, 1949; Srivastava, 1991). Eventually, a subset of all droplets can initiate coalescence (Kostinski and Shaw, 2005), where larger droplets collect smaller droplets to form drizzle. Condensational growth often considers relaxation to saturation, or is assumed to follow the adiabatic liquid water content with a prescribed shape of the droplet size distribution, whereas the first step of drizzle/precipitation formation is parameterised as *autoconversion*, in which cloud droplets larger than a threshold diameter (often approximately 50–80 μm) are assumed to form rain (Hsieh *et al.*, 2009). In other words, the shape of the cloud droplet size distribution is assumed invariant—often monodisperse—in all meteorological conditions without any effect of cloud dynamics or background aerosol population. As the growth of precipitating droplets mainly depends on collection, the magnitude of cloud adjustment to altered droplet concentration in global models is in practice largely determined by the strength of the autoconversion. As a result, in the models, increasing aerosol concentration always delays precipitation formation, leading to an increase in the cloud LWP (Sundqvist, 1978). However, estimates from satellite-based observations suggest that such an effect only occurs for very low droplet number concentrations, and that the opposite occurs when droplet concentration grows to ~30 cm^{-3} or above (e.g. Gryspeerdt *et al.*, 2019). The strength of this adjustment in models, and hence also the contribution to the aerosol indirect effect, depends on the exact formulation of the autoconversion parametrisation (Jing, Suzuki and Michibata, 2019). As already mentioned in Sect. 1.5, ESMs tend to produce warm precipitation with too little variability in strength. In addition, it is also common for global models that the formation of warm precipitation is too efficient (Suzuki *et al.*, 2015). This can be avoided, for example by decreasing the autoconversion efficiency either by increasing the cloud droplet threshold size for precipitation formation, or simply by scaling the autoconversion strength to account for resolution differences (e.g. Mülmenstädt *et al.*, 2020). However, changing the autoconversion strength needs to be balanced in some other processes as global models are constrained with observations of cloud fraction and liquid/ice water paths.

Various aspects related to specified cloud droplet size distribution have been studied before FORCeS. For example, the role of large aerosol particles, i.e. giant CCN, which form bigger cloud droplets already in the activation process, has been discussed in the literature (e.g. Jensen and Nugent, 2017; Johnson, 1982). In addition, cloud droplet growth is influenced by turbulence-induced variability in the saturation ratio (e.g. Chandrakar *et al.*, 2016) as well as by varying in-cloud residence time ("cloud contact time") of droplets (e.g. Feingold *et al.*, 2013), both of which are not taken into account by current parametrisations used within ESMs. A central hypothesis on how changes in CDNC may impact turbulent mixing and subsequently LWP and cloud fraction is the one formulated by Ackerman *et al.* (2004). It focuses on stratocumulus clouds that are driven by cloud-top radiative cooling which, in turn, is a function of cloud-top water content and temperature. At high CDNCs, with smaller droplets, the sedimentation flux is reduced and thus cloud-top water content is enhanced. This increases radiative and evaporative cooling at cloud top, enhancing the entrainment rate and mixing of dry air from above the cloud, reducing LWP and, in consequence, due to a shorter cloud lifetime, the cloud fraction (Bretherton, Blossey and Uchida, 2007). The effect depends on above-cloud relative humidity (RH): if the free troposphere is very dry, the evaporative

reduction in LWP is stronger than if it is humid (Ackerman *et al.*, 2004; Gryspeerdt *et al.*, 2019; Toll *et al.*, 2019). In summary, while GCMs and hence ESMs typically do include parametrisations of the effect of droplet number on the precipitation formation via autoconversion, it is much less common to include the effects on turbulent mixing and evaporation (Mülmenstädt *et al.*, 2024). As a consequence, GCMs and ESMs tend to simulate strongly positive responses of LWP to aerosol enhancements (Bender *et al.*, 2019; Michibata *et al.*, 2016; Quaas *et al.*, 2009; Sato *et al.*, 2018; Zhou and Penner, 2017).

1.7 ICE FORMATION AND MULTIPLICATION

Ice-containing clouds—whether fully glaciated or mixed-phase clouds (MPCs) with both ice crystals and supercooled liquid droplets—remain among the least understood cloud types due to the complex and highly nonlinear microphysical pathways that influence their evolution and properties (Griesche *et al.*, 2024; Korolev and Milbrandt, 2022; Morrison *et al.*, 2012). This complexity is further amplified in convective clouds, where the aerosol effects on microphysics are generally not considered in current ESMs, unlike in stratiform MPCs. Ice crystals can form in the atmosphere through homogenous freezing at temperatures below roughly –38°C or heterogenous nucleation, which requires the participation of insoluble aerosol particles known as INPs (Fukuta and Schaller, 1982; Heymsfield and Sabin, 1989; Hoose and Möhler, 2012; Kanji *et al.*, 2017; Murray, Carselaw and Field, 2005; Murray *et al.*, 2012). Several aerosol types have been identified to act as INPs, such as bioaerosols (O'Sullivan *et al.*, 2018; Pereira Freitas *et al.*, 2023, 2024), sea spray aerosols (e.g. McCluskey *et al.*, 2019) and dust (Kulkarni and Dobbie, 2010). Dust is considered to be the most important INP type globally, partly due to its high abundance (e.g. Murray *et al.*, 2012; Pratt *et al.*, 2009; Seinfeld *et al.*, 2016). Among dust minerals, alkali feldspar (especially potassium feldspar, K-feldspar) and quartz are known to be important INP components, especially in MPCs (Harrison *et al.*, 2016, 2019). In recent decades, research on atmospheric INPs has been intensified leading to advancements in measurement techniques and a wider range of observations (Kanji *et al.*, 2017). Within FORCeS, measurements of INPs during the NASCENT campaign (Sect. 2.2.1) provided valuable insight on the seasonality of INPs in the pristine Arctic atmosphere (Li *et al.*, 2022a; Pasquier *et al.*, 2022a, 2023; Pereira Freitas *et al.*, 2023).

Heterogenous ice nucleation dominates the primary ice formation in MPCs over the globe (e.g. (Burrows *et al.*, 2022), and can be triggered by four acknowledged pathways (see also Figure 1): (1) immersion freezing, where a cloud or solution droplet, already containing an INP, freezes upon cooling; (2) condensation freezing, where water condenses on an INP and then freezes; (3) contact freezing, where an INP collides with a supercooled droplet, triggering its freezing; and (4) deposition nucleation, where vapour directly deposits onto an INP (e.g. Lohmann, Mahrt and Lüönd, 2016). Burrows *et al.* (2022) concluded immersion freezing to be the dominant heterpgeneous ice formation pathway in MPCs. Through all these mechanisms, INPs can modulate the production rate of primary ice in clouds, which will then influence cloud structure, extent, microphysical and radiative properties, precipitation formation and properties, and ultimately weather and climate (e.g. Burrows *et al.*, 2022; Murray *et al.*, 2021). Within ESMs, primary ice formation can be treated with varying degree of complexity. Ice nucleation schemes were traditionally based only on thermodynamic state variables such as temperature and ice supersaturation (e.g. Meyers *et al.*, 1992), while recent advances in our understanding of the INP sources have led to the development of more aerosol-aware ice nucleation schemes that account for the particle number and size distribution and the different freezing modes (e.g. DeMott *et al.*, 2010).

Current ESMs differ in their representation of ice nucleation. In NorESM2, for example, primary ice formation follows classical nucleation theory (Hoose *et al.*, 2010) accounting for immersion, contact and deposition freezing from dust and soot. ECHAM models, on the other hand, consider the immersion freezing from mineral dust and BC, contact freezing on dust (Hoose *et al.*, 2008; Lohmann and Diehl, 2006) and include temperature dependency considering the INP ability of the particles. Evaluation of simulated INP in UKESM1 against global measurements shows that representation of dust as a mixture of mineralogical and organic ice-nucleating components, as present in many soils, provides a much better explanation for global INP (Herbert *et al.*, 2025). In the CMIP6, the majority of ESMs show no change in ice number in response to a perturbation in dust emissions suggesting a prevalence of aerosol-independent INP representations (Haugvaldstad *et al.*, 2025). The lack of aerosol-aware INP schemes represents a large structural uncertainty in estimates of dust radiative forcing (Haugvaldstad *et al.*, 2025).

Despite the growing understanding of primary ice formation and its various implementations in ESMs (e.g. Lohmann and Diehl, 2006; Spracklen and Heald, 2014; Wang *et al.*, 2014), observational data of MPCs has shown that measured ice crystal number concentration (ICNC) can exceed the nearby number of INPs by several orders of magnitude (Beck *et al.*, 2018; Geerts *et al.*, 2015; Järvinen *et al.*, 2022; Lowenthal *et al.*, 2019; Luke *et al.*, 2021; Mignani *et al.*, 2019; Pasquier *et al.*, 2022a). This discrepancy is often attributed to surface-based processes, such as in orographic MPCs (Geerts *et al.*, 2015; Beck *et al.*, 2018), or to ice particles falling into MPCs from either overlying clouds or higher levels within the same cloud—a process known as the seeder-feeder mechanism (e.g. Proske *et al.*, 2021; Vassel *et al.*, 2019).

However, in cases where MPCs are decoupled from the surface and lack seeding from upper-level clouds, the mismatch between INPs and ICNCs suggests the presence of subsequent cloud microphysical processes, known as secondary ice production (SIP), that allow pre-existing ice to multiply in the atmosphere. Over the course of the last decades, several proposed mechanisms for SIP have emerged (see also Figure 1), as pointed out by the reviews of Field *et al.* (2017) and Korolev and Leisner (2020). The most widely recognised SIP processes include the Hallett-Mossop (HM) or rime-splintering process (Hallett and Mossop, 1974), ice-ice collisional break-up (BR; Phillips, Yano and Khain, 2017; Phillips *et al.*, 2017; Takahashi *et al.*, 1995), and droplet-shattering (DS) during freezing (James, Phillips and Connolly, 2021; Lauber *et al.*, 2018).

Although SIP has been recognised in field (Korolev *et al.*, 2022; Wieder *et al.*, 2022) and laboratory studies (Grzegorczyk *et al.*, 2023; Kleinheins *et al.*, 2021; Seidel *et al.*, 2024), it is generally not represented in ESMs, except for simplified parametrisations of the HM process. For example, the activation of the HM process in models often relies on arbitrary thresholds that are found to limit its efficiency (Schäfer *et al.*, 2024; Young *et al.*, 2019). Consequently, models may overlook a critical source of ice particles, potentially compromising the accuracy of simulated cloud radiative effects and precipitation patterns (e.g. Vergara-Temprado *et al.*, 2018). Recently, more sophisticated formulations have been developed to better represent SIP by integrating experimental findings (Deshmukh *et al.*, 2022; Phillips, Yano and Khain, 2017; Phillips *et al.*, 2017). Several promising modelling initiatives have sought to integrate parametrisations for additional SIP mechanisms, although most have been limited to individual case studies with restricted spatial and temporal scopes (Dedekind *et al.*, 2024; Georgakaki *et al.*, 2024; Possner, Pfannkuch and Ramadoss, 2024). Only a few studies have assessed the global significance of SIP (Sotiropoulou *et al.*, 2024; Zhao and Liu, 2021). All modelling efforts consistently indicate a significant increase in ICNC due to SIP mechanisms in stratiform, frontal, multilayer, cumulus, orographic, and convective clouds (Hoose, 2022). Process investigation and potential description within ESMs is therefore warranted (e.g. Seidel *et al.*, 2024; Zhao and Liu, 2022).

1.8 AEROSOL PROCESSING AND SCAVENGING BY CLOUDS

Activation of aerosols into cloud droplets or ice crystals followed by precipitation (Radke, Hobbs and Eltgroth, 1980) is the most important removal pathway for particulate matter from the atmosphere (Ohata *et al.*, 2016). However, in addition to the scavenging of particulate mass, clouds also interact with aerosol precursor gases (Feingold and Kreidenweis, 2000; Hoppel *et al.*, 1986). Clouds, on the other hand, provide major transport pathways from the boundary layer to higher altitudes (Barth *et al.*, 2007, 2016; Wang and Crutzen, 1995). The transfer of gas phase products into the aqueous phase can initiate chemical reactions in the aqueous phase, e.g. the production of sulfate and organic material (Ervens, 2015; Ervens, Turpin and Weber, 2011). These can later be released to the atmosphere in the particle phase upon cloud hydrometeor evaporation. Generally, these processes are represented at least to some extent in ESMs, but obtaining overall consistency is challenging.

The scavenging processes are often divided into in- and below-cloud scavenging, in which the former refers to the scavenging by cloud hydrometeors and the latter to scavenging by falling precipitation. Wet scavenging of aerosols and their precursors involves many different dynamic and thermodynamic processes (e.g. nucleation, condensation, impaction, dissolution and reactive uptake), and is inherently intertwined with other processes that affect aerosol populations and cloud microphysics (especially cloud droplet activation, see also Sect. 1.5). An ideal ESM would therefore be able to capture all the relevant parameters, describing atmospheric aerosol populations and determining their evolution: the number and mass size distributions, the chemical composition, and the concentrations of the trace gases affecting gas-particle partitioning and secondary aerosol formation, as well as their processing in cloud water and potential re-release.

Nucleation scavenging in the ESMs follows generally the treatment of cloud droplet activation (see Sect. 1.5). The formation of sulfate from aqueous-phase chemistry tends to be included within ESMs (see e.g. Feichter *et al.*, 1996)for ECHAM-models), but the inclusion of formation of aqueous-phase organics depends on the model and how the formation of secondary aerosols in general are implemented (Irfan *et al.*, 2024; Kokkola *et al.*, 2018). ESMs usually neglect cloud droplet evaporation as an aerosol source, i.e. no aerosols are released back to the atmosphere after they are wet scavenged apart from the aqueous-phase sulfate formation. In the ECHAM family, however, a portion of the wet scavenged aerosols can re-evaporate back to the atmosphere (Stier *et al.*, 2005). Regarding gas-phase species, the partitioning between the air and the cloud water in these models is calculated based on Henry's law (Stier *et al.*, 2005).

2 OVERALL APPROACH, METHODOLOGY AND DATA

Due to the large range of temporal and spatial scales relevant for aerosol-cloud-climate interactions, a combination of experimental and theoretical methodologies was used within FORCeS (Figure 2). To arrive at recommendations for the targeted processes (Figure 1), the following key steps were conducted:

1. Review of the present representation of the selected processes in ESMs, benchmarking the sensitivity of model predictions to these processes and the related variables.
2. Collection and synthesis of current understanding of the processes, using empirical insights from laboratory experiments, in-situ observations and remote sensing data, interpreted using fundamental theory and high-resolution modelling (e.g. large-eddy simulations).
3. Formulations of recommendations for improvement of the targeted processes within ESMs, based on steps 1–2 above, balancing the accuracy in the description of the processes with computational demands and feasibility of implementation on the global scale.
4. Implementation and testing of the recommended improvements within the ESMs used within FORCeS.

This article focuses on steps 1–3 above, leaving the details of the implementation and testing of these recommendations to follow-up studies. The approach above was perhaps the key methodological development within FORCeS as compared to, and building on, previous large European projects with similar topics such as EUCAARI (Kulmala *et al.*, 2011), PEGASOS, and ACCENT (Fuzzi *et al.*, 2015). In addition to this "bottom up" approach, FORCES also developed a new "top down" approach to expose potential structural deficiencies in a global model based on analysis of a perturbed parameter ensemble (see Regayre *et al.*, 2023). The results of the top-down analysis relate to cloud processes, and are presented in section 3.6. Figure 2 illustrates the timeline that FORCeS was built upon based on the steps above, and provides examples of the various methodologies applied within the project. **In the sections below we give an overview of the ESMs used and measurement campaigns conducted explicitly for FORCeS.** Short descriptions of other data and methodologies applied within the project with key references used to obtain the recommendations (such as high-resolution modelling and laboratory experiments) are given in the Supplement.

2.1 EARTH SYSTEM MODELS

The research conducted under the framework of FORCeS primarily utilised three ESMs: EC-Earth3-AerChem, NorESM2, and ECHAM6.3-HAM2.3/MPI-ESM-1.2-HAM2.3. However, to derive additional insights and recommendations, simulations were also carried out using, for example, UKESM1 and ICON (see descriptions

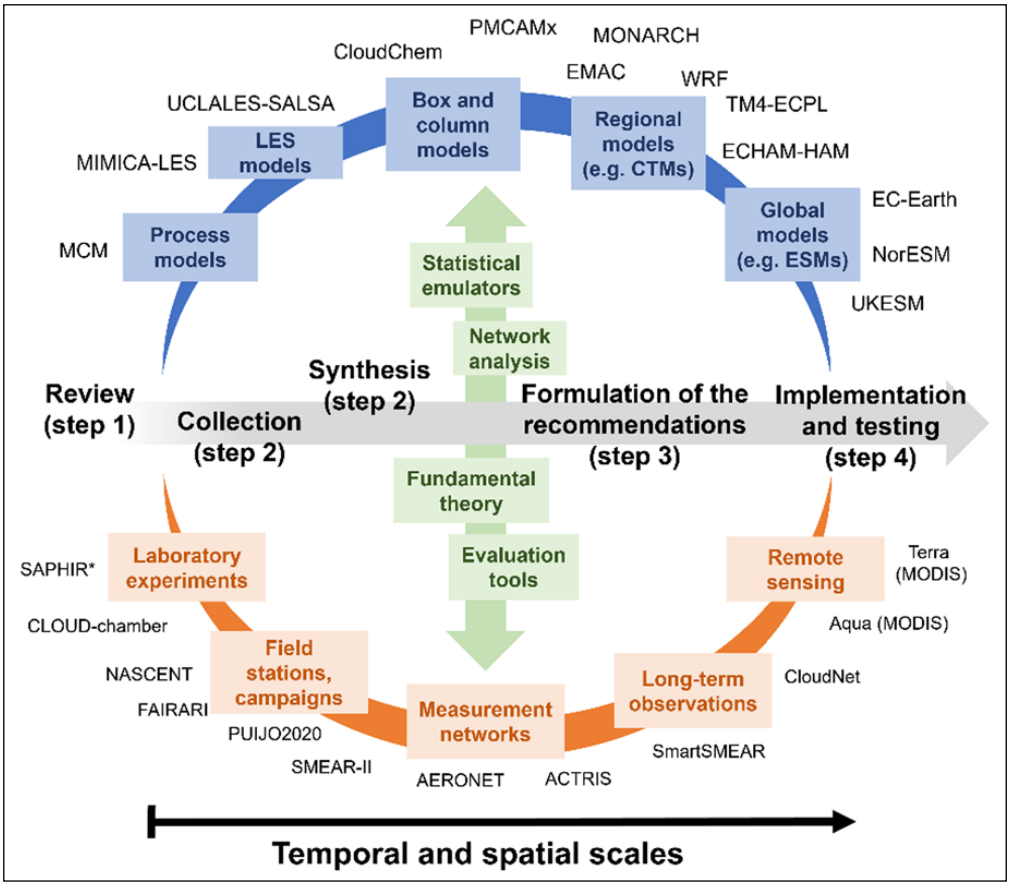

Figure 2 Schematic illustrating the overall approach, methodology and data within the FORCeS project. The timeline of the project is illustrated with grey arrows and steps from 1 to 4. The work within FORCeS has covered different temporal and spatial scales by utilising both models (shown in blue at the top) and observations (shown in orange at the bottom). Observations and models were intertwined with various analysis tools illustrated in the middle with green.

in Sect S1), including extensive analysis of perturbed parameter ensembles of UKESM1. The selection of models was based on their relatively advanced representations of aerosol and cloud microphysics, as well as chemistry. While different versions of these models were employed for various studies, the foundational benchmark for comparison was established through the Coupled Model Intercomparison Project Phase 6 (CMIP6, Eyring *et al.*, 2016) simulations.

2.1.1 EC-Earth3-AerChem

EC-Earth3-AerChem is a version of EC-Earth3 (Döscher *et al.*, 2022) with additional components to simulate aerosols and chemistry in the atmosphere (van Noije *et al.*, 2021). The atmospheric component of EC-Earth3-AerChem comprises an adapted iteration of the GCM employed in Cycle 36r4 of the Integrated Forecasting System (IFS) by the European Centre for Medium-Range Weather Forecasts (ECMWF). The IFS version applied in EC-Earth3-AerChem has a horizontal resolution of T_L255 (triangular truncation at wavenumber 255 in spectral space with a linear N128 reduced Gaussian grid, corresponding to a spacing of about 80 km), with 91 vertical layers in the atmosphere. The model top resides at 0.01 hPa.

The aerosol and chemistry model included within EC-Earth3-AerChem is the Tracer Model version 5 (TM5, Huijnen *et al.*, 2010; van Noije *et al.*, 2021), which employs an atmospheric grid characterised by reduced resolution in terms of longitude and latitude (3° × 2°), along with 34 vertical layers extending to approximately 0.1 hPa. The aerosol scheme used by TM5 is based on the modal aerosol microphysical scheme M7 (7 lognormal modes) introduced by Vignati *et al.* (2004), including sulfate, black carbon, organic aerosols, sea salt and mineral dust. Additionally, in TM5, ammonium nitrate and the associated water uptake is described using an equilibrium gas–particle partitioning model and the secondary organic aerosol formation is calculated following Bergman *et al.* (2022).

IFS Cycle 36r4 employs a 1-moment cloud microphysics scheme. Clouds and large-scale precipitation are described by prognostic equations for cloud liquid water, cloud ice, rain, snow, and a grid box fractional cloud cover. Cloud droplet formation is calculated diagnostically with an aerosol activation scheme in which the critical supersaturation and critical particle diameter for each of the relevant water-soluble modes is calculated from Köhler theory, assuming uniform internal mixing inside the modes. The subgrid-scale vertical velocities entering the scheme are assumed to be normally distributed with a fixed width and a mean equal to the large-scale vertical velocity. The ICNC is not predicted but diagnosed using the temperature-based scheme of Meyers *et al.* (1992). Water droplets freeze instantly below −38°C, while between −38°C and 0°C, ice and supercooled water can coexist, with ice growing via the Wegener-Bergeron-Findeisen process. Aerosol wet and dry removal is included as documented in van Noije *et al.* (2021).

2.1.2 NorESM2

The Norwegian Earth System Model version 2 (NorESM2, Seland *et al.*, 2020) is developed by the Norwegian Centre for Climate Services and based on the Community Earth System Model (CESM2.1, Danabasoglu *et al.*, 2020; Gettelman *et al.*, 2019), but with a different ocean model as well as a number of changes in the atmospheric component. Due to NorESM2's high computational cost, two model versions with varying horizontal resolution for the atmosphere and land components are available (Seland *et al.*, 2020). The "medium-resolution" has a grid spacing of 0.9375° × 1.25° (lat, lon), while the "low-resolution" version utilises 1.875° × 2.5°. In the vertical, NorESM2 has 32 vertical levels which extends to a "rigid" lid at 3.6 hPa, corresponding approximately to 40 km.

The aerosol scheme used in NorESM2 is OsloAero (Kirkevåg *et al.*, 2018) in which the aerosol mass is divided into background particles either from primary emissions or from new particle formation (e.g. dust, sea salt, biomass burning and recently nucleated sulfate and organics) and process tracers (e.g. sulfate condensate and coagulate, organic condensate). The background aerosols form the log-normal modes leading to the number concentrations. The process tracers are distributed onto the log-normal modes creating aerosol size distributions without any assumptions of the shape of distribution or mixing states. The explicit calculation of this is too costly for online calculations so optical properties are read from precalculated look-up tables, using added process mass as the indices in the table.

For aerosol activation, OsloAero applies the (Abdul-Razzak and Ghan, 2000) scheme, and given that the aerosol cloud activation scheme requires a log-normal distribution, the size distributions are calculated by the sum of the background and process as described above and are approximated by a best fit to a log-normal size distribution.

2.1.3 ECHAM6.3-HAM2.3/MPI-ESM-1.2-HAM2.3

The global aerosol-climate model ECHAM6.3-HAM2.3 is based on the atmospheric circulation model ECHAM6 (Stevens *et al.*, 2013). For solving atmospheric circulation in three dimensions, it employs spectral truncation at T63 (indicative of an approximate horizontal resolution of 1.875° × 1.875°). The vertical grid comprises 47 model levels and extends up to 0.01 hPa. MPI-ESM-1.2-HAM is based on the MPI-ESM1.2 model (Mauritsen *et al.*, 2019) and comprises ECHAM6.3-HAM2.3, coupled with the ocean model MPIOM1.6 and the ocean biogeochemistry model HAMOCC6.

The aerosol module within ECHAM6.3-HAM2.3 originates from the Hamburg Aerosol Model HAM

(Neubauer *et al.*, 2019; Stier *et al.*, 2005; Tegen *et al.*, 2019), which computes the aerosol mixture taking into account sulfate, black carbon, organic carbon, sea salt and mineral dust. The default version of ECHAM6.3-HAM2.3 is complemented with the modal aerosol model M7 (Stier *et al.*, 2005; Tegen *et al.*, 2019; Vignati *et al.*, 2004) but the sectional module SALSA (Kokkola *et al.*, 2008, 2018)—comprising size bins distributed between 3 nm and 10 μm of aerosol diameter—can also be used. Additionally, ECHAM6.3-HAM2.3 can be complemented with the chemistry model MOZ (Schultz *et al.*, 2018), depending on the application.

For cloud droplet activation, two alternative parametrisations are implemented into ECHAM6.3-HAM2.3. One is the empirical scheme by Lin and Leaitch, (1997), which was implemented by Lohmann *et al.* (2007). The other is the Abdul-Razzak and Ghan parametrisation that is explicitly based on Köhler theory (for modal setup, Abdul-Razzak, Ghan and Rivera-Carpio, 1998 and Abdul-Razzak and Ghan, 2000, and for sectional setup, Abdul-Razzak and Ghan, 2002), which were introduced by Stier (2016) for M7 and by Kokkola *et al.* (2008; 2018) for SALSA. Next to activation, the two-moment cloud microphysics scheme (Lohmann and Neubauer, 2018) includes homogeneous nucleation of ice crystals in cirrus clouds and heterogeneous nucleation in MPCs as well as size dependent in-cloud and below-cloud wet scavenging of aerosol particles.

2.2 MEASUREMENT CAMPAIGNS

Within FORCeS, three in-situ measurement campaigns were conducted to study the interactions between aerosols and clouds in three very different environments (Figure 3). NASCENT (the Ny-Ålesund Aerosol Cloud Experiment) took place in the high Arctic in Ny-Ålesund, Norway which is an extremely clean environment. The PUIJO campaign was conducted in south-east of Finland in Kuopio, which is characterised as a semi-urban environment. FAIRARI (Fog and Aerosol InteRAction Research Italy) was conducted in Po Valley, Italy, which is characterised with very high pollution and frequent fog events. The common denominator for all three sites is the availability of in-situ measurements of both aerosols and cloud microphysics, enabling process-level studies across contrasting conditions. Together, these campaigns provide complementary observational coverage that is specifically suited to address the key science gaps targeted in the FORCeS project, capturing the influence of clean, semi-urban, and highly polluted environments on aerosol-cloud interactions. Studies emerging from these measurement campaigns have provided a variety of observational constraints for the modelling work conducted within FORCeS. Short descriptions with key references for these campaigns are presented below.

2.2.1 NASCENT

Observations during NASCENT (September 2019 to August 2020) were conducted at multiple sites close to Ny-Ålesund (78.9°N, 11.9°E). One of the key locations was the Zeppelin Observatory (485 m.a.s.l) located 2 km southwest of Ny-Ålesund on Mt. Zeppelin. Because of its location in a pristine Arctic environment, far from significant sources of contamination, interference from local pollution is minimal. Additionally, the prevailing meteorological conditions in the area further reduce the impact of local pollution. During NASCENT (from September 2019 to August 2020) the monthly cloud cover varied between 50% to 80% and from those

Figure 3 Overview of the in-situ measurement campaigns conducted within FORCeS: NASCENT in Ny-Ålesund, Norway, FAIRARI in Po Valley, Italy and PUIJO-campaign in Kuopio, Finland.

30 to 70% could be classified as low-level clouds. The measurements during NASCENT comprised a multitude of different variables to characterise the aerosols, clouds, radiation and meteorological conditions. Aerosol and cloud characteristics were observed with great detail, including e.g. the particle shape for the aerosols and both ice and liquid water content for the cloud measurements. Full details of the deployed instrumentation and measured parameters at each of the sites are given in Pasquier *et al.* (2022b).

2.2.2 PUIJO-campaign

The measurements during the PUIJO campaign (SMEAR IV station, 62.90°N, 27.65°E) included observations (from 15.09.2020 to 24.11.2020) at the top of the Puijo tower (306 m.a.s.l) and at ground level 200 metres below the tower station. The station represents a semi-urban environment, surrounded by forest and lakes but still resides in the vicinity (distance ~2 km) of Kuopio city centre. The site has been designed to investigate the interactions of aerosol particles and clouds, especially the activation of aerosol particles into cloud droplets. More details on the tower station can be found in Leskinen *et al.* (2009). The tower is frequently inside low-level clouds, and the ground station was used to obtain comparable observations for out-of-cloud conditions. At both stations, aerosol particle number size distribution and the chemical composition of the particles (d_p < 1 µm) were measured. In the tower station, the particulate molecular composition was also measured along with droplet number concentrations and size distributions. Details of the measurements and instrumentation conducted during this campaign can be found from earlier work (Calderón *et al.*, 2022; Kommula *et al.*, 2024; Tiitta *et al.*, 2022).

2.2.3 FAIRARI

The FAIRARI campaign took place at the research station San Pietro Capofiume in the Italian Po Valley (44.65°N, 11.62°E, 11 m.a.s.l) during winter/spring 2021/22 (with a pre-campaign in Feb 2021). The geography of the Po Valley, which is enclosed between the Alps in the North and West, and the Apennines in the South, promotes air stagnation under anticyclonic conditions. During winter, those, together with high concentrations of anthropogenic pollution (e.g. annual average $PM_{2.5}$ > 25 µg m^{-3}, Neuberger *et al.* 2025), often lead to long-lasting and dense fog events, affecting both visibility and human health. To evaluate the aerosol-fog interactions and their impact on secondary aerosol formation during this period as well as the transition to the following period of frequent new particle formation events, physical and chemical properties of gas molecules up to fog droplets were measured in situ. More details about the FAIRARI campaign, including a detailed description of the set-up, can be found in Neuberger *et al.* (2025).

3 RECOMMENDATIONS ON AEROSOL AND CLOUD PROCESSES FOR EARTH SYSTEM MODELS

3.1 RECOMMENDATIONS FOR ORGANIC AEROSOL

Given the demonstrated structural uncertainties in the representation of OA impacts on the aerosol levels and ACI, with implications for, e.g. the representation of biogenic climate feedbacks (e.g. Blichner *et al.*, 2024) and absorbing aerosol (e.g. Brown *et al.*, 2021; Li *et al.*, 2022b), it is evident that continued work on the representation of OA in ESMs is needed. The contribution of OA to the PNSD seems pertinent, as well as finding ways to simplify the complexity of the chemical system driving OA in terms of the number of simulated surrogate compounds and their assumed properties.

It is also evident that due to the large range of molecular species present in OA and the fact that many of them can change phase within the atmosphere, some form of treatment with various volatilities present in OA is needed. To address this issue, an ESM module called ORACLE-lite has been developed within FORCeS (Tsimpidi *et al.*, 2025). Previously, the more detailed ORACLE module (Tsimpidi *et al.*, 2014, 2018) was developed and implemented in the ECHAM/MESSy (Jöckel *et al.*, 2006) Atmospheric Chemistry model EMAC (Sect. S1.3). ORACLE is based on the VBS approach (e.g. Donahue *et al.*, 2006, see also Sect 1.1), uses fixed logarithmically-spaced saturation concentration bins and assumes the formation of pseudo-ideal solutions in the organic aerosol phase.

The overall aim of the ORACLE-lite is to combine advanced air quality features and recent experimental discoveries regarding the complexity of OA into a flexible, publicly available system. To meet the computational requirements for ESMs, the number of surrogate species describing OA and their volatility is reduced from 92 in ORACLE to 16 in ORACLE-lite (Figure 4). ORACLE-lite uses three surrogate species with effective saturation concentration at 298 K of $C^* = 10^{-2}$, 10^{1}, and 10^{4} µg m^{-3} to represent the volatility range of low volatility (LVOCs), semi volatile (SVOCs), intermediate volatility organic compounds (IVOCs) emissions. These compounds are allowed to partition between the gas and aerosol phases, contributing to the formation of POA. Photochemical reactions that alter the volatility of gas-phase organic compounds are accounted for, and their oxidation products are tracked separately to simulate SOA formation from SVOC and IVOC emissions. Additionally, the oxidation of VOC precursors yields two products per species, distributed into two volatility bins with effective saturation concentrations of 1 and 10^{3} µg m^{-3}, which also partition into the aerosol phase and contribute to SOA formation. Overall, despite the simplifications applied to reduce the computational cost,

ORACLE-lite is able to simulate the contribution of LVOCs, SVOCs, IVOCs and VOCs to OA formation with reasonable accuracy, underestimating total OA concentrations with normalised mean bias ranging from –4% over North America to –53% over Europe (Tsimpidi *et al.*, 2025). **Other existing ESMs could explore the implementation of ORACLE-lite, especially if their current simulations do not consider the variable volatility of organic species.** The addition of 16 OA components comes at a computational cost and simpler approaches for OA representation could be desirable in some applications (Pai *et al.*, 2020). In this regard, an evaluation of the ability of a given ESM to represent OA impacts on PNSD is encouraged—particularly, if capturing ACI is important for the model experiments in question. IOA species participate in NPF and early growth (e.g. Kupc *et al.*, 2020), which implies the need for simulating the low-volatility components of OA. **The approach developed and evaluated for EC-Earth-AerChem by Bergman *et al.* (2022) might therefore be of interest to models that seek a simple, yet thermodynamically-based representation of OA.** This approach (noted as NEWSOA in Figure 5) focuses on two lumped species, namely semi-volatile and extremely low-volatile organic species (SVOCs and ELVOCs), results in generally improved predictions, though still underestimates aerosol number (Figure 5a)

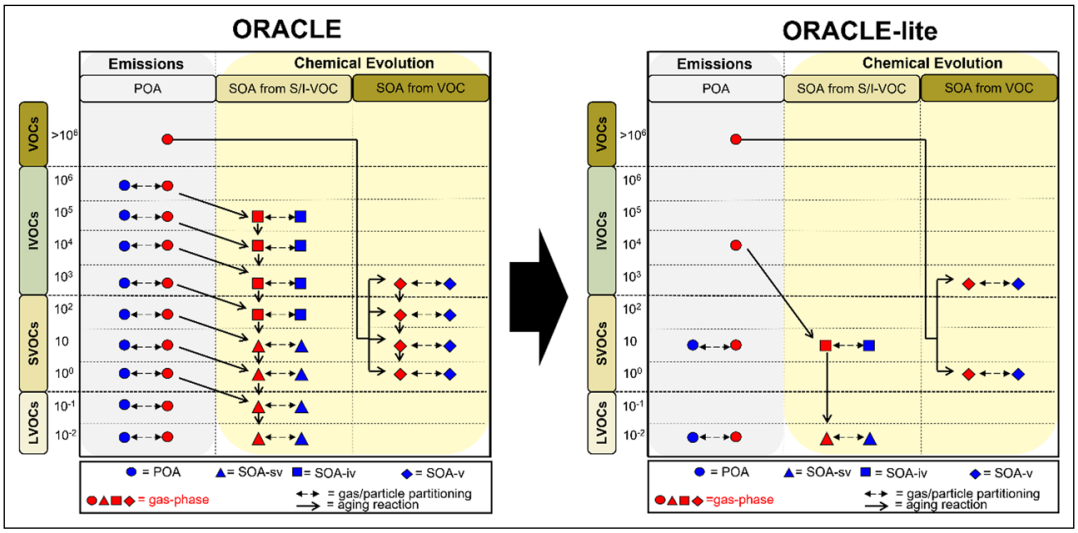

Figure 4 Schematic illustrating the difference between the full ORACLE (Tsimpidi *et al.*, 2014, 2017) and ORACLE-Lite (Tsimpidi *et al.*, 2025). Reproduced and modified under the Creative Commons 4.0 (CC 4.0) license.

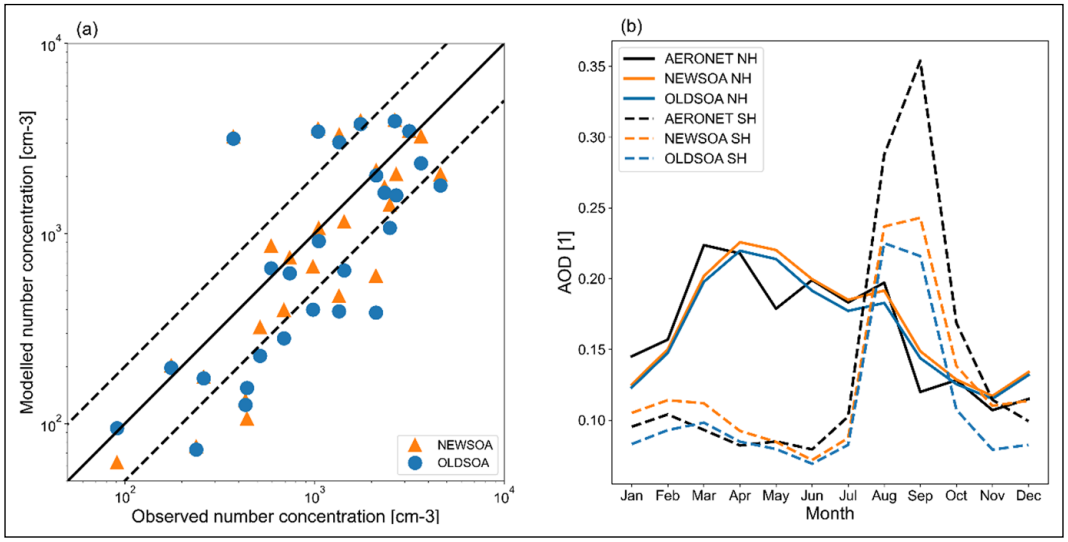

Figure 5 Evaluation of the performance between model simulations and observations presented in Bergman *et al.* (2022). Scatter plot in **(a)** shows the annual mean number concentrations at the stations (Table S3 in Bergman *et al.*, 2022) in the year 2010, orange triangles indicate simulations with NEWSOA (online approach with lumped SVOCs and ELVOCs) and blue dots represent OLDSOA (offline calculation of SOA production). The black solid line shows the 1:1 line, and the dashed lines indicate a deviation of a factor of 2. Panel **(b)** shows the seasonal cycle of the mean AOD across all AERONET stations for Northern Hemisphere (NH, solid lines), and Southern Hemisphere (SH, dashed lines). Black lines indicate the derived AERONET AOD and the orange and blue colours are the NEWSOA and OLDSOA simulations, respectively. Figure adopted and modified from Bergman *et al.* (2022) under the Creative Commons 4.0 (CC 4.0) license.

and optical depth (Figure 5b) compared with the earlier approach (noted as OLDSOA in Figure 5) in which SOA production was calculated offline (Bergman *et al.*, 2022). Applicability of these recommendations naturally requires organic aerosol species to be represented in the model of interest, coupled to a gas-phase chemistry scheme and secondary aerosol formation processes.

As there are still large uncertainties in the volatilities of organics, Irfan *et al.* (2024) evaluated the sensitivity of globally simulated organic aerosol to the volatility of secondary organic aerosols. This study showed that although the growth of newly formed particles depends mainly on the organics with lowest volatilities, the simulated organic mass is most sensitive to semi-volatile organics due to the higher abundance of those species as well as the higher sensitivity to the partitioning process itself. Lowest volatility organics mainly reside in the particle phase, and this is not influenced by the small variability in their assumed volatility. Similarly, high volatility organics reside mainly in the gas phase and their partitioning is also insensitive to the variability in their volatility. Based on the same study, reducing the number of volatility classes by combining them requires a careful consideration of the mean volatility of the combined classes since the simulated organic mass and CCN are sensitive to these assumptions.

3.2 RECOMMENDATIONS FOR PARTICULATE NITRATE

As anthropogenic SO_2 emissions are decreasing, the importance of particulate nitrate will likely increase and ammonium nitrate is expected to surpass ammonium sulfate in the aerosol composition in many regions (Aksoyoglu *et al.*, 2017; Tsimpidi *et al.*, 2025; Wang *et al.*, 2020). **It is therefore recommended to review the treatment and consider the addition of nitrate within any ESM targeting on interactions between air quality and climate.** We explored the key mechanisms driving nitrate formation on dust and sea-salt particles and evaluated how these processes are represented in models. By integrating different levels of complexity of the dust heterogeneous chemistry into the MONARCH model (see Sect. S2.2), we assessed the sensitivity of nitrate formation to various processes (Soussé Villa *et al.*, 2025). The analysis focused on the condensation of gas species onto dust (both reversible and irreversible pathways), the impact of nitrate representation on species burdens, lifetimes, size distributions, and the role of dust alkalinity (mineral composition). Accounting for the alkalinity of dust and sea salt improved model agreement with observations, particularly when assuming reversible gas condensation onto dust particles and accounting for kinetic limitations. In contrast, irreversible uptake led to an overestimation of coarse particulate nitrate. As stated in Sect. 1.2 the main issue related to modelling inorganic aerosol thermodynamics in ESMs is related to the computational cost of these calculations. **A computationally efficient atmospheric aerosol thermodynamics module, ISORROPIA-lite, has therefore been developed within FORCeS with the aim to be incorporated into ESMs with little additional computational cost.** Special emphasis was placed on reducing the computational cost of the formation and evaporation of ammonium nitrate, the reactions of nitric acid with coarse sea salt and dust particles, and the competition between fine and coarse particles for the available nitric acid. The implementation of ISORROPIA-lite naturally becomes meaningful in models in which the key inorganic species described in the model are represented, together with a scheme aiming at predicting the thermodynamics of atmospheric water.

The ISORROPIA-lite module is described in detail by Kakavas, Pandis and Nenes (2022), and is based on the well-documented aerosol thermodynamics model ISORROPIA-II (see e.g. Fountoukis and Nenes, 2007). The main differences between the lite version and ISORROPIA-II are that it (1) assumes the aerosol is always in metastable (i.e. aqueous state) equilibrium, (2) treats the thermodynamics of Na^+–NH_4^+–SO_4^{2-}–NO_3^-–Cl^-–Ca^{2+}–K^+–Mg^{2+}–Organics–H_2O aerosols using binary activity coefficients from precalculated look-up tables, and (3) accounts for the contribution of organic aerosol water. The assumption of a metastable state greatly simplifies the phase diagrams, but is, however, supported by observations (Bougiatioti *et al.*, 2016; Guo *et al.*, 2015, 2018). The evaluation of ISORROPIA-lite compared to ISORROPIA-II within the chemical transport model PMCAMx (Sect. S2.1 and references therein), showed that the lite version is 35% faster accelerating the PMCAMx 3D simulations by ~10% (Kakavas, Pandis and Nenes, 2022). Further evaluation of ISORROPIA-lite in the EMAC (ECHAM5/MESSy, Sect. S1.3) atmospheric and chemistry-climate model compared to ISORROPIA II in stable mode showed relatively good agreement for global daily mean surface concentrations of inorganic aerosols, mineral ions and aerosol water (Milousis *et al.*, 2024). Greater differences were found for intermediate humidity ranges (RH between 20% and 60%), where ISORROPIA-lite predicted higher aerosol water and lower particulate nitrate concentrations, due to the metastable assumption. The differences in particulate nitrate between the two versions were localised to specific regions, including the Middle East, the Himalayan Plateau and East Asia, with a strong dependence on RH. Meanwhile, the estimates from ISORROPIA-lite closely reproduced the AMS measurements of particulate nitrate, showing good overall agreement (Figure 6). While some scatter is evident, particularly in regions like North America, the model captures average nitrate concentrations well across regions, with normalised mean biases below 10% (Tsimpidi *et al.*, 2025). This variability is typical of global models and originates from known limitations such as

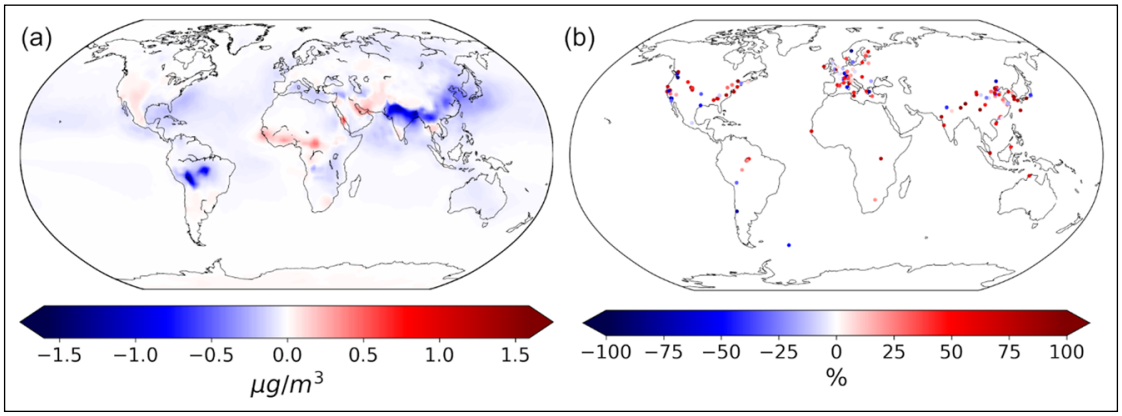

Figure 6 The change of the EMAC-simulated nitrate concentrations at surface after employing ISORROPIA-lite (vs. ISORROPIA II) is presented in **(a)**, with blue colour indicating lower concentrations by ISORROPIA-lite. The coloured points in **(b)** show the deviations between EMAC results (with ISORROPIA-lite) and nitrate derived from observations with aerosol mass spectrometers around the world over the period 2000–2020.

coarse spatial resolution and uncertainties in precursor emissions, as discussed in Milousis *et al.* (2025a).

Since the partitioning or semivolatile inorganic components is usually not simulated in ESMs and yet it might change under future conditions, our recommendation from FORCeS is to use a thermodynamic model within the ESM to perform these calculations if possible. This module could be, for example, the ISORROPIA-lite developed within FORCeS due to its reduced computational cost and good overall performance compared to the standard version of ISORROPIA-II (Figure 6a). Within FORCeS, the EQSAM module in EC-Earth3-AerChem has been replaced by ISORROPIA-II (Myriokefalitakis *et al.*, 2022), in which nitrates are now simulated for both the accumulation and coarse mode, in contrast to the bulk aerosol approximation used earlier. Due to the good agreement between ISORROPIA-II and ISORROPIA-lite, a similar behaviour is expected with ISORROPIA-lite except for the reduced computational time.

Minerals present in dust, such as calcite, influence the aerosol pH and thus the distribution of nitrate between the gas and particulate phases (e.g. Karydis *et al.*, 2021). However, deserts around the world have different mineral compositions due to their discrete soil characteristics, which can affect the coating of the emitted mineral dust with inorganic acids such as nitrate (Karydis *et al.*, 2016; Klingmüller *et al.*, 2018). ESMs typically assume a globally uniform dust chemical composition. Representing calcite in ESMs requires at least two additional tracers (for accumulation and coarse modes). This is now included in EC-Earth3-AerChem (Myriokefalitakis *et al.*, 2022). Another potential option to avoid the extra computational cost is to use precalculated monthly climatologies of calcite fractions in dust. Within FORCeS, a new dust climatology has been developed that can allow ESMs broadly characterising regional changes in dust composition and its potential impact on aerosol pH and nitrate (Gonçalves Ageitos *et al.*, 2023). **In applications in which an accurate prediction of the distribution of nitrate between the fine and coarse mode is essential, our recommendation is therefore to consider implementing a dust minearology climatology** (see also Sect. 3.3.2). These recommendations are meaningful additions for models that have dust represented as an aerosol species, coupled to some form of size-resolved composition (i.e., to separate between fine and coarse particles) and secondary aerosol formation.

3.3 RECOMMENDATIONS FOR ABSORBING AEROSOL

3.3.1 Black carbon

It is recommended that models align with the recent experimental determinations of fresh black carbon (BC) MAC at 500 nm by (Liu *et al.*, 2020), who reviewed the available literature on BC absorption properties, and found an average of 8 ± 0.7 m^2 g^{-1}. This value is close to the MAC value of 7.5 ± 1.2 m^2 g^{-1} recommended by Bond and Bergstrom (2006). Most of the numerical modelling studies align with this MAC recommendation, and use a refractive index of BC of 1.95 + 0.79i, which, however, according to Liu *et al.* (2020), can fail to reproduce the measured MAC values, resulting in a potential negative bias in the simulated BC absorbivity. Note that the recent AeroCom Phase III intercomparison exercise for absorbing aerosol by Sand *et al.* (2021) has reported that the BC MAC at 550 nm in 15 participating models ranged between 3.1 m^2 g^{-1} and 16.6 m^2 g^{-1}, with a mean of 9.8 m^2 g^{-1} and a median of 10 m^2 g^{-1}. However, not all models within the intercomparison provided values for BC MAC. While MAC values for aged (coated) BC larger than 10 m^2 g^{-1} have been confirmed by several field observations, the values smaller than 7.5 m^2 g^{-1} even for fresh uncoated (fresh or externally mixed) BC seem unsupported by the observations, and may require revision of the employed refractive index in the model.

In general, BC MAC is highly site-specific and can vary substantially, particularly in remote regions where

aerosols are aged. This variability adds complexity, and sensitivities of models to updated MAC values are not yet fully known. MAC is also influenced by black carbon density, and the choice of the actual combination of values of density and refractive indexes can significantly impact the estimate of BC radiative forcing in global models (Digby *et al.*, 2025). According to Liu *et al.* (2020), the density of black carbon aerosols is reasonably well constrained by laboratory measurements in the range 1.7–1.9 g cm^{-3}. Nevertheless, the determination of black carbon density in ambient, internally mixed particles remains a topic of open investigation. Despite these uncertainties, **MAC remains a powerful diagnostic of BC absorption and its evaluation in ESM output is highly recommended.**

3.3.2 Dust

The direct influence of dust aerosols on climate is largely through their shortwave (SW) optical properties, which depend on mineral composition. ESMs often simplify dust as a single, homogeneous aerosol, ignoring regional differences in mineralogy. Studies have shown that variations in dust mineralogy, especially iron oxides like hematite that strongly absorb solar radiation, can significantly alter dust's SW radiative effects (Li *et al.*, 2021a; Perlwitz, Pérez García-Pando and Miller, 2015). We provide specific recommendations to improve dust mineralogy representation in ESMs, drawn from FORCeS investigations in collaboration with other projects like FRAGMENT and NASA EMIT (Earth Surface Mineral Dust Source Investigation) using the MONARCH model and other ESMs (CESM, NASA GISS ModelE and GFDL AM4) (Gonçalves Ageitos *et al.*, 2023; Li *et al.*, 2024a; Obiso *et al.*, 2024; Song *et al.*, 2024 and references therein). The focus of these recommendations is on levaraging new data (e.g. NASA's EMIT mission surface mineralogy altas) and on refining iron oxide optical properties and mixing assumptions, while balancing accuracy with computational efficiency. These recommendations naturally become meaningful for models that simulate dust as an absorbing species.

The first recommendation is to move beyond globally uniform dust properties by allowing dust optical properties to vary geographically according to source mineral composition. Dust mineralogy differs by source region, which in turn affects optical behaviour. Yet many state-of-the-art ESMs still assume dust has invariant composition everywhere. Obiso *et al.* (2024) shows that by implementing individual tracers for key minerals and integrating region-specific soil mineral profiles from Claquin *et al.* (1999) into a model (with iron oxides as a key variable), the model produced higher SSA and thus a stronger cooling than the previous uniform-composition case, in substantially better agreement with dust-filtered SSA retrievals derived from AERONET (see also S5.2) sun photometers. Song *et al.* (2024) likewise found that explicitly resolving eight mineral types in the GFDL model reduced dust SW absorption compared to the homogeneous dust assumption, leading to better agreement with observations. **The recommendation is to implement individual tracers for key minerals to spatially resolved dust composition in ESMs.**

Underlying soil mineralogical atlases drive the modeled dust composition, so using the best available data is essential. Gonçalves Ageitos *et al.* (2023) examined two existing global soil mineralogy datasets (Claquin *et al.*, 1999; Journet, Balkanski and Harrison, 2014) and found large discrepancies – for impactful components like iron oxides, different soil atlases led to 100% differences in the dust iron fraction in some regions. Such uncertainty directly translates to uncertainty in dust SW absorption in models as shown in (Li *et al.*, 2021a, 2024a). Li et al. (2024a) likewise reported substantial bias in modeled hematite abundance when using current surface mineral datasets, underscoring the need for improved sources. **The recommendation is to update model surface mineral inputs with new high-quality observations. The NASA EMIT mission offers a breakthrough dataset, using imaging spectroscopy to map surface mineral composition across major dust source regions** (Clark *et al.*, 2024; Green *et al.*, 2023; Thompson *et al.*, 2024). EMIT's measurements can capture the spatial variability of minerals such as hematite with unprecedented detail. The first version of the new dataset has been implemented in four models (MONARCH, CESM, ModelE and AM4) to simulate the spatially and temporally varying refractive indices consistent with the varying mineralogical composition of dust aerosols, showing good agreement with SSA observations, and reduced uncertainty in the direct radiative impacts of dust in both present-day and future climates (Li *et al.*, 2024b).

We furthermore recommend to update refractive indices for hematite and goethite, using improved optical constants for hematite and goethite based on recent laboratory constraints. Li et al. (2024a) and Obiso *et al.* (2024) highlight that hematite's absorption capacity in dust has been highly uncertain (varying over two orders of magnitude) and substantially narrow this range by exploring mixing assumptions using lab measurements of dust composition, absorption, and scattering from Di Biagio *et al.* (2019) and mineralogy-aware dust modeling. Incorporating these refined properties in model radiative calculations reduced uncertainty in dust absorption. This ensures dust optical properties (like single-scattering albedo) are more realistically presented, directly improving estimates of dust's direct radiative effect. In practice, **ESM developers may replace older hematite optical parameters with the new values from Li *et al.* (2024a) or Obiso *et al.* (2024) based on Di Biagio *et al.* (2019) to better capture dust's solar absorption.** Model evaluation against observations (e.g. AERONET aerosol optical depth and single-scattering albedo) can confirm

that this update leads to improved agreement. Since mineralogy also partly determines the desert surface albedo, updates to the dust composition will need to be accompanied by updates in the desert surface albedo to avoid biases in the dust direct forcing efficiency due inconsistencies between the optical properties of the dust and the desert surface.

Key minerals should be targeted, considering computational efficiency. We suggest focusing on representing those minerals that most strongly influence shortwave optics—primarily iron oxides (hematite/goethite)—for absorption. Other minerals such as calcite, feldspar and quartz may be of relevance when considering dust heterogeneous chemistry and the impact of dust on ice nucleation. All in all, modeling every individual mineral is impractical and computationally expensive, and the choice should depend on the application. Song *et al.* (2024) suggest grouping similar minerals to save computation: for example, treat all clay minerals (illite, kaolinite, smectite) as one category with shared optical properties, while keeping iron oxide-rich particles separate, since hematite and goethite have unique absorption characteristics. In their tests, lumping clays together and explicitly isolating hematite (and gypsum, another distinct mineral) maintained accuracy in radiative effects but with lower computational cost. Song *et al.* (2024) also found that a homogeneous dust tuned to a certain amount of hematite could mimic the global-mean radiative effect of a full mineralogy model. This implies that much of the climate impact comes from the overall dust absorption level. Thus, if computational resources are constrained, one minimum step is to adjust the assumed global dust iron oxide content together with the associated dust refractive index to observation-constrained values, to at least get the correct average SW absorption. However, for regional accuracy and mechanistic studies (e.g. impacts on monsoons), explicit spatial variation of mineralogy is preferable despite the extra computation. **ESM developers should therefore represent at least the iron oxide fraction as a separate entity (or a separate optical property calculation), and possibly group the rest into a few broad classes (e.g. clays, quartz/feldspar, carbonates).** An additional alternative is to use a globally resolved climatology of mineral fractions, representing some regional variability in dust optical properties, while avoiding the computational burden of additional mineral tracers. All in all, this balances detail with efficiency: the model gains realism in SW absorption by iron oxides without needing to track a dozen mineral tracers.

3.3.3 Brown carbon

Representing BrC in ESMs naturally requires OA to be explicitly parametrised, as BrC stands for the absorbing part of it. Only the absorption by BrC (i.e., the imaginary part of the refractive index) therefore has to be considered, while the scattering properties (real part of the refractive index) are considered through the OA direct climate effect. For a simple but explicit calculation of BrC, three different BrC species can be be considered: two primary strongly absorbing species and one photobleached very weakly absorbing species, denoted as pbBrC. The BrC produced during the oxidation of aromatic VOCs is weakly absorbing compared with the primary BrC and has rapidly decreasing absorbing properties due to ageing (Schnitzler *et al.*, 2022). Thus, it could be neglected as a first approximation. The first primary BrC component to be considered is inert and insoluble and does not lose its absorbing properties, corresponding to 6–10% of BrC emissions (Forrister *et al.*, 2015; Skyllakou *et al.*, 2024). The second primary BrC component is soluble and loses its absorbing properties by photobleaching and is transformed to pbBrC. **For this reaction, a rate constant $k = 3.4 \times 10^{-5}$ s^{-1} (Wong *et al.*, 2019) or alternatively a rate depending on OH radical concentration (Wang *et al.*, 2018) should be used. All BrC species to be considered are in the accumulation mode and are subject to atmospheric deposition.** However, ongoing and future research is expected to clarify the key environmental factors that influence BrC photobleaching (Schnitzler *et al.*, 2022) and regional patterns (Carter *et al.*, 2021). These recommendations naturally require the OA scheme to be coupled to an atmospheric oxidation chemistry module.

For primary BrC, the imaginary part of the refractive index of BrC ($k_{BrC,\lambda}$) is derived from the Mass Absorption Efficiency (MAE) and depends on wavelength. A value of 0.045 (MAE of 1 m^2 g^{-1}) is used for primary BrC at 550 nm and an Absorption Angstrom Exponent (AAE) of 5 for wavelength $\lambda < 2$ µm in the equations by (Zhang *et al.*, 2020). Importantly, a particle density ρ of 1.3 g cm^{-3} is used for all BrC tracers in these recommendations. For the photobleached BrC at 550 nm, a MAE of 0.19 m^2g^{-1}, a k_{pbBrC} of 10^{-3} and an AAE of 5 can be used within the range provided by (Saleh, 2020). Primary BrC sources to be considered result from biomass burning and biofuel combustion and can be calculated (as mass equivalent to absorption) in two ways: either using the BC/OA emission ratio (see Zhang *et al.*, 2020), or as associated to the ELVOC species in the model (Skyllakou *et al.*, 2024; Tasoglou *et al.*, 2020). The second approach is found to lead to about 10 times lower BrC emissions from biomass burning over Europe (Skyllakou *et al.*, 2024), pointing to the need to further improve the emissions of BrC from its various sources through targeted field and laboratory studies.

The OA effective absorptivity at 550 nm ($A_{OA,550}$) and the equivalent mass emissions of BrC have been parameterised by Zhang *et al.* (2020) as a function of the BC to OA emission ratio by (Saleh *et al.*, 2014) based on multiple laboratory experiments on fresh and aged BrC emissions, and using source-specific emission rates

of OA, BC and BrC (E_{OA}, E_{BC}, E_{BrC}, respectively) in g m^{-2} s^{-1}. Figure 7a shows the global AAOD at 440 nm of BrC in TM5 (the atmospheric chemistry and aerosol model component of EC-Earth3-AerChem). As the aerosols are internally mixed in the model, BrC AAOD for Figure 7a was extracted by running two separate simulations; one without BrC and with OA being only scattering (imaginary part of the refractive index being zero), and the other as described above. The difference between these two simulations in the total AAOD was then taken to obtain the AAOD for BrC. It is clear that AAOD maxima appear in central Africa, India and Eastern China, and high values over the Amazon, which are areas affected by biomass burning events.

In Figure 7b, the difference in BrC AAOD at 440 nm is shown between a simulation in which all OA are considered slightly absorbing (referred to as FORCeS) and a simulation that accounts for both only scaterring OA, i.e. the imaginary part of the refractive index is set to zero, and only absorbing BrC, i.e. the real part of refractive index is set to one. This simulation is referred as BrC in Figure 7b. The latter—i.e. the BrC simulation—shows higher AAOD over biomass-burning affected areas, and slightly lower AAOD at remote areas where in the FORCeS simulation OA was slightly absorbing. **These results demonstrate the importance of individual consideration of BrC absorption in climate models.**

An evaluation of BrC absorption, simulated by the MONARCH atmospheric chemistry model adopting the parametrisation described above, showed reasonably good correlations with aethalometer observations across Europe (Navarro-Barboza *et al.*, 2025). However, despite accounting for primary biomass burning and biofuel sources, the simulated BrC absorption was still notably underestimated at the sites analysed. These underestimations could be attributed to unaccounted or underrepresented sources, highlighting the need for further studies to derive refined anthropogenic BrC emission inventories (Xiong *et al.*, 2022).

3.4 RECOMMENDATIONS FOR NEW PARTICLE FORMATION AND ULTRAFINE AEROSOL

Numerous global and regional scale modelling studies have demonstrated that the formation of new secondary aerosol particles through NPF is a key process modifying the aerosol PNSD and CCN concentrations, and hence should be accounted for in some way within any ESM that aims to investigate ACI (Dunne *et al.*, 2016; Stolzenburg *et al.*, 2023; Zhao *et al.*, 2024). **The representation of NPF within ESMs can, on the one hand, rely on (essentially semi-empirical) parametrisations of field observations, or on the other hand on laboratory observations of NPF involving known chemical systems, or some kind of combination thereof.** Balancing the need to reproduce present particle number concentrations with a reasonable accuracy with the need for mechanistic parameterisations with maximal predicting power in different environments and conditions requires following both of these development tracks in parallel. Besides the chemical systems considered for NPF within models, the size range into which new particles are added also varies, depending on the PNSD description and NPF schemes used within the model. Again, extending the PNSD description to the sizes that allow for a more mechanistic description of NPF instead of saving computation resources for more important processes is a delicate balancing act. However, recent studies demonstrate the ability of Aitken mode particles with diameters well below 50 nm to contribute to CCN concentrations (e.g. Bulatovic *et al.*, 2021; Karlsson *et al.*, 2021), particularly in clean environments (see also Sect. 3.5). To capture ACI, a PNSD representation is of importance, including the key processes modifying the Aitken mode (including the contribution of NPF to particle number within it). **For the applicability**

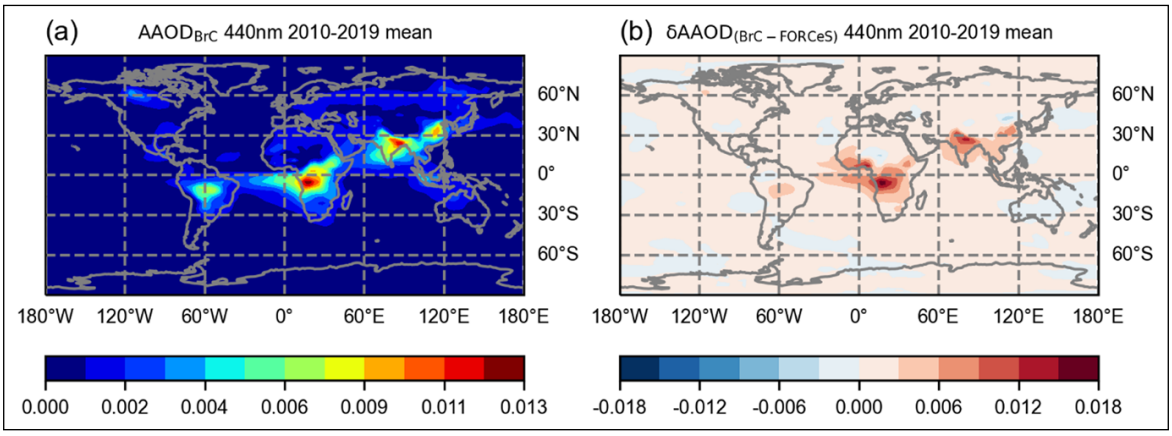

Figure 7 Absorption Aerosol Optical Depth (AAOD) for BrC at 440 nm is presented in **(a)**. AAOD for BrC is calculated by the difference between two ten-year simulations, one accounting for BrC and the second one neglecting its absorption. In **(b)**, the difference in AAOD at 440 nm between a simulation in which all OA is considered slightly absorbing (referred to as FORCeS) and a simulation where OA are only considered scattering and BrC only absorbing (referred to as BrC). Both subfigures display averages over ten-year periods (2010–2019).

of recommendations related to NPF, it is therefore important to ensure that Aitken mode dynamics are also represented within ESMs, Blichner *et al.* (2021) implemented a sectional scheme for the smallest particles (5–39.6 nm diameter) in NorESM2. This improved the concentrations of the smaller particles (50 nm < d_p < 100 nm) compared with observations. In addition, this led to an increased concentration of cloud droplets in remote regions, implying that an inadequate representation of the smallest aerosols can indeed have considerable impacts on the predicted aerosol-cloud interactions.

Within FORCeS, we have investigated the observed atmospheric formation rates (J) of particles in different environments (Figure 8a): boreal forests (the SMEAR I and II stations in Hyytiälä and Värriö in Finland), urban areas (Beijing, China and Budapest, Hungary) and rural sites (Agia Marina Xyliatou in Cyprus and Maracapuru in Brazil). Using data from such different environments hopefully allows the creation of parametrisations that are simple yet applicable in various environments globally (Li *et al.*, 2025). Based on these observations, the formation rate of 5–9 nm particles (J_5) was parametrised by using RH, observed sulfuric acid concentration (H_2SO_4) and condensation sink (CS) as input variables – these are also then needed for the applicability of the parameterisation. The obtained equation can be expressed as

$$J_5 = k_0[H_2SO_4]^{k_{SA}} RH^{k_{RH}} CS^{k_{CS}}, \quad (1)$$

where $k_0 = 1490.02$, $k_{SA} = 0.23$, $k_{RH} = -2.53$ and $k_{CS} = 0.67$ are the experimentally derived coefficients (Li *et al.*, 2025). It is known that various oxidation products of VOCs, highly oxygenated molecules (HOM), also participate in the first steps of new particle formation and growth (see Sect. 3.1). Despite the insufficient long-term VOC data, sulfuric acid is assumed to be the main vapour for the purpose of this parametrisation due to its global abundance. The developed parametrisation for J_5 has been preliminary evaluated with the TM5 module (employed, for example, in EC-Earth3-AerChem). The results (Figure 8b, blue line) show that the underestimation of Aitken mode aerosols is fixed with the new parametrisation compared to the simulation without nucleation (orange line). **This parametrisation, presented in Eq. (1), can therefore be recommended if a field-based semi-empirical approach is desired.**

A complementary approach to using field observations for parametrising NPF is to use well-controlled laboratory observations of known chemical systems, and to sum up these NPF parametrisations within a potential ESM application (see e.g. Dunne et al., 2016; Zhao *et al.*, 2024 for examples). The CLOUD chamber (Sect. S4.1) is one of the most important laboratory facilities used at present to investigate NPF, and the chemical systems studied by CLOUD up to the end of 2022 have been summarised in a recent review by Kirkby *et al.* (2023). These systems include those involving sulfuric, nitric and iodic acids, water, ammonia, various amines, as well as some biogenic and anthropogenic organic species. In general, the NPF studies from CLOUD report particle formation rates (J) at the low-end of the particle number size distribution measurements, usually

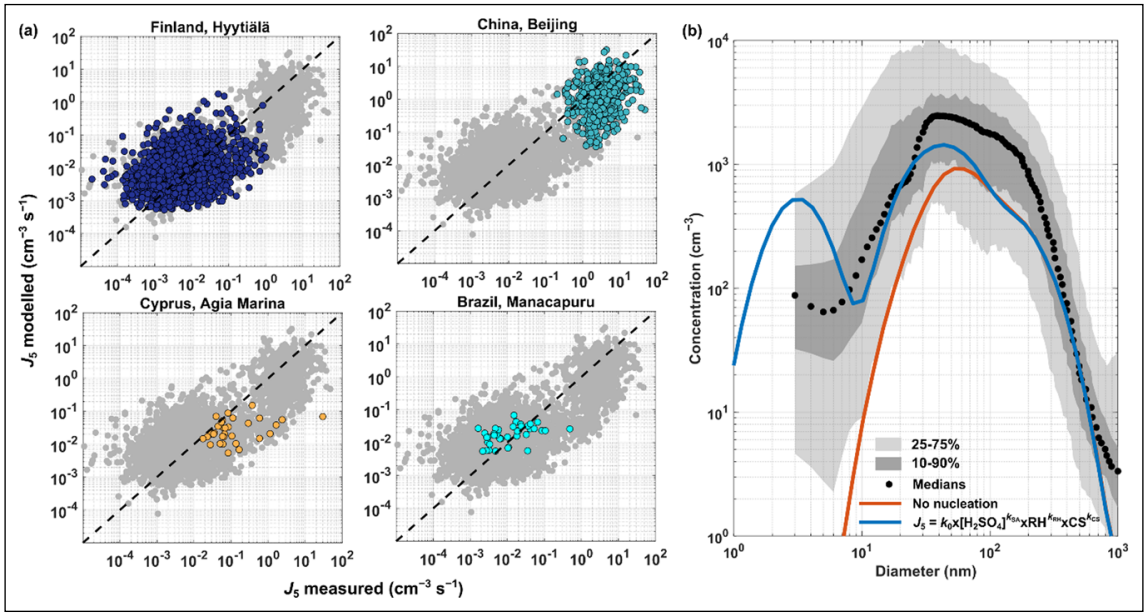

Figure 8 Preliminary J_5 parametrisation testing results on several environment types involving boreal forests, giga-city, rural and rural/rain forest zone is shown in **(a)**. Coloured points refer to the measurements at the specific sites and grey points show all measured data as presented in Li *et al.* (2025). The dashed lines are 1:1 line for the comparison between the measured and the modelled J5 values. In **(b)**, TM5 simulation results for particle number concentration using Eq. (1) are shown as 2018 December medians (black dots and their shades) from pristine boreal forest, arctic remote boreal forest, urban, and rural regions as tests. "No nucleation" refers to no applied nucleation mechanism in TM5 simulation, and Eq. (1) showed promising prediction power, especially for particles at CCN size.

around 2 nm, as a function of the concentrations of the relevant nucleating vapours—most importantly sulfuric acid, the least volatile oxidation products on the organic precursors, or iodic acid. **In many of the studies reviewed within Kirkby *et al.* (2023) these laboratory observations have then been cast into simplified parametrisations (Dunne *et al.*, 2016; Gordon *et al.*, 2016; Lehtipalo *et al.*, 2018), that can be utilised within larger-scale models, including ESMs (see also Zhao *et al.*, 2024).** A complementary, less empirical, method with great potential in reproducing observed NPF and its impacts of ambient PNSD uses look-up tables or other simplifications of predictions from kinetic cluster models (McGrath *et al.*, 2012) with the cluster energetics constrained by laboratory observations (e.g. Roldin *et al.*, 2019) instead of essentially semi-empirical fits. Additional work conducted in the SAPHIR* chamber (Sect. S4.2) has shown, for example, that shifting chemical regimes from RO_2 dominated to HO_2 and NO dominated has a clear effect on HOM product distribution, thus also having impact on the SOA yields (Baker *et al.*, 2024).

The issues that remain to be specified in any respective ESM application are therefore 1) which gas phase species to involve in the NPF parametrisation (based on the which tracers are simulated in the model); 2) which size range the particles are (based on the PNSD representation present in the model); and 3) how the condensation growth and coagulation of these new particles are treated (based on both, see e.g. Stolzenburg *et al.* (2023) for a review on nanoparticle growth, including its representation and effects within ESM applications).

Observational and theoretical studies (Bardakov *et al.*, 2024; Brock *et al.*, 1995; Curtius *et al.*, 2024; Kupc *et al.*, 2020; Weigel *et al.*, 2011; Williamson *et al.*, 2019) have shown that besides NPF taking place in the atmospheric boundary layer (BL), some of the CCN might have actually originated from NPF at higher altitudes (i.e. upper troposphere, UT) and are transported downwards within the atmosphere. However, NPF in the UT is limited to whether the necessary precursors can be transported to the UT in the required quantities. Wang *et al.* (2022) for example, demonstrated the possibility of intense synergistic nucleation of HNO_3, H_2SO_4 and NH_3 (available in necessary amounts) in the UT. Nucleation of organic species in the UT is also an important mechanism contributing to aerosol abundances in the UT. Of all organic species, especially isoprene and monoterpenes are the most important reactive organic species emitted by plants in the tropics. In addition to contributing to the growth of newly formed particles, they can also directly contribute to particle formation in combination with other species (see e.g. Ehn *et al.*, 2014; Kirkby *et al.*, 2016; Lehtipalo *et al.*, 2018; Riccobono *et al.*, 2014; Tröstl *et al.*, 2016) or nucleate on its own (e.g. Simon *et al.*, 2020). Palmer *et al.* (2022) linked overnight convective transport of isoprene to large amounts of tropospheric aerosols later in the day. Particle nucleation from isoprene was subsequently confirmed and analysed in detail by (Bardakov *et al.*, 2024; Curtius *et al.*, 2024; Shen *et al.*, 2024). **While the nucleation processes itself can, in principle, be captured with the same particle formation rate parametrisations as NPF within the BL, a proper understanding of aerosol precursor loss and chemical transformation during cycles of deep convection is essential (see also Sect. 3.8.3) to accurately predict aerosol, and further CCN abundances in the UT.** Given the recent knowledge accumulated on the potential role of multiple different chemical systems capable of nucleating new particles in the Earth's atmosphere, the applicability of the laboratory-based parameterisations mentioned above depends on the comprehensiveness of the chemical systems required. Representing all potentially nucleating species explicitly in ESMs is probably not cost-effective given present computational resources and other priorities, hence there is a continued need for reconciling the insights from laboratory studies with field observations, and developing simple yet general schemes for new generations of NPF parameterisations with improved predictive power.

3.5 RECOMMENDATIONS FOR DROPLET ACTIVATION AND DROPLET CONCENTRATION SUSCEPTIBILITY

3.5.1 Cloud droplet activation

On a principal level, the recipe for predicting the activation of aerosol particles to cloud droplets is relatively well established: if the particle number size distribution, chemical composition and ambient water vapour supersaturation is known, the fraction of particles that can grow into cloud droplets can be rather accurately predicted using the Köhler theory (Calderón *et al.*, 2022; Köhler, 1936). In the atmospheric context, the supersaturation is often driven by cooling caused by several small-scale processes such as buoyancy, orographic effects, radiation or atmospheric mixing.

A comprehensive review of the numerous available droplet parameterisations was performed by Ghan *et al.* (2011). They found that the more complex iterative-based schemes, such as the one from Fountoukis and Nenes (2005), performed well when compared against an adiabatic cloud parcel model under a wider range of environmental conditions, and usually performed better when compared to the non-iterative schemes. In the non-interactive schemes, more N_{act} was estimated for higher aerosol concentrations, and lower N_{act} for low aerosol concentrations, compared to the iterative scheme from Fountoukis and Nenes (2005).

The study of Simpson *et al.* (2014) performed an evaluation against a cloud parcel model of the Abdul-Razzak and Ghan (2000) and Fountoukis and Nenes (2005) schemes and its subsequent updates (Barahona *et al.*, 2010; Morales Betancourt and Nenes, 2014) which

include updates to account for the growth of inertially limited particles, and their subsequent contribution to the water vapour sink. They found that all these schemes tended to underestimate the fraction of activated drops compared to the parcel model due to the methods used by the parametrisations to approximate the sink of water vapour. Furthermore, Simpson, Connolly and McFiggans (2014) highlighteded a tendency of the parameterisations to overestimate the fraction of activated aerosol particles for simulations in which the aerosol particle median diameter of a single lognormal mode is large (between 250 and 2000 nm). They attributed this overestimation to the parametrisations having an infinite "effective simulation time" compared to the simulation time prescribed in the parcel model due to the assumption in parametrisations that the parcel rises to the altitude of S_{max}, regardless of whether this is greater than cloud top (Simpson, Connolly and McFiggans, 2014). This characteristic of existing droplet activation schemes requires further study, and should be considered carefully, for example, in future GCM simulations of geoengineering experiments such as marine cloud brightening.

A recent study found the performance of the Abdul-Razzak and Ghan (2000) scheme against a cloud parcel model to be sensitive to the geometric standard deviations (widths) of the lognormal aerosol modes (Ghosh *et al.*, 2025). By adjusting three constant parameters within this scheme they were able to improve the performance of the parametrisation under polluted aerosol conditions. They compared both the original and modified Abdul-Razzak and Ghan (2000) scheme and the population splitting scheme of Morales Betancourt and Nenes (2014) against a cloud parcel model and found that the original Abdul-Razzak and Ghan (2000) scheme tended to underpredict S_{max} for almost all environmental conditions explored. The more complex scheme (Morales Betancourt and Nenes, 2014) was found to be in generally good agreement with the parcel model for all input parameters explored with similar agreement found from the updated Abdul-Razzak and Ghan (2000) scheme.

In summary, considering the importance of constraining GCM ACI forcing estimates which are strongly dependant on the accurate calculation of N_{act} in the present day, and during cleaner aerosol conditions during the pre-industrial period (Carslaw *et al.*, 2013) **it is recommended that GCMs and ESMs embrace the complex iterative based droplet activation parametrisation of Morales Betancourt and Nenes (2014) or the recently updated version (Ghosh *et al.*, 2025) of Abdul-Razzak and Ghan (2000).** It is also recommended that future development and evaluation of these parametrisations be undertaken against an ensemble of detailed cloud parcel models in a consistent way (e.g. Shipway and Hill, 2012), given that the reported performance will depend on differences in the numerical cloud models used to develop the original schemes. Additionally, the warm bias in sea surface temperature over the Southern Oceans simulated by the CMIP6 models has been a persistent issue (see Sect. 1.2). This bias is mainly attributed to the deficiencies in cloud processes, such as the lack of supercooled liquid water clouds resulting in insufficient reflection of SW radiation, exacerbating the warm bias. Recently, updates in the IFS cloud scheme (employed in EC-Earth-AerChem), including employment of the Morales and Nenes activation scheme, have been applied and shown to reduce this bias. For example, the work by Thomas *et al.* (2024) quantified the impact on biases in the cloud radiative effects, and observed reduction of approximately 40–50% over the Southern Oceans.

An important aspect to consider is the relative role of PNSD and OA hygroscopicity in governing ACI in ESMs. While PNSD typically dominates CCN activation by controlling the number of particles that can activate, hygroscopicity and mixing state provide crucial secondary influences, particularly in organic-rich or biomass-burning environments. Eventually, accurate representation of both factors is essential for reliable ACI estimates (Mandariya *et al.*, 2024; Pöhlker *et al.*, 2023; Shen *et al.*, 2025; Xu *et al.*, 2021b). In ESMs, their relative importance depends on the CCN activation parameterisation—simplified schemes could overemphasise PNSD effects, whereas those incorporating size-dependent chemistry or κ-based activation could, in theory, capture the coupled microphysical and chemical controls more realistically.

3.5.2 Susceptibility of cloud droplet number concentration to aerosol perturbations

Examining the relationship between the aerosol particle concentration (for different lower cut-off diameters) and the CDNC from long-term in-situ observations, remote sensing data, and ESMs reveals an important trend. The susceptibility of CDNC to perturbations in aerosol particle concentrations derived from ground-based in-situ observations is considerably higher than the corresponding response inferred from global ocean satellite data (Virtanen *et al.*, 2025). Furthermore, the analysis reveals significant issues in how this process is currently represented within ESMs, calling for further work on this key driver behind ACI predictions. The data show that the typical critical activation diameter at Puijo (located in Kuopio, Finland) is around 125 nm, around 110 nm in Pallas (located in northern Finland), and as small as 40 nm for Zeppelin in the Arctic (Bulatovic *et al.*, 2021; Karlsson *et al.*, 2021). The findings support previous observational studies by Kecorius *et al.* (2019), Koike *et al.* (2019) and Willis *et al.* (2016), which indicate that Aitken mode aerosol particles are important for cloud droplet formation in clean environments. Parcel model calculations suggest activation diameters as small as 30 nm for some arctic conditions (Motos *et al.*, 2023). The

small activation diameters in the Arctic could also be linked to high contribution of marine sulfate to the total aerosol mass, especially during summer (Gramlich *et al.*, 2023; Siegel *et al.*, 2023).

High-resolution modelling (see also Sect. S3) work by FORCeS members also shows that Aitken mode particles significantly affect cloud microphysical and radiative properties in the summertime high Arctic when accumulation mode number concentrations are low (<10–20 cm^3, Bulatovic *et al.*, 2021). The modelling results obtained during FORCeS agree with observations of the Hoppel minimum obtained from multiple expeditions in the high Arctic (Bulatovic *et al.*, 2021 and references therein). **The results show that accumulation mode particles should not be considered as the only potential CCN in models, as this may lead to inaccuracies in CCN concentrations and their sensitivity to perturbations in various emissions.** Even more subtle effects were observed in the Po Valley fogs (see also Sect. 2.2.3), where activation diameters are as large as 300–400 nm (Gilardoni *et al.*, 2014), and aerosol number concentrations are in great excess with respect to the potential CDNC. Based on ongoing research, the actual supersaturation reached during activation and the number of activated droplets is first affected by the dispersion in the accumulation mode size distribution and secondly by the chemical composition. In aerosol-fog interactions in polluted environments, as a typology of an "updraft-limited regime" (Reutter *et al.*, 2009), a realistic representation of the standard deviation of the accumulation-mode size distribution along with an at least synthetic formulation of aerosol hygroscopicity are therefore recommended.

The process-based evaluation of the ESMs by Virtanen *et al.* (2025) reveals that further development work is required on how the driving force for water vapour supersaturation—in practice the parametrisation of the cloud-scale updraft velocity—is represented in the models. The results from the three field sites presented in Virtanen *et al.* (2025) are generally in line with the findings from a review article led by and involving FORCeS partners, which pointed out the general need to improve satellite-based methods to derive aerosol-cloud relationships (Quaas *et al.*, 2020). Combining constraints from satellite data, in-situ observations and high-resolution modelling show promise in providing further insights into cloud droplet activation processes. Taken together, the analysis conducted within FORCeS shows that, despite the fact that the fundamental microscale thermodynamics of cloud droplet activation are in most cases well understood (see, however, also e.g. Heikkinen *et al.*, 2024; Lowe *et al.*, 2019), the inputs (particularly PNSD and cloud-scale updraft velocity) required for the common parametrisations are not yet well enough constrained within current ESMs to provide an entirely consistent and robust representation of susceptibility and hence ACI (Virtanen *et al.*, 2025). **Furthermore, care must be taken when inferring the susceptibility of clouds to aerosol perturbations from remote sensing observations, as the potential link between aerosol products derived from remote sensing data and CCN concentration is not always straightforward** (see also e.g. Jia *et al.*, 2022; Manshausen *et al.*, 2022), and the observations at the cloud top do not necessarily represent the condition at the cloud base where activation takes place. It is also important to note that perturbation of the local background aerosol conditions has different impacts in different environments (Kommula *et al.*, 2024).

Additional work using the above mentioned LES modelling to develop ESM parametrisations was also conducted within FORCeS. ESMs and other large-scale models rely mainly on parameterising the subgrid component of the updraft velocity based on turbulent kinetic energy. In FORCeS, we have used an ensemble of marine stratocumulus clouds simulated with a large eddy model to develop a parametrisation that can be used to estimate the updrafts driven by radiative cooling (Ahola *et al.*, 2022). The use of the new parametrisation in ECHAM shows that the method is a promising candidate and should be extended to cover other cloud types (Nordling *et al.*, 2024). However, the work conducted within FORCeS also points out that the time step limitations on LES modelling can lead to overestimation of the susceptibility at very high aerosol concentrations or low updraughts in warm stratocumulus clouds (Schwarz *et al.*, 2024).

3.6 RECOMMENDATIONS RELATED TO CLOUD MICROPHYSICAL PROCESSES BEYOND ACTIVATION

As mentioned in Sect. 1.6, most current ESMs form precipitation through some form of autoconversion parametrisation (see e.g. Khairoutdinov and Kogan, 2000; Sundqvist, 1978). **The work conducted within FORCeS (Prank *et al.*, 2022, 2025) supports previous studies (Jensen and Lee, 2008; Jensen and Nugent, 2017) on the importance of considering coarse mode aerosol particles and giant CCN in the representation of autoconversion for capturing this process correctly.** This update will most likely act to substantially modulate the timing of the drizzle onset in shallow cumulus clouds. The stratiform cloud cases are expected to show similar or possibly even stronger signal, which has substantial repercussions for the description of marine clouds in global models. For example, current methods are very likely to produce a delayed onset of drizzle in subtropical stratocumulus outflow regions near the coasts (see e.g., Magaritz-Ronen, Pinsky and Khain, 2016), where droplet concentrations are typically too high for drizzle initiation when autoconversion schemes neglect the presence of giant sea-salt particles. In these clouds, drizzle and precipitation formation can lead to reorganisation of the mesoscale cloud structure, transforming the cloud deck

from a closed to an open cellular structure and causing dramatic changes in the overall albedo (e.g., Stevens *et al.*, 2005). Accounting these particles is therefore critical for describing the aerosol-cloud interactions and the aerosol indirect effect. As contemporary climate models usually carry at least some information about the aerosol size distribution, it is therefore recommended that coarse mode aerosol is accounted for in the autoconversion parametrisation. Before the onset of autoconversion, the large end of the droplet size distribution is affected by sedimentation fluxes (as evident also in fogs, see e.g. Boutle *et al.*, 2022). Additionally, given the high subgrid-scale variability of the processes and variables relevant for cloud microphysics, further work in the development of the ESM resolution is warranted.

Fogs can be considered as special cases of clouds that are in contact with the Earth surface. However, compared to other clouds, the growth in liquid water content is strongly controlled by the sedimentation of cloud droplets. As sedimentation becomes efficient already for droplets that are smaller than those typically formed from the autoconversion process, and thus the employment of autoconversion can lead to too efficient water removal. This is demonstrated in Figure 9, which visualises the evolution of radiation fog simulated with UCLALES-SALSA (Sect. S3.1): the droplets do not have time to grow to drizzling sizes (d_p~100 µm, Figure 9c) before they are removed due to sedimentation. This is the case especially if the fog does not reach altitudes higher than 100 m, after which both droplet concentration (Figure 9a) and liquid water content (Figure 9b) reach high values due to the change in fog dynamics (Boutle *et al.*, 2018). **Our recommendation is to not use the autoconversion process at all when simulating fog, especially if the fog droplet formation is based on physically valid parametrisations that account for radiative cooling at the top of and activation processes within the fog.** This recommendation is, however, most relevant for high-resolution models, as present ESMs do not generally have high enough resolution to explicitly simulate fog, although low-level clouds are common. Also, the assumption of the droplet size distribution shape in bulk models is affecting the water removal and thus liquid water content strongly (Boutle *et al.*, 2022), and it is recommended that the bulk schemes should be evaluated against observation such as those performed during the FAIRARI campaign.

To include the effect of entrainment (see Sect. 1.6) there are two necessary ingredients: 1) Turbulence at cloud top needs to be a function of cloud-top radiative and evaporative cooling; and 2) cloud droplet sedimentation has to be a function of cloud droplet number/size, and has to be accounted for in the first place. Point (1) is to some extent fulfilled in all turbulence parametrisations directly or indirectly (via cooling rates). It is, however, not clear whether the effect is realistic enough. One of the potential problems is the lack of inversion strength and sharpness, due to the coarse vertical resolution (e.g. Pelucchi, Neubauer and Lohmann, 2021). The other problem is that not only turbulence, but also numerical diffusion leads to mixing and entrainment. It is only the former that is responsive to the aerosol-induced

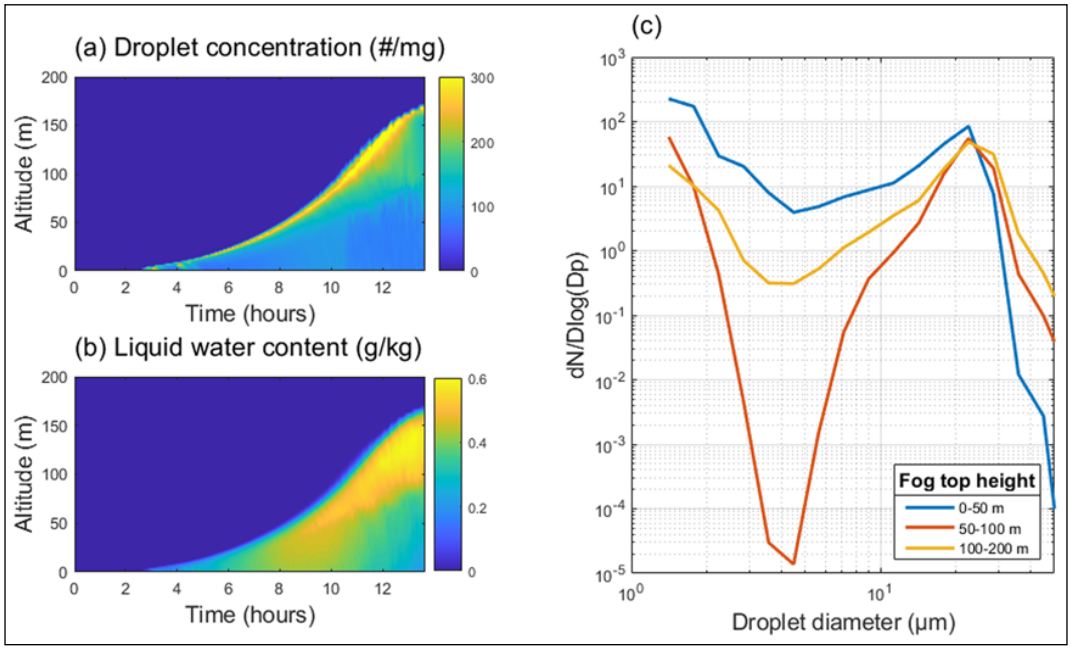

Figure 9 Example of the evolution of radiation fog. **(a)** droplet number concentration, **(b)** liquid water content, and **(c)** average fog droplet size distribution for the lowest 15 m during three different fog periods according to the fog top height. Simulations are conducted with UCLALES-SALSA (Sect. S3.1) in 2D setup employing the mean aerosol size distribution from the FAIRARI campaign (Sect. 2.2.3) and assuming constant aerosol hygroscopicity of 0.6. Vertical and horizontal resolution in the simulations were 1.5 m and 4 m. Atmospheric background sounding for initial conditions is typical for the nighttime radiation fogs observed in the area.

perturbation; the latter should be as small and irrelevant as possible. Point (2) is accounted for in several cloud microphysical schemes, but in many others it is not. The ones that consider cloud droplet sedimentation include the schemes by Morrison and Gettelman (2008) (see also Gettelman and Morrison, 2015; Seifert and Beheng, 2006).

The effect of mixing and evaporation on the impact of enhanced CDNC on cloud liquid water path and cloud fraction should be examined using observations. This should involve a statistical analysis as well as an analysis of the response of clouds to external perturbations. If ESMs simulate a reduction in LWP due to enhanced entrainment that is not large enough compared to observations, or if it is even overwhelmed by a positive LWP response, the first aim would be to reduce the impact of drizzle formation rather than attempting to directly increase the effect of entrainment. **The results from FORCeS suggest that great care should be taken when inferring LWP responses to aerosol from remote sensing data.** Arola *et al.* (2022) showed that the propagation of natural spatial variability and errors in satellite retrievals of cloud optical depth and cloud effective radius strongly impact estimates of aerosol indirect effects. They used satellite and synthetic measurements to demonstrate that, because of this propagation, even a positive LWP adjustment to an aerosol increase is likely to be misinterpreted as negative. This biasing effect would likely result in an underestimate of the aerosol-cloud-climate cooling. Similarly, Zipfel *et al.* (2022, 2024) showed that the relationship is modulated by precipitation fraction and sea-surface temperature, and that the sensitivity of LWP to CDNC is weaker at higher CDNC, based on a machine-learning approach. These conclusions were supported by a study from Kokkola *et al.* (2025) in which model outputs from UCLALES-SALSA (Sect. S3.1) for stratiform clouds were analysed using satellite retrieval equations. Similarly to the Arola *et al.* (2022) analysis, satellite retrieval equations biased the correlation between CDNC and LWP negative at higher CDNC values. However, this study indicated that, **by carefully selecting cloud cases with similar meteorological conditions, and ensuring that cloud condensation nuclei concentrations are well-defined, changes in liquid water can be reliably determined using satellite data.** Such data would also be useful for evaluating the description of LWP response to aerosol in ESMs.

Christensen *et al.* (2022) reviewed available satellite datasets and field campaigns to find opportunistic experiments of aerosol influence on cloud microphysics. Based on the satellite data analysis, they found that cloud albedo perturbations were strongly sensitive to background meteorological conditions and that LWP increases due to aerosol perturbations could generally not be distinguished from the data (in line with Arola *et al.*, 2022). While they found these opportunistic experiments to give significantly improved process-level understanding of ACI, they also concluded that it remains unclear if the relationships found can be reliably scaled to the global level. Manshausen *et al.* (2022), on the other hand, took a closer look at ship tracks, leveraging from the fact that only a small fraction of the clouds polluted by shipping show ship tracks in satellite images. They showed aerosols emissions led to substantial changes in cloud properties even when no ship tracks were visible in satellite images. The study by Manshausen *et al.* (2022) indicated selection biases in previous studies of ship tracks, and found a strong LWP response to clouds to aerosols perturbations, which in turn potentially indicates a higher climate sensitivity than observed temperature trends would otherwise suggest (see also Watson-Parris *et al.*, 2022, which discusses the importance of shipping regulations for climate). Machine learning approaches were also exploited within FORCeS in the investigation of cloud microphysical properties. Bender *et al.* (2024) found, for example, that the cloud droplet effective radius can be successfully estimated by gradient boosting regression using only meteorological data as input, and limited improvement in model skill with inclusion of aerosol information. The work highlights the importance of local meteorology on controlling cloud properties. Similarly, Jia *et al.* (2024) used explainable machine learning to quantify cloud-fraction adjustments to aerosol in the context of meteorological conditions. Proske *et al.* (2024) tested a drastically simplified approach and replaced the aerosol model in ECHAM-HAM with a CCN and INP climatology, as input for either of the two available aerosol activation schemes (Abdul-Razzak *et al.*, 1998; Abdul-Razzak and Ghan, 2000 or Lin and Leaitch, 1997). The simplification reduced the computational time up to ~65%, while deviations in results from the simplified model stayed mostly close to inter-annual variability of the full model version. Depending on the purpose of a modeling project, a simplified model version may indeed be more apt than a complex one. **In particular, the work from Proske *et al.* (2024) highlights the role of simplification for understanding: it generates an easier-to-understand model version, but also creates understanding through the simplification work itself.**

An important aspect of model evaluation is to **determine the extent to which the model is simultaneously consistent with multiple observation types. A model that is skilful at simulating one aerosol or cloud property (e.g., droplet number concentration) but inconsistent with another (e.g. aerosol optical depth) or vice versa** is not a realistic model. In normal global model development in which adjustments to parameter values are usually made one at a time, such "cross-variable consistency" is difficult to establish because not all potential combinations of parameter values are explored (i.e. retuning could

eliminate cross-variable inconsistency). In FORCeS, a new approach was developed that exploited a perturbed parameter ensemble to detect such cross-variable inconsistency by examining model-observation skill across 37-dimensional space of uncertain parameter combinations in UKESM1 (Regayre *et al.*, 2023). In this study, one million model 'variants' were created using emulators trained on UKESM1 (Sect. S1.1) simulations and were then evaluated against observations of several cloud properties in several ocean regions and months of the year (in total 450 observational constraint variables). The study then constrained to each of these observation variables separately and quantified the effect on the model-observation agreement with the other variables. This approach exposed a very large number of pair-wise inconsistencies that indicate potential structural deficiencies in UKESM1 – i.e. achieving model consistency with two variables simultaneously would require changes to the model structure (the process parameterisations) rather than just changes to parameter values in the existing parameterisations. In particular, the study found that droplet number concentration and liquid water path of shallow clouds were inconsistent, which the authors associated with the limitations of a single-moment cloud microphysics scheme in UKESM1. **A key result for FORCeS is that the reduction in uncertainty in aerosol ERF is likely to be hindered by such model internal inconsistencies, which should become a priority for model development efforts.** The results also point to the importance of using rigorous model evaluation procedures and multiple observation types to avoid overfitting models to very limited sets of observations (for example in emergent constraint studies) and reaching incorrect conclusions about the uncertainty in aerosol forcing.

3.7 ICE FORMATION AND MULTIPLICATION

3.7.1 Primary ice nucleation from dust and other sources

During FORCeS, the contributions from K-feldspar and quartz dust minerals together with marine and terrestrial bioaerosols for ice nucleation were investigated. In the work conducted by (Chatziparaschos *et al.*, 2023), the global 3D chemistry climate model TM4-ECPL (Sect. S1.4 and references therein) was extended by including prediction of INPs with parametrisations representing the ice-active surface site immersion freezing process based on laboratory-derived active site parametrisations provided in Harrison *et al.* (2019). Simulations using the model indicate that INPs originating from quartz dominate at lower altitudes which are characterised by higher dust concentrations, but relatively low INP concentrations (Figure 10b). They also show that in some regions, such as high and middle latitudes in Asia, quartz can contribute to over 60% of the total INP concentration. The INP concentrations derived from the TM4-ECPL model with the added dust components were evaluated against the BACCHUS database (http://www.bacchus-env.eu/in/index.php, last access 31.03.2025) and data from Wex *et al.* (2019). The results showed agreement within 1.5 orders of magnitude. Further analysis showed that the annual means in the surface concentrations of dust are often underestimated in the model over regions in Europe and Southern Ocean. This could potentially explain part of the bias that is often seen between observed and modelled concentrations of INPs (Figure 10e).

In Chatziparaschos *et al.* (2025) TM4-ECPL was further developed to investigate the importance of marine primary organic aerosol (MPOA), and terrestrial primary biological aerosol particles (PBAP) for ice nucleation in MPCs based on the parametrisations of Wilson *et al.* (2015) and Tobo *et al.* (2013), respectively. INP originating from PBAP were estimated to be the primary source of INP at low altitudes between –10°C and –20°C (Figure 10d), while INP from marine bioaerosol dominate in the Southern Hemisphere (SH), particularly at low altitudes at subpolar and polar latitudes, having maximums at temperatures around –16°C (Figure 10d). When compared with available global observational INP data, the model demonstrates its highest predictive power across all temperature ranges when both dust and MPOA are included (Figure 10f). The inclusion of PBAP slightly decreases the model performance (Figure 10g) by overestimating INP concentrations. However, it should be noted that PBAP could be a key contributor to ice nucleation events (Figure 10d) at warmer temperatures despite the large uncertainties in its parameterisations (Chatziparaschos *et al.*, 2025).

The INP schemes for quartz, K-feldspar (Harrison *et al.*, 2019) and MPOA (Wilson *et al.*, 2015) were then implemented in the EC-Earth3-AerChem model in combination with a secondary ice production parametrisation (Sect. 3.7.2, Georgakaki and Nenes, 2024), replacing the deposition-condensation-freezing temperature-based parametrisation by Meyers *et al.* (1992). Simulations demonstrate improved agreement with INP observations when using a parametrisation that accounts for the sensitivity of heterogeneous ice nucleation to mineral dust (K-feldspar and quartz) and marine organic aerosols, as opposed to the traditional temperature-dependent approach. **To summarise: Our findings support the inclusion of aerosol aware INP parametrisations into ESMs, in particular for dust (K-feldspar and quartz), but also potentially for PBAPs and MPOA (Chatziparaschos *et al.*, 2023, 2025), however their sources remains highly uncertain.** The applicability of this recommendation naturally depends on the description of dust and primary particle sources within a given ESM.

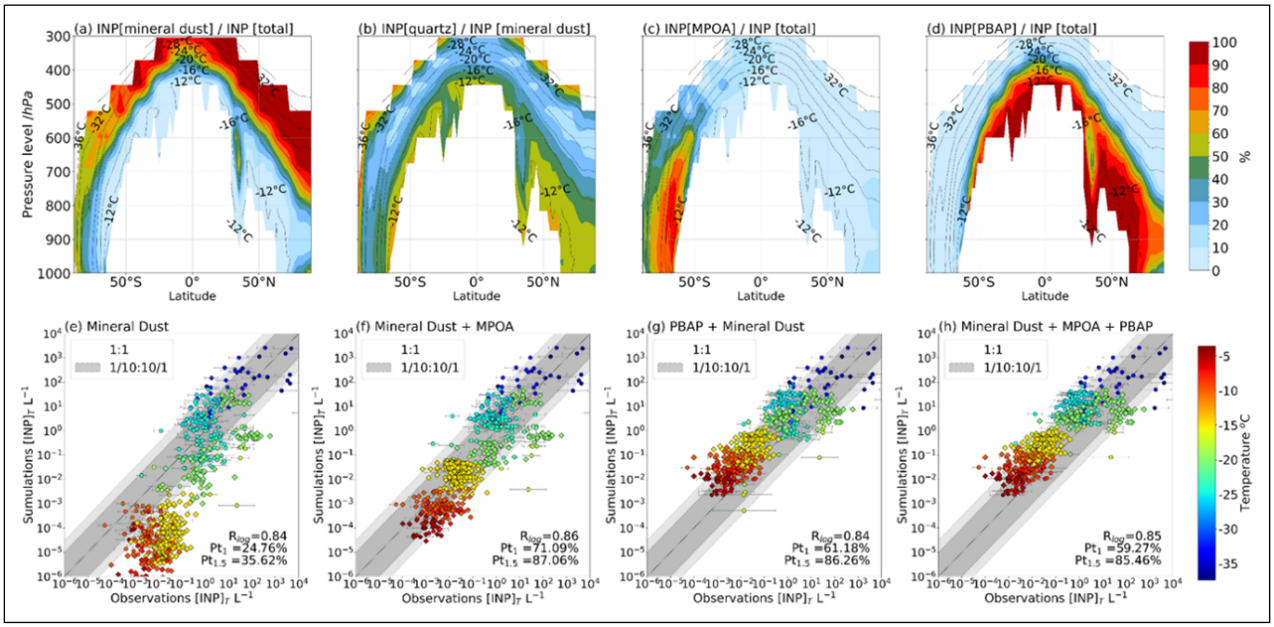

Figure 10 Top row: percentage contribution of each species to the total INP concentration **(a–d)**, calculated using multi-year averaged zonal mean profiles of INP number concentration at modelled ambient temperatures. Panels show the contribution of: (a) quartz and feldspar, (b) the relative contribution of INP from quartz within the quartz and feldspar, (c) marine bioaerosols and (d) fungal spores and bacteria. The black contour dashed lines show the annual mean temperature of the model. Bottom row: Comparison of INP concentrations calculated at the temperature of the measurements against observations accounting for mineral dust **(e)**, mineral dust and MPOA **(f)**, mineral dust and PBAP **(g)** and all these combined (g). The dark grey dashed lines represent one order of magnitude difference between modelled and observed concentrations, and the light-grey dashed lines depict 1.5 orders of magnitude. The simulated values correspond to monthly mean concentrations, and the error bars correspond to the error of the observed monthly mean INP values. The colour bar shows the corresponding instrument temperature of the measurement in Celsius. Pt1 and Pt1.5 are the percentages of data points reproduced by the model within an order of magnitude and 1.5 orders of magnitude, respectively. Correlation coefficient is denoted with R, which is calculated with the logarithm of the values. Figure adapted from Chatziparaschos *et al.* (2025) under the Creative Commons 4.0 (CC 4.0) license.

3.7.2 Secondary ice production processes

Observations of significant numbers of ICNCs that significantly surpass the concentration of INPs in warm MPCs (at around –25°C and above) most likely indicate the presence of SIP. **It is therefore recommended that key SIP processes are included in regional and global climate model simulations.** However, how much the addition or refinement of a single process can improve model results depends on the model's structure and other included processes. **For example, the studies by Proske *et al.* (2022, 2023) identified SIP as one potential candidate for simplification (among others),** at least within the context of the current representation of ice formation processes in ECHAM-HAM (See Sect. 2.1.3 and Table S7). That is because other processes dwarf SIP's influence on key global cloud variables in this specific model. Ongoing work utilising all three FORCeS models (Ickes *et al.*, 2025) highlights the intricate interconnections between all relevant cloud microphysical processes: the impact of modifying a specific process within one model may vary significantly from its effect in another model with a different microphysics scheme. Further research and exploration of this topic and the level of detailed required in various applications is therefore warranted.

Initial comparisons within FORCeS between observed ice-phase cloud properties during the NASCENT campaign (Sect. 2.2.1), obtained using a holographic imager mounted on the tethered balloon system (Pasquier *et al.*, 2022a), and simulations from the Weather Research and Forecasting (WRF, Sect. S2.3) model (Skamarock *et al.*, 2021) revealed that the model's representation of these properties is inadequate without fine-tuning the cloud microphysics scheme (Schäfer *et al.*, 2024). Indeed, measurements taken in Ny-Ålesund highlighted the importance of SIP in the form of drizzle shattering in Arctic MPCs (Pasquier *et al.*, 2022a), and also pointed out the complexity of the shape of the ice crystals affecting their radiative properties (Pasquier *et al.*, 2023). Focusing on a single cloud event, Schäfer *et al.* (2024) performed WRF simulations with two different microphysics schemes (Milbrandt and Yau, 2005; Morrison, Thompson and Tatarskii, 2009), constrained by observed CCN and INP concentrations. Their simulations underscored the necessity of accurately representing both primary and secondary ice formation processes in the model. The best alignment with observed hydrometeor profiles and precipitation was achieved after enhancing the efficiency of the Hallett-Mossop (HM; rime-splintering) process and incorporating descriptions of collisional fracturing and breakup (BR) as well as droplet freezing and

shattering (DS). These modifications were implemented in the Morrison microphysics scheme, following the methodologies of Sotiropoulou *et al.* (2021) and Georgakaki *et al.* (2022), respectively.

Similar results were obtained by Han, Hoose and Dürlich's (2024) simulations for convective clouds with the ICON model (Sect S1.2) with parameterisations for BR and DS included. Recognising the critical role of SIP in polar MPCs and the need for their accurate representation in large-scale models led to the development of the Random Forest SIP parametrisation (Georgakaki and Nenes, 2024). RaFSIP is a data-driven parametrisation created using machine learning techniques, leveraging comprehensive mesoscale WRF simulations with advanced SIP descriptions. This work is presented in detail in Georgakaki and Nenes (2024) and thus a short overview is given here.

The development of RaFSIP was based on a training dataset derived from two years of regional climate simulations using the WRF model, focusing on polar stratiform clouds across the pan-Arctic region from 2016 to 2017. Two nested domains were employed (Figure 11), and cloud microphysics were parameterised using an updated version of the Morrison, Thompson and Tatarskii, (2009) scheme including the three most significant SIP processes: HM, BR and DS (Georgakaki, Sotiropoulou and Nenes, 2024). Two variations of the RaFSIP scheme were developed: RaFSIPv1, which indirectly expresses the effect of SIP through the so-called Ice Enhancement Factor, and RaFSIPv2, which directly predicts SIP rates (see Georgakaki and Nenes, (2024), for details). These both consider SIP in temperatures as low as –25°C, as supported by the recent observational findings (Korolev *et al.*, 2022; Pasquier *et al.*, 2022a; Wieder *et al.*, 2022). As demonstrated in Figure 11, the absolute differences between the ICNCs predicted by the detailed SIP microphysics simulation of WRF (referred to as ALLSIP) and those predicted by the simulation that ran with RaFSIPv2 (referred to as RaFSIP) demonstrated that RaFSIP effectively replicates the mean horizontal distribution of ICNCs, with mean biases below 30 # L^{-1}. These biases in modelled cloud-phase partitioning do not appear to translate into significant radiative biases. The largest radiative biases were observed during the summer (Figure 11d), compared to the slower build-up (Figure 11b) and Arctic Haze periods (Figure 11c), likely due to slight differences in the glaciation fraction of the simulated clouds, which allowed more shortwave radiation to reach the surface.

The design of the RaFSIP scheme allows for straightforward implementation in the dynamical core of any ESM that lacks detailed microphysics, as long as the relevant input features (i.e. temperature and RH with respect to ice) are properly integrated within the stratiform cloud microphysics routine. **Our recommendation is therefore that the RaFSIP v2 scheme, as presented by Georgakaki and Nenes, (2024), should be used for a comprehensive emulation of SIP processes in ESMs.** The RaFSIP approach outlines a way towards model simplification that can maintain the "essence" of complex physics in model versions that require limited complexity. Its design strikes a balance between detailed process representation and computational efficiency, making it a valuable tool for improving the accuracy of SIP in ESMs without the need for highly complex microphysics schemes.

Within FORCeS, RaFSIP has now been successfully incorporated into the microphysics modules of the three participating ESMs: EC-Earth3-AerChem, NorESM2 and ECHAM-HAM (see Table S1 in Sect. S7). Preliminary results from the model intercomparison study (utilising RaFSIPv2), however, show that the addition of a unified SIP parameterisation leads to varied model responses in terms of the simulated supercooled liquid fraction (Ickes *et al.*, 2025). This highlights the complexity of

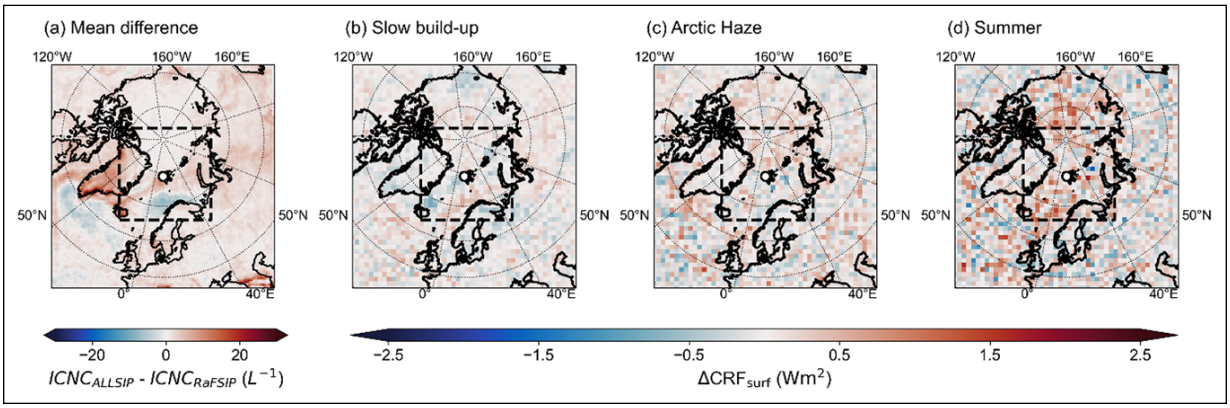

Figure 11 The first panel **(a)** shows the difference between mean ice crystal number concentrations predicted by the detailed microphysics simulation of WRF (ALLSIP) minus the simulation that ran with RaFSIPv2. The mean is derived from the entire year of simulations (September 2019–August 2020), focusing on the cases where: ICNC > 10^{-5} L^{-1} and temperature was between –25°C and 0°C (where ice multiplication was enabled in the WRF model). Panels **(b)** to **(d)** show the radiative biases in the predicted cloud radiative forcing at the surface calculated for the three periods: slow build-up (October–January), Arctic haze (February–May), and summer (June–September). Figure is adapted from Georgakaki and Nenes (2024) under the Creative Commons 4.0 (CC 4.0) license.

microphysical process interactions as mentioned at the beginning of this section, and suggests that robust conclusions about real-world process importance cannot be drawn from individual models alone.

3.8 RECOMMENDATIONS FOR AEROSOL PROCESSING AND SCAVENGING BY CLOUDS

3.8.1 Aerosol number and mass scavenging by clouds and precipitation

Nucleation scavenging is the main loss mechanism affecting sub-micron aerosol particle number size distributions (Isokääntä *et al.*, 2022; Tunved *et al.*, 2013; Wang, Zhang and Moran, 2010; Wang, Xia and Zhang, 2021). This highlights the importance of getting CCN activation right in atmospheric models (see also Sect. 1.5 and 3.5). **A systematic investigation of the implications of activation descriptions for wet scavenging and predicted aerosol size distributions in ESMs is therefore recommended** (see also Sect 3.5). Studies using direct and simultaneous observations of total PM, cloud water and interstitial aerosol population suggest a less efficient uptake of BC to cloud water as compared with the more soluble components – probably due to effects of external mixing and the distribution of the BC material in the aerosol size distribution (e.g. Ruuskanen *et al.*, 2021). Trajectory-based studies indicate that during cold seasons ($T < 10°C$) SO_4, OA and BC are scavenged by precipitation equally efficiently in air masses arriving at Hyytiälä, Finland (Isokääntä *et al.*, 2022; Talvinen *et al.*, 2025), indicating internal mixing of these aged aerosol components. During the warm season ($T > 10°C$) SO_4 is scavenged less efficiently than OA and BC indicating that SO_4 might be distributed to smaller sizes than OA and BC (Isokääntä *et al.*, 2022).

Similar relationships between precipitation and BC concentration as as well as overall number size distribution were also reported by Tunved *et al.* (2021) for Ny Ålesund in the Arctic. Heslin-Rees *et al.* (2024) followed on the work and showed that about 25% of the long-term trends of absorbing aerosol in the Arctic is explained by changing precipitation patterns. Together with the recent evaluation of a new wet scavenging scheme within ECHAM-SALSA (Holopainen *et al.*, 2020) and the ongoing ESM intercomparison by Cremer *et al.* (2024) with regards to transport of BC to the Arctic, these results highlight the importance of an accurate description of the level of external mixing of soluble and insoluble compounds in modeled emissions and size-dependent composition of the aerosol population for getting the wet removal mechanisms right. Further studies on the size-dependent aerosol composition distribution and mixing state are therefore warranted to allow for the accurate description of aerosol-cloud interactions and wet removal.

A modelling closure between boundary layer dynamics, aerosol, and cloud properties can be achieved in well characterised cases such as those specified for the FORCeS 2020 campaign at the SMEAR IV site in Puijo, Finland (Calderón *et al.*, 2022, see also Sect. 2.2.2). Observation-based sounding profiles were fundamental to achieve closure between large eddy simulations and observations of the cloud structure and the vertical wind velocity probability distribution. Likewise, the initialisation of aerosol properties using observation-based aerosol number concentrations and aerosol composition had a relevant role for obtaining closure of the activation efficiency curves. Moreover, as shown in Figure 12, the cloud droplet size distribution was also reproduced after accounting for the larger, supermicron aerosol particles, which produce drizzle most efficiently. As the effect of cloud processing on aerosol properties is difficult

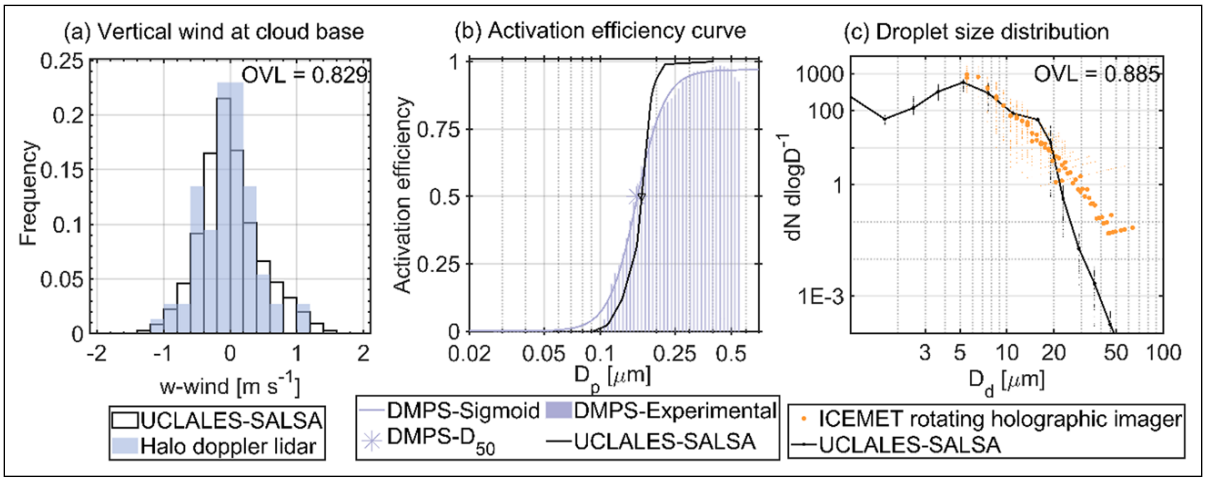

Figure 12 Modelled and observed cloud properties during the 5th hour of the cloud event of 24 September 2020 during the Puijo 2020 campaign. In **(a)**, vertical wind at cloud base compared to Halo Doppler lidar observations is shown. Activation efficiency curve retrieved from Differential Mobility Particle Sizer observations with the twin-inlet system compared to modelled equivalent of total and interstitial aerosol particles is presented in **(b)**. Droplet size distribution compared to observations with the ICEMET rotating holographic imaging system is shown in **(c)**. Values of the overlapping index (OVL) have been added to indicate the degree of agreement between distributions. If two distributions are equivalent the OVL index tends to the unity.

to observationally constrain, the findings support the further employment of models like UCLALES-SALSA (Sect S3.1) for the development of wet scavenging schemes accounting for different chemical compounds in global models. Simultaneous observations of atmospheric thermodynamic profiles (or updrafts) together with high-resolution measurements of aerosol number size distribution and chemical composition are important for obtaining closure for CCN activation and predicting cloud hydrometeor populations in liquid-phase clouds. **Where possible, we therefore recommend the use of LES-type models for developing parametrisations for larger-scale models also, when it comes to wet scavenging.** Given the importance of coarse mode aerosols for cloud microphysics and e.g., autoconversion (see also Sect. 3.6), LES-based closure studies could also help provide constraints on coarse-mode aerosol emissions and concentrations.

3.8.2 Chemical processing and secondary aerosol generation within clouds

Aqueous formation of sulfate is visible in sub-micron aerosol in the boreal forest environment (Figure 13a), thus at least it is qualitatively in line with the mechanisms applied at present within the ESMs. The sulfate mass concentrations observed in Hyytiälä, Finland by Isokääntä *et al.* (2022) increased 44–61% due to in-cloud sulfate formation, and the increase was largest during the cold season and with more polluted air masses (Figure 13a and Isokääntä *et al.*, 2022). The same conclusion (Figure 13b–c) was also obtained for two ESMs also utilised within FORCeS: UKESM1 and ECHAM6.3-HAM2.3-MOZ1.0 with the sectional aerosol module SALSA2.0 (Talvinen *et al.*, 2025). In addition to increased sulfate mass, the mass fraction also increased (Figure 13d–f) implying changes in particle composition. The formed aerosol mass ended up between 200 and 600 nm in the aerosol size distribution, as expected from observations of cloud-processed sub-micron aerosol size distributions (Isokääntä *et al.*, 2022). Aqueous-phase formation of sulfate has been implemented in ESMs since the 1990s. **Based on previous work (e.g. Roelofs *et al.*, 2006) and the work conducted within FORCeS, we recommend that the sulfate formed in the aqueous-phase should be distributed over the Aitken, accumulation and coarse modes.** No signs of significant aqueous SOA formation, on the other hand, were observed in this boreal environment a) during the warmer season ($T > 10$°C) over areas with monoterpenes (MTs) dominating the biogenic volatile organic compound (VOC) emissions and total VOC; or b) during the colder season ($T < 10$°C) when anthropogenic emissions dominate over biogenic emissions (Isokääntä *et al.*, 2022). Similar observations have also been made by Graham *et al.* (2020) for Swedish boreal forest environments. **Based on studies within the boreal zone and the Arctic, no traces of significant aqueous SOA production have been observed and can therefore probably be neglected within these environments in**

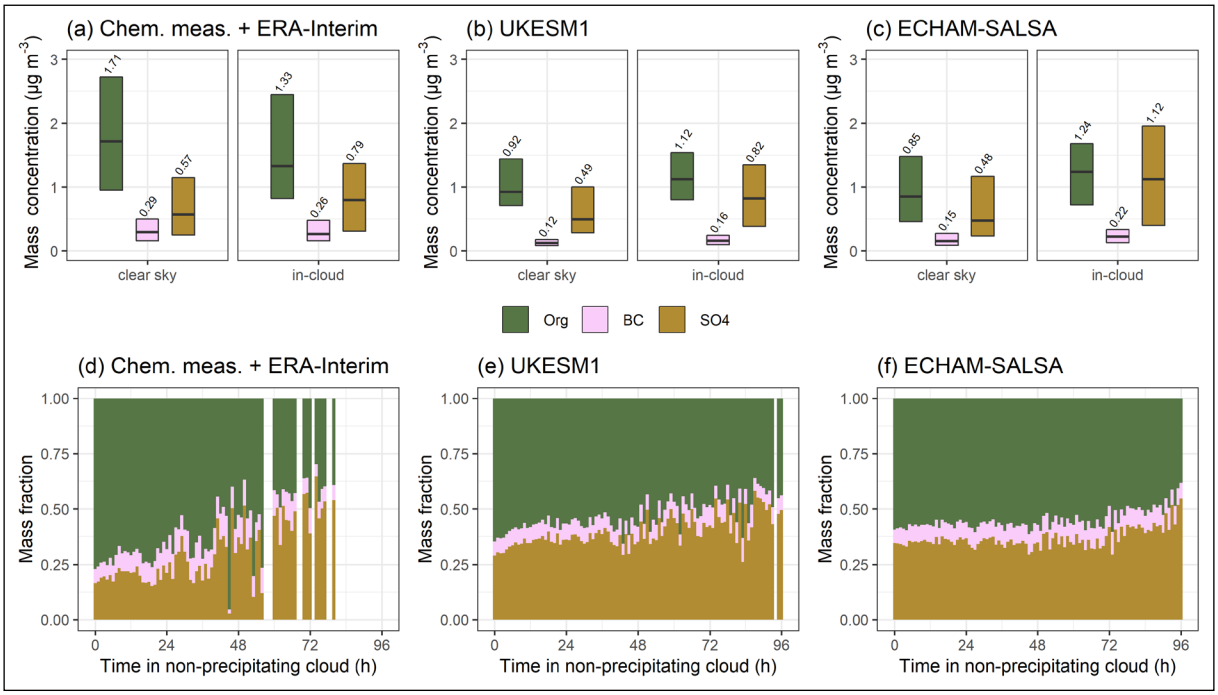

Figure 13 Top row: Median (black horizontal lines and numerical values) particle mass concentrations with 25th–75th percentiles (boxes) for OA (noted here, and in Isokääntä et al., 2022 as Org), eBC, and SO_4 for the cold and polluted airmass sector at SMEAR II station, Hyytiälä, Finland. The experienced conditions by the air mass are denoted as clear sky and in-cloud (non-precipitating), and the data is temporally harmonised across observations and GCMs. Bottom row: The mass fractions of OA, SO4, and BC (derived from median concentrations at each 1-hour bin) for the more polluted air masses as a function of time spent in in non-precipitating cloud. Figure created from the data used in Isokääntä *et al.* (2022) and Talvinen *et al.* (2025).

ESMs. It is important to note, however, that aqueous-phase SOA is routinely observed and a well-established phenomenon in isoprene-dominated environments (e.g. Ervens, Turpin and Weber, 2011; Marais *et al.*, 2016; Surratt *et al.*, 2010).

3.8.3 Aerosol precursor scavenging by convective clouds

Understanding the details of trace gas transport through convective clouds is important for better predictions of upper tropospheric (UT) NPF as source of particle number at higher altitudes (see e.g. Williamson *et al.*, 2019). In addition to the removal of particulate mass by clouds and precipitation, we have also investigated the processes that affect gas transport and removal within deep convective clouds (Bardakov *et al.*, 2020, 2021, 2022, 2024; Wang *et al.*, 2022).

Using the LES model MIMICA (Sect. S3.2), Bardakov *et al.* (2021) produced individual parcel trajectories within simulated deep convective clouds. A box model was then coupled to these trajectories to calculate e.g. gas condensation on hydrometeors, gas-phase chemical reactions, gas scavenging by hydrometeors and turbulent dilution. Trace gas transport followed approximately one out of three scenarios, determined by a combination of the equilibrium vapour pressure (containing information about water-solubility and pure component saturation vapour pressure) and the enthalpy of vapourisation for the ranges of molecular properties for isoprene system considered by Bardakov *et al.* (2021). At one extreme, the trace gas will eventually be completely removed by uptake to hydrometeors and precipitation. At the other extreme, there is almost no vapour condensation on hydrometeors and most of the gas is transported to the top of the cloud**. Any physically-based description of scavenging by clouds should therefore couple effective volatility and chemical reactivity to the cloud liquid and ice water content in a dynamically evolving atmosphere.**

Nucleation of organic species is one of the most important mechanisms contributing to the aerosol concentrations in the UT. Isoprene nucleation has been in focus with recent studies (Bardakov *et al.*, 2024; Curtius *et al.*, 2024; Shen *et al.*, 2024), especially looking at the night-day transition. Before sunrise, a convective event can transport around 20% of the highly volatile isoprene emitted to the upper troposphere, as shown in Figure 14. Figure 14 displays the isoprene gas system surviving to

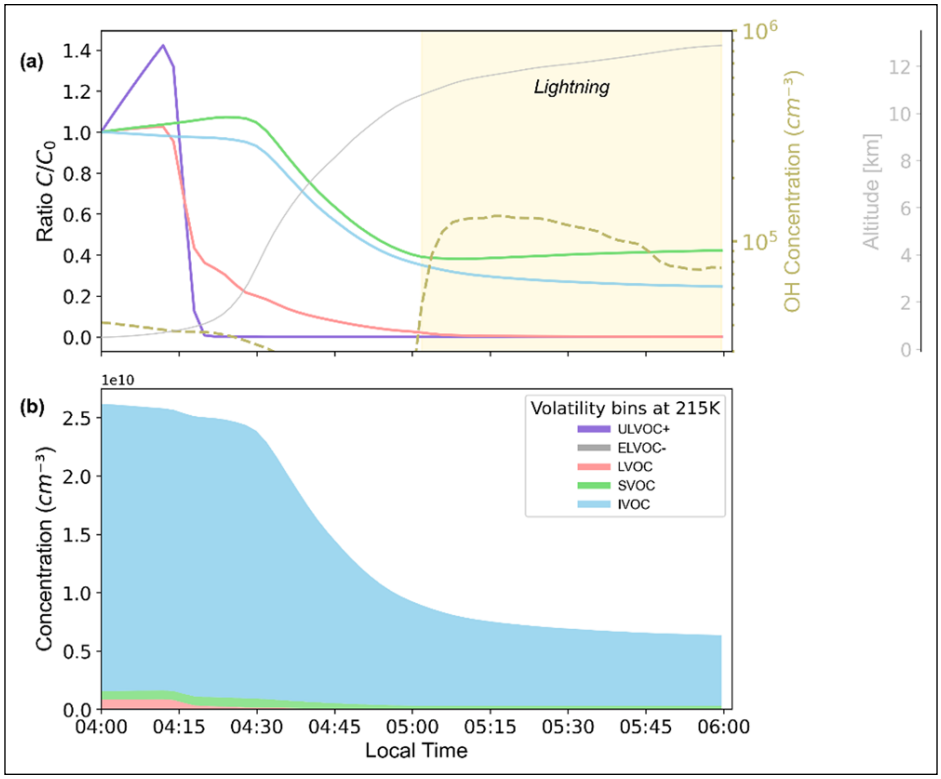

Figure 14 Transport of the isoprene gas-phase system during night-time convection over the Amazon. In **(a)** the fraction of the initial gas-phase concentration within volatility bins that survives night-time transport (chemistry and microphysics processes) is presented, and the altitude is shown with thin grey line and the OH concentration by the dashed olive yellow line. In **(b)** the contribution of different volatility bins to the total gas-phase concentration during transport is shown. Organic compounds are categorised according to their volatility with C* obtained for T = 215K: ULVOC+, extended ultra-low volatility organic compound, with the equilibrium saturation concentration $C^*(T) \leq 3 \times 10^{-7}$ μg m^{-3} (7 compounds) in purple; ELVOC-, reduced extremely low-volatility organic compound, with $3 \times 10^{-7} < C^*(T) \leq 3 \times 10^{-5}$ μg m^{-3} (1 compound = $C_4H_5O_3$) in grey; LVOC, low-volatility organic compound, with $3 \times 10^{-5} < C^*(T) \leq 0.3$ μg m^{-3} (8 compounds) in red; SVOC, semi-volatile organic compound, with $0.3 < C^*(T) \leq 300$ μg m^{-3} (1 compound = MVK/MACR = C_4H_6O) in green and the IVOC, intermediate volatile organic compound, with $300 < C^*(T) \leq 3 \times 10^6$ μg m^{-3} (1 compound = Isoprene = C_5H_8) in blue.

the convective updraft, using the CloudChem box model (Sect. S3.3), with isoprene in blue (IVOC). After sunrise, isoprene is then oxidised to form large amounts of ultra-low volatility species, which can reach concentrations of about 10^7 molecules cm^{-3}. Finally, these species directly nucleate at high rates and lead to typically observed nanoparticle concentrations of 10^3–10^5 particles cm^{-3} over the tropics (Andreae *et al.*, 2018).

The results from Bardakov *et al.* (2021) on the isoprene system also show that gas uptake to anvil ice is an important parameter for regulating the intensity of the isoprene oxidation and associated low volatility organic vapour concentrations in the outflow. This result is corroborated also by the study by Wang *et al.* (2022), which studied a completely different system, namely synergistic NPF of ammonia, nitric acid and sulfuric acids at high altitudes. This study suggests that transport of the trace gases through convective clouds, particularly ammonia, plays a large role in NPF in the upper troposphere in Asian monsoon. The trace gas scavenging onto ice is highly uncertain, and hence further studies on vapour uptake on and retention from ice hydrometeors are warranted.

The work towards parameterising the findings from the LES and box model frameworks discussed above for potential use in larger scale models is ongoing, in relation to, e.g., the descriptions of Jeuken *et al.* (2001) and Roelofs and Lelieveld (1995) that are currently used within EC-Earth. **If NPF in the UT was to be explored within ESMs, the description of the transport and chemical transformation of the precursor VOCs in the convective systems needs to be explored and parameterised in a way that is physically consistent and in line with present observations** (Bardakov *et al.*, 2020, 2021, 2022, 2024; Curtius *et al.*, 2024).

4 SUMMARY, CONCLUSIONS AND OUTLOOK

Uncertainties in anthropogenic aerosol radiative forcing estimates are still a bottleneck for confidence in future climate projections (e.g. Im *et al.*, 2021; Samset *et al.*, 2018). One way to address this issue is to improve current descriptions of aerosol and cloud processes in Earth System Models (ESMs). Other key developments include increased model resolution, enhanced observational constraints and using simplified models and statistical emulation to obtain comprehensive yet computationally efficient parametrisations (see also Shaw and Stevens, 2025). In the framework of the FORCeS project, we reviewed current representations of aerosol and cloud processes (Figure 1) in a number of ESMs and scrutinised them against state-of-the-art knowledge. We then conducted new research to enhance our process understanding and to push the development of the model parametrisations. As a result, we arrived at a number of recommendations for ESMs regarding key chemical and microphysical processes. In the following, we summarise our recommendations, which are currently in various implementation phases within the ESMs covered in this article (see Sect. S7).

Organic aerosol (OA) is chemically complex and thus challenging to describe in models, yet important for climate feedbacks involving natural aerosol, for example, but also for capturing the sources and properties of human-driven emissions—including partly absorbing brown carbon (BrC), whose emissions remain particularly uncertain. Its representation is always a balance between an accurate enough description of the OA evolution and properties and limiting the number of additional tracers to include in the model. Our recommendation for ESMs is to consider implementing ORACLE-lite (Tsimpidi *et al.*, 2025), especially if their current parametrisations do not consider the large variation in volatility of organic species. In addition, the approach developed for EC-Earth-AerChem by Bergman *et al.* (2022) focusing on two lumped species, namely semi-volatile and extremely low-volatile organic species might be of interest to models that seek an even simpler, yet thermodynamically-based representation of OA.

Particulate nitrate is expected to become more important in the future as reductions in anthropogenic SO_2 emissions will increase the fraction of ammonium-containing species, such as ammonium nitrate. We therefore recommend adding nitrate to any ESM, but most importantly when simulating interactions between air quality and climate. The computationally efficient atmospheric aerosol thermodynamics module, ISORROPIA-lite (Kakavas, Pandis and Nenes, 2022; Milousis *et al.*, 2024), developed within FORCeS, is well-suited for this purpose. As inorganic partitioning is often not included in ESMs, we recommend incorporating a thermodynamic model, such as ISORROPIA-lite, which offers reduced computational cost and good performance compared to the standard ISORROPIA-II. In applications in which accurate prediction of the distribution of nitrate between the fine and coarse modes is critical, we recommend reviewing relevant studies and considering the implementation of a dust mineralogy climatology.

For **black carbon** (BC), models should align with recent experimental findings. Liu *et al.* (2020) reviewed available literature on BC absorption properties and determined an average MAC of 8 ± 0.7 m^2 g^{-1} at 500 nm from ten different measurements. Regarding **BrC**, three different BrC species are ideally considered: two primary strongly absorbing species and one photobleached very weakly absorbing species, denoted as pbBrC. Based on current knowledge, the BrC from oxidation of aromatic VOCs could be neglected as a first approximation. The first primary BrC tracer (about 10% of the total BrC emission) to be considered is inert and insoluble

and does not lose its absorbing properties. The second primary BrC tracer is soluble and loses its absorbing properties by photobleaching and is transformed to pbBrC. For this reaction, a rate constant $k = 3.4 \times 10^{-5}$ s^{-1} or a rate depending on OH radical concentration should be used. All BrC species to be considered are in the accumulation mode and are subject to atmospheric deposition. For improving the representation of the single scattering albedo of **dust**, we recommend updating optical constants using recent lab constraints (Di Biagio *et al.*, 2019; Li *et al.*, 2024a; Obiso *et al.*, 2024) and calibrating absorption to observed iron oxide fractions. Models should incorporate region-specific soil mineral data, leveraging high-resolution datasets such as NASA's EMIT mission. For computational efficiency, options include representing key iron oxides as separate tracers while grouping similar minerals (e.g. clays) or employing precomputed lookup tables to dynamically adjust optical properties. These approaches balance improved realism with manageable computational cost.

The representation of **ultrafine aerosols and new particle formation** (NPF) within ESMs varies; it can rely on semi-empirical parametrisations of field observations or laboratory observations of NPF involving known chemical systems or some combination thereof. The work conducted within FORCeS showed that Eq. (1) provides good results and can therefore be recommended if a field-based semi-empirical approach is desired. If a laboratory-based approach is desired, many of the experimental studies reviewed by Kirkby *et al.* (2023) have been cast into simplified parametrisations (Dunne *et al.*, 2016; Gordon *et al.*, 2016; Lehtipalo *et al.*, 2018; Zhao *et al.*, 2024), that can be utilised within larger-scale models such as ESMs. It is also important to ensure that Aitken mode dynamics are properly represented within ESMs, as smaller aerosols can act as cloud condensation nuclei (CCN), especially in cleaner environments. In the upper troposphere, these processes can be captured with NPF parametrisations derived for boundary layer conditions, but an accurate simulation requires proper representation of trace gas transport, chemistry, and also particle downward transport.

Accurate calculation of the number of activated droplets (N_{act}) is crucial for constraining the ACI forcing estimates, and thus the **cloud droplet activation** schemes in both GCMs (general circulation models) and ESMs should be carefully selected. Recent work by Ghosh *et al.* (2025) has shown that the complex iterative based droplet activation parametrisation of Morales Betancourt and Nenes (2014) and a modified version of Abdul-Razzak and Ghan (2000) scheme provide relatively good agreement with adiabatic cloud parcel models, and are therefore recommended for treating droplet activation in the FORCeS ESMs. Recent results highlight the importance of accurately characterising the aerosol lifecycle in models to ensure a realistic representation of the size distribution, which is crucial for droplet activation parameterisations. While models account for all aerosol modes, under certain conditions—such as clean environments—both Aitken and coarse mode particles can significantly contribute to CCN populations, and their influence may be underestimated if the input size distribution is not sufficiently resolved.

For **liquid cloud microphysics,** we obtained a number of insights that might be helpful in the development of cloud schemes in ESMs, but also in using and interpreting observations for model evaluation. The work conducted within FORCeS (Prank *et al.*, 2022, 2025) supports earlier findings that giant CCN, and also coarse mode particles, are important to consider in autoconversion parametrisations for capturing the formation of drizzle correctly. For fog specifically, we recommend avoiding autoconversion parametrisations, especially if the fog droplet formation is simulated realistically based on physically valid parametrisations that account for radiative cooling at the top of fog, sedimentation and activation processes within the fog. FORCeS recommends that the impact of increased aerosol concentrations on droplet evaporation and mixing, and thus cloud droplet number concentration (CDNC), cloud liquid water path (LWP) and cloud fraction, should be examined against observations. The results from FORCeS suggest that great care should be taken when inferring LWP responses to aerosol from remote sensing data. However, by carefully selecting cloud cases with similar meteorological conditions and ensuring that cloud condensation nuclei concentrations are well-defined, changes in liquid water can also be reliably determined using satellite data.

The general understanding of **primary ice formation processes** has increased substantially in the past two decades (Lohmann and Diehl, 2006; Spracklen and Heald, 2014; Wang *et al.*, 2014; Zhao and Liu, 2022). FORCeS findings support that ESMs should include aerosol aware INP (ice nucleating particle) parametrisations, for dust in particular, although large uncertainties remain in the representation of aerosol sources of INPs. A mismatch between observed ICNCs and INPs for mixed-phase clouds (MPCs) that are decoupled from the surface and lack seeding from upper-level clouds can be attributed to **secondary ice production** (SIP). To address this, we recommend that key SIP processes be incorporated into ESM simulations to better capture realistic ICNCs. A data-driven parameterisation trained on physically detailed WRF simulations is the RaFSIPv2 scheme, presented by Georgakaki and Nenes (2024), which parameterises the combined effects of the three dominant SIP mechanisms and is designed for straightforward implementation in large-scale models (e.g. with horizontal grid spacings >10 km). The use of RaFSIP can support ongoing efforts to improve the representation of MPCs in climate models and deepen our understanding of cloud-phase processes and their role in the climate system.

In addition to investigating the ways that aerosol perturbations influence atmospheric radiation and cloud microphysics, several studies within FORCeS targeted different aspects of **aerosol and precursor gas scavenging and processing** by clouds. FORCeS findings (Isokääntä *et al.*, 2022; Talvinen *et al.*, 2025) confirm the established importance of aqueous-phase sulfate formation within clouds and suggest that this source is well-captured by state-of-the-art approaches. Based on studies within the boreal zone and the Arctic (Graham *et al.*, 2020; Isokääntä *et al.*, 2022), however, no trace of significant aqueous secondary organic aerosol production was observed in these environments and can therefore probably be neglected for these regions in ESMs. Given the importance of upper tropospheric NPF, the description of the transport and scavenging of the relevant precursor gases through convective clouds is also highly relevant to represent. Any physically-based description of scavenging of gas-phase species by clouds should couple volatility, solubility and chemical reactivity to the cloud liquid and ice water content in a dynamically evolving atmosphere. Given the non-linearity of the associated phenomena, we recommend the enhanced use of high-resolution modelling such as LES for developing parametrisations for larger-scale models for wet scavenging. If such processes were to be explored within ESMs, the description of the transport and chemical transformation of the precursor VOCs in the convective systems needs to be explored and parametrised in a way that is physically consistent and in line with present observations.

Continued efforts are required in prioritising model development and evaluation. Although advocating for improving aerosol and cloud representation in ESMs, we realise that model development always faces a trade-off between partially contradicting goals: increasing the number and detail of representations to enhance representational accuracy; using the model to generate understanding; and increasing model performance (in terms of decreasing computing time or increasing the match with observations). In particular, representative accuracy leads to model complexity, which is sometimes problematic for various reasons: (1) complexity hinders the understanding of the model and the ability to generate understanding with it, (2) a more complex model includes more free parameters that allow for multiple equally plausible model realisations (equifinality), (3) including processes in large detail increases the risk of overinterpreting the processes that are included while overlooking those that are not, (4) increasing model detail may not be decreasing uncertainty and finally, (5) more complexity and authority from included processes conceal non-epistemic influences such as values and habits (Proske *et al.*, 2023 and references therein). Thus, adding more detailed representation and complexity comes with a price. That being said, the results from the FORCeS project do demonstrate the importance of capturing the key drivers of ACI better in the next generation of ESMs: **it is hard to imagine a substantial decrease in the uncertainties associated with ACI with ESMs that do not include physically reasonable and high-enough resolution descriptions of particle number size distributions, water vapour concentrations, emission sources** (critically characterised and constrained by the chemical fingerprint present in the particles) **and cloud microphysics** (including hydrometeor size distributions and phase). The reduction in aerosol ERF uncertainty should also be targeted through addressing **internal model inconsistencies** and **rigorous model evaluation** procedures. Related to the former, structural errors in present ESMs may result in inconsistencies in key parameters for ACI, LWP and CDNC as examples. **Such inconsistencies could be remedied with thoughtful application of high-resolution and LES modelling constrained by a combination of in-situ and remote-sensed observations.** As needed, **such developments can be facilitated with large ensemble simulations using e.g., statistical emulation.** For model evaluation, multiple observation types should be used to avoid overfitting models to very limited sets of observations. Our results therefore demonstrate the importance of long-term, high-resolution empirical data (both in-situ and remote sensing) and the potential of using detailed process models to facilitate direct upscaling such observations for direct comparisons with ESMs (see e.g., Arola *et al.*, 2022). Furthermore, we advocate prioritising process-based evaluation approaches that complement the traditional parameter-based evaluations (e.g., Blichner *et al.*, 2024; Virtanen *et al.*, 2025). Continued dialogue is needed between the research communities working with detailed microphysical and chemical processes relevant to the Earth system, and those developing and using global models. Likewise, our results have demonstrated the critical importance of open discussion on the limitations and potential of various data sets used for ESM evaluation, and have pinpointed areas where methodological developments are critical for pushing the research frontiers in this field of climate science.

ACKNOWLEDGEMENTS

We gratefully aknowlegde the key contributions from Trude Storelvmo, Ulrike Lohmann and David Neubauer during the FORCeS project. Sini Talvinen would like to extend personal thanks to Roman Bardakov from all the helpful discussions during the writing process of this work.

FUNDING INFORMATION

This work has been supported by the European Research Council by the Union's Horizon 2020 research and innovation programme (FORCeS, grant No. 821205 and CERTAINTY, grant No. 10113768), consolidator grants

INTEGRATE (grant No. 865799) and FRAGMENT (grant No. 773051) and Marie Sklodowska-Curie Actions (grant No. 754433 from the call H2020-MSCA-COFUND-2016).

Further support has been provided by the Swiss National Science foundation (grant No. 225474, 217899 and 216181), UK Natural Environment Research Council (NERC, grant No. NE/W001713/1), the Spanish Ministerio de Economía y Competitividad through the HEAVY project (grant PID2022-140365OB-I funded by MICIU/AEI/10.13039/501100011033 and by ERDF, EU), the AXA Research Fund through the AXA Chair on Sand and Dust Storms at the Barcelona Supercomputing Center (BSC), and National Academic Infrastructure for Supercomputing in Sweden (NAISS) at NSC (Linköping University), partially funded by the Swedish Research Council (grant No. 2022-06725), for computational resources. We also acknowledge the Earth Surface Mineral Dust Source Investigation (EMIT), a NASA Earth Ventures Instrument (EVI-4) mission.

COMPETING INTERESTS

The authors have no competing interests to declare.

AUTHOR CONTRIBUTIONS

Ilona Riipinen and Annica M. L. Ekman proposed the study and designed the concept with contribution from Sini Talvinen.

Ilona Riipinen and Sini Talvinen wrote the original manuscript with support from Annica M. L. Ekman, Paraskevi Georgakaki, Carlos Pérez García-Pando, Ulrike Proske, Lubna Dada, Øyvind Seland, Daniel G. Partridge, Almuth Neuberger, Snehitha M. Kommula, Stefano Decesari and Twan van Noije.

The figures were created by Sini Talvinen together with Anouck Chassaing, Paraskevi Georgakaki, Xinyang Li, Tommi Bergman, Snehitha M. Kommula, Angelos Gkouvousis, Alexandra P. Tsimpidi, Marios Chatziparaschos, Almuth Neuberger, Vlassis A. Karydis, Silvia M. Calderón, Sami Romakkaniemi, Théodore Khadir and Paul Zieger.

All co-authors edited the manuscript and provided valuable feedback.

AUTHOR AFFILIATIONS

Ilona Riipinen
Department of Environmental Science, Stockholm University, Stockholm, Sweden; Bolin Centre for Climate Research, Stockholm University, Stockholm, Sweden

Sini Talvinen orcid.org/0000-0001-6307-7206
Department of Environmental Science, Stockholm University, Stockholm, Sweden; Bolin Centre for Climate Research, Stockholm University, Stockholm, Sweden; Now at Department of Technical physics, University of Eastern Finland, Kuopio, Finland

Anouck Chassaing
Department of Environmental Science, Stockholm University, Stockholm, Sweden; Bolin Centre for Climate Research, Stockholm University, Stockholm, Sweden

Paraskevi Georgakaki
Laboratory of Atmospheric Processes and their Impacts, School of Architecture, Civil & Environmental Engineering, Ecole Polytechnique Fédérale de Lausanne, Lausanne, Switzerland; Now at Leipzig Institute for Meteorology, Leipzig University, Leipzig, Germany

Xinyang Li
Institute for Atmospheric and Earth System Research, University of Helsinki, Helsinki, Finland

Carlos Pérez García-Pando
Barcelona Supercomputing Center, Barcelona, Spain; ICREA, Calatan Institution for Research and Advanced Studies, Barcelona, Spain

Tommi Bergman
Finnish Meteorological Institute, Helsinki, Finland

Snehitha M. Kommula
Department of Technical Physics, University of Eastern Finland, Kuopio, Finland

Ulrike Proske
Institute for Atmospheric and Climate Science, ETH Zürich, Zürich, Switzerland; Now at Hydrology and Environmental Hydraulics Group, Wageningen University, Wageningen, Netherlands

Angelos Gkouvousis
Environmental Chemical Processes Laboratory, Department of Chemistry, University of Crete, Heraklion – Crete, Greece; Institute of Chemical Engineering Sciences, Foundation for Research and Technology Hellas, Patras, Greece

Alexandra P. Tsimpidi
Institute of Climate and Energy Systems: Troposphere, Forschungszentrum Jülich GmbH, Jülich, Germany

Marios Chatziparaschos
Environmental Chemical Processes Laboratory, Department of Chemistry, University of Crete, Heraklion – Crete, Greece; Now at Barcelona Supercomputing Center, Barcelona, Spain

Almuth Neuberger
Department of Environmental Science, Stockholm University, Stockholm, Sweden; Bolin Centre for Climate Research, Stockholm University, Stockholm, Sweden

Vlassis A. Karydis
Institute of Climate and Energy Systems: Troposphere, Forschungszentrum Jülich GmbH, Jülich, Germany

Silvia M. Calderón
Finnish Meteorological Institute, Kuopio, Finland

Sami Romakkaniemi
Finnish Meteorological Institute, Kuopio, Finland

Daniel G. Partridge
Department of Mathematics and Statistics, University of Exeter, Exeter, United Kingdom

Théodore Khadir
Department of Environmental Science, Stockholm University, Stockholm, Sweden; Bolin Centre for Climate Research, Stockholm University, Stockholm, Sweden

Lubna Dada
Institute for Atmospheric and Earth System Research, University of Helsinki, Helsinki, Finland; PSI Center for Energy and Environmental Sciences, Villigen PSI, Switzerland

Twan van Noije
Royal Netherlands Meteorological Institute, De Bilt, Netherlands

Stefano Decesari
Institute of Atmospheric Sciences and Climate, National Research Council of Italy, Bologna, Italy

Øyvind Seland
Norwegian Meteorological Institute, Oslo, Norway

Paul Zieger
Department of Environmental Science, Stockholm University, Stockholm, Sweden; Bolin Centre for Climate Research, Stockholm University, Stockholm, Sweden

Frida Bender
Department of Meteorology, Stockholm University, Stockholm, Sweden

Ken Carslaw
School of Earth and Environment, University of Leeds, Leeds, United Kingdom

Jan Cermak
Institute of Meteorology and Climate Research, Karlsruhe Institute of Technology, Germany; Institute of Photogrammetry and Remote Sensing, Karlsruhe Institute of Technology, Germany

Montserrat Costa-Surós
Barcelona Supercomputing Center, Barcelona, Spain

Maria Gonçalves Ageitos
Barcelona Supercomputing Center, Barcelona, Spain; Universitat Politècnica de Catalunya, Barcelona, Spain

Yvette Gramlich
Department of Environmental Science, Stockholm University, Stockholm, Sweden; PSI Center for Energy and Environmental Sciences, Villigen PSI, Switzerland

Ove W. Haugvaldstad
Norwegian Meteorological Institute, Oslo, Norway; Department of Geosciences, University of Oslo, Oslo, Norway

Eemeli Holopainen
Institute of Chemical Engineering Sciences, Foundation for Research and Technology Hellas, Patras, Greece; Finnish Meteorological Institute, Kuopio, Finland

Corinna Hoose
Institute of Meteorology and Climate Research, Karlsruhe Institute of Technology, Germany

Oriol Jorba
Barcelona Supercomputing Center, Barcelona, Spain

Stylianos Kakavas
Institute of Chemical Engineering Sciences, Foundation for Research and Technology Hellas, Patras, Greece

Maria Kanakidou
Environmental Chemical Processes Laboratory, Department of Chemistry, University of Crete, Heraklion – Crete, Greece; Institute of Chemical Engineering Sciences, Foundation for Research and Technology Hellas, Patras, Greece

Harri Kokkola
Department of Technical Physics, University of Eastern Finland, Kuopio, Finland; Finnish Meteorological Institute, Kuopio, Finland

Radovan Krejci
Department of Environmental Science, Stockholm University, Stockholm, Sweden; Bolin Centre for Climate Research, Stockholm University, Stockholm, Sweden

Thomas Kühn
Finnish Meteorological Institute, Helsinki, Finland

Markku Kulmala
Institute for Atmospheric and Earth System Research, University of Helsinki, Helsinki, Finland

Philippe Le Sager
Royal Netherlands Meteorological Institute, De Bilt, Netherlands

Risto Makkonen
Finnish Meteorological Institute, Helsinki, Finland

Stella E. I. Manavi
Department of Chemical Engineering, University of Patras, Greece

Thomas F. Mentel
Institute of Climate and Energy Systems: Troposphere, Forschungszentrum Jülich GmbH, Jülich, Germany; Retired

Alexandros Milousis
Institute of Climate and Energy Systems: Troposphere, Forschungszentrum Jülich GmbH, Jülich, Germany

Stelios Myriokefalitakis
Institute for Environmental Research and Sustainable Development, National Observatory of Athens, Penteli, Greece

Athanasios Nenes
Laboratory of Atmospheric Processes and their Impacts, School of Architecture, Civil & Environmental Engineering, Ecole Polytechnique Fédérale de Lausanne, Lausanne, Switzerland; Institute of Chemical Engineering Sciences, Foundation for Research and Technology Hellas, Patras, Greece

Tuomo Nieminen
Institute for Atmospheric and Earth System Research, University of Helsinki, Helsinki, Finland; Department of Physics, University of Helsinki, Helsinki, Finland

Spyros N. Pandis
Department of Chemical Engineering, University of Patras, Greece

David Patoulias
Institute of Chemical Engineering Sciences, Foundation for Research and Technology Hellas, Patras, Greece

Tuukka Petäjä
Bolin Centre for Climate Research, Stockholm University, Stockholm, Sweden

Johannes Quaas
Leipzig Institute for Meteorology, Leipzig University, Leipzig, Germany; German Centre for Integrative Biodiversity Science Halle-Jena-Leipzig, Leipzig, Germany

Leighton Regayre
School of Earth and Environment, University of Leeds, Leeds, United Kingdom; Met Office Hadley Centre, Exeter, Fitzroy Road, Exeter, Devon, United Kingdom; Centre for Environmental Modelling and Computation, University of Leeds, Leeds, United Kingdom

Susanne M. C. Scholz
Institute of Climate and Energy Systems: Troposphere, Forschungszentrum Jülich GmbH, Jülich, Germany

Michael Schulz
Norwegian Meteorological Institute, Oslo, Norway

Ksakousti Skyllakou
Institute of Chemical Engineering Sciences, Foundation for Research and Technology Hellas, Patras, Greece

Ruben Sousse
Barcelona Supercomputing Center, Barcelona, Spain

Philip Stier
Department of Physics, University of Oxford, Oxford, United Kingdom

Manu Anna Thomas
Meteorology Research Unit – Environment and Climate, Swedish Meteorological and Hydrological Institute, Sweden

Julie T. Villinger
Institute for Atmospheric and Climate Science, ETH Zürich, Zürich, Switzerland; Now at Meteomatics AG, St Gallen, Switzerland

Annele Virtanen
Department of Technical Physics, University of Eastern Finland, Kuopio, Finland

Klaus Wyser
Rossby Centre, Swedish Meteorological and Hydrological Institute, Norrköping, Sweden

Annica M. L. Ekman
Bolin Centre for Climate Research, Stockholm University, Stockholm, Sweden; School of Earth and Environment, University of Leeds, Leeds, United Kingdom

REFERENCES

Abdul-Razzak, H. and **Ghan, S.J.** (2000) A parameterization of aerosol activation: 2. Multiple aerosol types. *J. Geophys. Res. Atmospheres*, 105: 6837–6844. DOI: https://doi.org/10.1029/1999JD901161

Abdul-Razzak, H. and **Ghan, S.J.** (2002) A parameterization of aerosol activation 3. Sectional representation. *J. Geophys. Res. Atmospheres*, 107: AAC 1-1–AAC 1-6. DOI: https://doi.org/10.1029/2001JD000483

Abdul-Razzak, H., Ghan, S.J. and **Rivera-Carpio, C.** (1998) A parameterization of aerosol activation: 1. Single aerosol type. *J. Geophys. Res. Atmospheres*, 103: 6123–6131. DOI: https://doi.org/10.1029/97JD03735

Ackerley, D., Highwood, E.J., Frame, D.J. and **Booth, B.B.B.** (2009) Changes in the Global Sulfate Burden due to Perturbations in Global CO_2 Concentrations. *J. Clim.*, 22: 5421–5432. DOI: https://doi.org/10.1175/2009JCLI2536.1

Ackerman, A.S., Kirkpatrick, M.P., Stevens, D.E. and **Toon, O.B.** (2004) The impact of humidity above stratiform clouds on indirect aerosol climate forcing. *Nature*, 432: 1014–1017. DOI: https://doi.org/10.1038/nature03174

Ahola, J., Raatikainen, T., Alper, M.E., Keskinen, J.-P., Kokkola, H., Kukkurainen, A., Lipponen, A., Liu, J., Nordling, K., Partanen, A.-I., Romakkaniemi, S., Räisänen, P., Tonttila, J. and **Korhonen, H.** (2022) Technical note: Parameterising cloud base updraft velocity of marine stratocumuli. *Atmospheric Chem. Phys.*, 22: 4523–4537. DOI: https://doi.org/10.5194/acp-22-4523-2022

Aksoyoglu, S., Ciarelli, G., El-Haddad, I., Baltensperger, U. and **Prévôt, A.S.H.** (2017) Secondary inorganic aerosols in Europe: sources and the significant influence of biogenic VOC emissions, especially on ammonium nitrate. *Atmospheric Chem. Phys.*, 17: 7757–7773. DOI: https://doi.org/10.5194/acp-17-7757-2017

Albrecht, B.A. (1989) Aerosols, Cloud Microphysics, and Fractional Cloudiness. *Science*, 24: 1227–1230. DOI: https://doi.org/10.1126/science.245.4923.1227

Andreae, M.O., Afchine, A., Albrecht, R., Holanda, B.A., Artaxo, P., Barbosa, H.M.J., Borrmann, S., Cecchini, M.A., Costa, A., Dollner, M., Fütterer, D., Järvinen, E., Jurkat, T., Klimach, T., Konemann, T., Knote, C., Krämer, M., Krisna, T., Machado, L.A.T., Mertes, S., Minikin, A., Pöhlker, C., Pöhlker, M.L., Pöschl, U., Rosenfeld, D., Sauer, D., Schlager, H., Schnaiter, M., Schneider, J., Schulz, C., Spanu, A., Sperling, V.B., Voigt, C., Walser, A., Wang, J., Weinzierl, B., Wendisch, M. and **Ziereis, H.** (2018) Aerosol characteristics and particle production in the upper troposphere over the Amazon Basin. *Atmospheric Chem. Phys.*, 18: 921–961. DOI: https://doi.org/10.5194/acp-18-921-2018

Andreae, M.O. and **Gelencsér, A.** (2006) Black carbon or brown carbon? The nature of light-absorbing carbonaceous aerosols. *Atmospheric Chem. Phys.*, 6: 3131–3148. DOI: https://doi.org/10.5194/acp-6-3131-2006

Arola, A., Lipponen, A., Kolmonen, P., Virtanen, T.H., Bellouin, N., Grosvenor, D.P., Gryspeerdt, E., Quaas, J. and **Kokkola, H.** (2022) Aerosol effects on clouds are concealed by natural cloud heterogeneity and satellite retrieval errors. *Nat. Commun.*, 13: 7357. DOI: https://doi.org/10.1038/s41467-022-34948-5

Atkinson, J.D., Murray, B.J., Woodhouse, M.T., Whale, T.F., Baustian, K.J., Carslaw, K.S., Dobbie, S., O'Sullivan, D. and **Malkin, T.L.** (2013) The importance of feldspar for ice nucleation by mineral dust in mixed-phase clouds, *Nature*. 498: 355–358. DOI: https://doi.org/10.1038/nature12278

Baccarini, A., Karlsson, L., Dommen, J., Duplessis, P., Vüllers, J., Brooks, I.M., Saiz-Lopez, A., Salter, M., Tjernström, M., Baltensperger, U., Zieger, P. and **Schmale, J.** (2020) Frequent new particle formation over the high Arctic pack ice by enhanced iodine emissions. *Nat. Commun.*, 11: 4924. DOI: https://doi.org/10.1038/s41467-020-18551-0

Baker, A.R., Kanakidou, M., Nenes, A., Myriokefalitakis, S., Croot, P.L., Duce, R.A., Gao, Y., Guieu, C., Ito, A., Jickells, T.D., Mahowald, N.M., Middag, R., Perron, M.M.G., Sarin, M.M., Shelley, R. and **Turner, D.R.** (2021) Changing atmospheric acidity as a modulator of nutrient deposition and ocean biogeochemistry. *Sci. Adv.*, 7: eabd8800. DOI: https://doi.org/10.1126/sciadv.abd8800

Baker, Y., Kang, S., Wang, H., Wu, R., Xu, J., Zanders, A., He, Q., Hohaus, T., Ziehm, T., Geretti, V., Bannan, T.J., O'Meara, S.P., Voliotis, A., Hallquist, M., McFiggans, G., Zorn, S.R., Wahner, A. and **Mentel, T.F.** (2024) Impact of HO_2/RO_2 ratio on highly oxygenated α-pinene photooxidation products and secondary organic aerosol formation potential. *Atmospheric Chem. Phys.*, 24: 4789–4807. DOI: https://doi.org/10.5194/acp-24-4789-2024

Barahona, D., West, R.E.L., Stier, P., Romakkaniemi, S., Kokkola, H. and **Nenes, A.** (2010) Comprehensively accounting for the effect of giant CCN in cloud activation parameterizations. *Atmospheric Chem. Phys.*, 10: 2467–2473. DOI: https://doi.org/10.5194/acp-10-2467-2010

Barati, A.A., Zhoolideh, M., Azadi, H., Lee, J.-H. and **Scheffran, J.** (2023) Interactions of land-use cover and climate

change at global level: How to mitigate the environmental risks and warming effects. *Ecol. Indic.*, 146: 109829. DOI: https://doi.org/10.1016/j.ecolind.2022.109829

Bardakov, R., Krejci, R., Riipinen, I. and **Ekman, A.M.L.** (2022) The Role of Convective Up- and Downdrafts in the Transport of Trace Gases in the Amazon. *J. Geophys. Res. Atmospheres*, 127: e2022JD037265. DOI: https://doi.org/10.1029/2022JD037265

Bardakov, R., Riipinen, I., Krejci, R., Savre, J., Thornton, J.A. and **Ekman, A.M.L.** (2020) A Novel Framework to Study Trace Gas Transport in Deep Convective Clouds. *J. Adv. Model. Earth Syst.*, 12: e2019MS001931. DOI: https://doi.org/10.1029/2019MS001931

Bardakov, R., Thornton, J.A., Ekman, A.M.L., Krejci, R., Pöhlker, M.L., Curtius, J., Williams, J., Lelieveld, J. and **Riipinen, I.** (2024) High Concentrations of Nanoparticles From Isoprene Nitrates Predicted in Convective Outflow Over the Amazon. *Geophys. Res. Lett.*, 51: e2024GL109919. DOI: https://doi.org/10.1029/2024GL109919

Bardakov, R., Thornton, J.A., Riipinen, I., Krejci, R. and **Ekman, A.M.L.** (2021) Transport and chemistry of isoprene and its oxidation products in deep convective clouds. *Tellus B Chem. Phys. Meteorol.*, 73: 1979856. DOI: https://doi.org/10.1080/16000889.2021.1979856

Barth, M.C., Bela, M.M., Fried, A., Wennberg, P.O., Crounse, J.D., St. Clair, J.M., Blake, N.J., Blake, D.R., Homeyer, C.R., Brune, W.H., Zhang, L., Mao, J., Ren, X., Ryerson, T.B., Pollack, I.B., Peischl, J., Cohen, R.C., Nault, B.A., Huey, L.G., Liu, X. and **Cantrell, C.A**. (2016) Convective transport and scavenging of peroxides by thunderstorms observed over the central U.S. during DC3. *J. Geophys. Res. Atmospheres*, 121: 4272–4295. DOI: https://doi.org/10.1002/2015JD024570

Barth, M.C., Kim, S.-W., Wang, C., Pickering, K.E., Ott, L.E., Stenchikov, G., Leriche, M., Cautenet, S., Pinty, J.-P., Barthe, C., Mari, C., Helsdon, J.H., Farley, R.D., Fridlind, A.M., Ackerman, A.S., Spiridonov, V. and **Telenta, B.** (2007) Cloud-scale model intercomparison of chemical constituent transport in deep convection. *Atmospheric Chem. Phys.*, 7: 4709–4731. DOI: https://doi.org/10.5194/acp-7-4709-2007

Basnet, S., Hartikainen, A., Virkkula, A., Yli-Pirilä, P., Kortelainen, M., Suhonen, H., Kilpeläinen, L., Ihalainen, M., Väätäinen, S., Louhisalmi, J., Somero, M., Tissari, J., Jakobi, G., Zimmermann, R., Kilpeläinen, A. and **Sippula, O.** (2024) Contribution of brown carbon to light absorption in emissions of European residential biomass combustion appliances. *Atmospheric Chem. Phys.*, 24: 3197–3215. DOI: https://doi.org/10.5194/acp-24-3197-2024

Bauer, S.E., Koch, D., Unger, N., Metzger, S.M., Shindell, D.T. and **Streets, D.G.** (2007) Nitrate aerosols today and in 2030: a global simulation including aerosols and tropospheric ozone. *Atmospheric Chem. Phys.*, 7: 5043–5059. DOI: https://doi.org/10.5194/acp-7-5043-2007

Bauer, S.E., Tsigaridis, K., Faluvegi, G., Nazarenko, L., Miller, R.L., Kelley, M. and **Schmidt, G.** (2022) The Turning Point of the Aerosol Era. *J. Adv. Model. Earth Syst.*, 14: e2022MS003070. DOI: https://doi.org/10.1029/2022MS003070

Beck, A., Henneberger, J., Fugal, J.P., David, R.O., Lacher, L. and **Lohmann, U.** (2018) Impact of surface and near-surface processes on ice crystal concentrations measured at mountain-top research stations. *Atmospheric Chem. Phys.*, 18: 8909–8927. DOI: https://doi.org/10.5194/acp-18-8909-2018

Bellouin, N., Quaas, J., Gryspeerdt, E., Kinne, S., Stier, P., Watson-Parris, D., Boucher, O., Carslaw, K.S., Christensen, M., Daniau, A.-L., Dufresne, J.-L., Feingold, G., Fiedler, S., Forster, P., Gettelman, A., Haywood, J.M., Lohmann, U., Malavelle, F., Mauritsen, T., McCoy, D.T., Myhre, G., Mülmenstädt, J., Neubauer, D., Possner, A., Rugenstein, M., Sato, Y., Schulz, M., Schwartz, S.E., Sourdeval, O., Storelvmo, T., Toll, V., Winker, D. and **Stevens, B.** (2020) Bounding Global Aerosol Radiative Forcing of Climate Change. *Rev. Geophys.*, 58: e2019RG000660. DOI: https://doi.org/10.1029/2019RG000660

Bender, F.A.-M., Engström, A. and **Karlsson, J.** (2016) Factors Controlling Cloud Albedo in Marine Subtropical Stratocumulus Regions in Climate Models and Satellite Observations. *J. Climate*, 29: 3559–3587. DOI: https://doi.org/10.1175/JCLI-D-15-0095.1

Bender, F.A.-M., Frey, L., McCoy, D.T., Grosvenor, D.P. and **Mohrmann, J.K.** (2019) Assessment of aerosol–cloud–radiation correlations in satellite observations, climate models and reanalysis. *Clim. Dyn.*, 52: 4371–4392. DOI: https://doi.org/10.1007/s00382-018-4384-z

Bender, F.A.-M., Lord, T., Staffansdotter, A., Jung, V. and **Undorf, S.** (2024) Machine Learning Approach to Investigating the Relative Importance of Meteorological and Aerosol-Related Parameters in Determining Cloud Microphysical Properties. *Tellus B Chem. Phys. Meteorol.*, 76(1): 1–18. DOI: https://doi.org/10.16993/tellusb.1868

Bergman, T., Makkonen, R., Schrödner, R., Swietlicki, E., Phillips, V.T.J., Le Sager, P. and **van Noije, T.** (2022) Description and evaluation of a secondary organic aerosol and new particle formation scheme within TM5-MP v1.2. *Geosci. Model Dev.*, 15: 683–713. DOI: https://doi.org/10.5194/gmd-15-683-2022

Bergström, R., Hallquist, M., Simpson, D., Wildt, J. and **Mentel, T.F.** (2014) Biotic stress: a significant contributor to organic aerosol in Europe? *Atmospheric Chem. Phys.*, 14: 13643–13660. DOI: https://doi.org/10.5194/acp-14-13643-2014

Bian, H., Chin, M., Hauglustaine, D.A., Schulz, M., Myhre, G., Bauer, S.E., Lund, M.T., Karydis, V.A., Kucsera, T.L., Pan, X., Pozzer, A., Skeie, R.B., Steenrod, S.D., Sudo, K., Tsigaridis, K., Tsimpidi, A.P. and **Tsyro, S.G.** (2017) Investigation of global particulate nitrate from the AeroCom phase III experiment. *Atmospheric Chem. Phys.*, 17: 12911–12940. DOI: https://doi.org/10.5194/acp-17-12911-2017

Blichner, S.M., Sporre, M.K., Makkonen, R. and **Berntsen, T.K.** (2021) Implementing a sectional scheme for early aerosol growth from new particle formation in the Norwegian

Earth System Model v2: comparison to observations and climate impacts. *Geosci. Model Dev.*, 14: 3335–3359. DOI: https://doi.org/10.5194/gmd-14-3335-2021

Blichner, S.M., Yli-Juuti, T., Mielonen, T., Pöhlker, C., Holopainen, E., Heikkinen, L., Mohr, C., Artaxo, P., Carbone, S., Meller, B.B., Quaresma Dias-Júnior, C., Kulmala, M., Petäjä, T., Scott, C.E., Svenhag, C., Nieradzik, L., Sporre, M., Partridge, D.G., Tovazzi, E., Virtanen, A., Kokkola, H. and **Riipinen, I.** (2024) Process-evaluation of forest aerosol-cloud-climate feedback shows clear evidence from observations and large uncertainty in models. *Nat. Commun.*, 15: 969. DOI: https://doi.org/10.1038/s41467-024-45001-y

Bond, T.C. and **Bergstrom, R.W.** (2006) Light Absorption by Carbonaceous Particles: An Investigative Review. *Aerosol Sci. Technol.*, 40: 27–67. DOI: https://doi.org/10.1080/02786820500421521

Bond, T.C., Doherty, S.J., Fahey, D.W., Forster, P.M., Berntsen, T., DeAngelo, B.J., Flanner, M.G., Ghan, S., Kärcher, B., Koch, D., Kinne, S., Kondo, Y., Quinn, P.K., Sarofim, M.C., Schultz, M.G., Schulz, M., Venkataraman, C., Zhang, H., Zhang, S., Bellouin, N., Guttikunda, S.K., Hopke, P.K., Jacobson, M.Z., Kaiser, J.W., Klimont, Z., Lohmann, U., Schwarz, J.P., Shindell, D., Storelvmo, T., Warren, S.G. and **Zender, C.S.** (2013) Bounding the role of black carbon in the climate system: A scientific assessment. *J. Geophys. Res. Atmospheres*, 118: 5380–5552. DOI: https://doi.org/10.1002/jgrd.50171

Bougiatioti, A., Nikolaou, P., Stavroulas, I., Kouvarakis, G., Weber, R., Nenes, A., Kanakidou, M. and **Mihalopoulos, N.** (2016) Particle water and pH in the eastern Mediterranean: source variability and implications for nutrient availability. *Atmospheric Chem. Phys.*, 16: 4579–4591. DOI: https://doi.org/10.5194/acp-16-4579-2016

Boutle, I., Angevine, W., Bao, J.-W., Bergot, T., Bhattacharya, R., Bott, A., Ducongé, L., Forbes, R., Goecke, T., Grell, E., Hill, A., Igel, A.L., Kudzotsa, I., Lac, C., Maronga, B., Romakkaniemi, S., Schmidli, J., Schwenkel, J., Steeneveld, G.-J. and **Vié, B.** (2022) Demistify: a large-eddy simulation (LES) and single-column model (SCM) intercomparison of radiation fog. *Atmospheric Chem. Phys.*, 22: 319–333. DOI: https://doi.org/10.5194/acp-22-319-2022

Boutle, I., Price, J., Kudzotsa, I., Kokkola, H. and **Romakkaniemi, S.** (2018) Aerosol–fog interaction and the transition to well-mixed radiation fog. *Atmospheric Chem. Phys.*, 18: 7827–7840. DOI: https://doi.org/10.5194/acp-18-7827-2018

Bretherton, C.S., Blossey, P.N. and **Uchida, J.** (2007) Cloud droplet sedimentation, entrainment efficiency, and subtropical stratocumulus albedo. *Geophys. Res. Lett.*, 34. DOI: https://doi.org/10.1029/2006GL027648

Brock, C.A., Hamill, P., Wilson, J.C., Jonsson, H.H. and **Chan, K.R.** (1995) Particle Formation in the Upper Tropical Troposphere: A Source of Nuclei for the Stratospheric Aerosol. *Science*, 270: 1650–1653. DOI: https://doi.org/10.1126/science.270.5242.1650

Brown, H., Liu, X., Pokhrel, R., Murphy, S., Lu, Z., Saleh, R., Mielonen, T., Kokkola, H., Bergman, T., Myhre, G., Skeie, R.B., Watson-Paris, D., Stier, P., Johnson, B., Bellouin, N., Schulz, M., Vakkari, V., Beukes, J.P., van Zyl, P.G., Liu, S. and **Chand, D.** (2021) Biomass burning aerosols in most climate models are too absorbing. *Nat. Commun.*, 12: 277. DOI: https://doi.org/10.1038/s41467-020-20482-9

Bulatovic, I., Ekman, A.M.L., Savre, J., Riipinen, I. and **Leck, C.** (2019) Aerosol Indirect Effects in Marine Stratocumulus: The Importance of Explicitly Predicting Cloud Droplet Activation. *Geophys. Res. Lett.*, 46: 3473–3481. DOI: https://doi.org/10.1029/2018GL081746

Bulatovic, I., Igel, A.L., Leck, C., Heintzenberg, J., Riipinen, I. and **Ekman, A.M.L.** (2021) The importance of Aitken mode aerosol particles for cloud sustenance in the summertime high Arctic – a simulation study supported by observational data. *Atmospheric Chem. Phys.*, 21: 3871–3897. DOI: https://doi.org/10.5194/acp-21-3871-2021

Burgos, M.A., Andrews, E., Titos, G., Benedetti, A., Bian, H., Buchard, V., Curci, G., Kipling, Z., Kirkevåg, A., Kokkola, H., Laakso, A., Letertre-Danczak, J., Lund, M.T., Matsui, H., Myhre, G., Randles, C., Schulz, M., van Noije, T., Zhang, K., Alados-Arboledas, L., Baltensperger, U., Jefferson, A., Sherman, J., Sun, J., Weingartner, E. and **Zieger, P.** (2020) A global model–measurement evaluation of particle light scattering coefficients at elevated relative humidity. *Atmospheric Chem. Phys.*, 20: 10231–10258. DOI: https://doi.org/10.5194/acp-20-10231-2020

Burrows, S.M., McCluskey, C.S., Cornwell, G., Steinke, I., Zhang, K., Zhao, B., Zawadowicz, M., Raman, A., Kulkarni, G., China, S., Zelenyuk, A. and **DeMott, P.J.** (2022) Ice-Nucleating Particles That Impact Clouds and Climate: Observational and Modeling Research Needs. *Rev. Geophys.*, 60: e2021RG000745. DOI: https://doi.org/10.1029/2021RG000745

Cai, J., Sulo, J., Gu, Y., Holm, S., Cai, R., Thomas, S., Neuberger, A., Mattsson, F., Paglione, M., Decesari, S., Rinaldi, M., Yin, R., Aliaga, D., Huang, W., Li, Y., Gramlich, Y., Ciarelli, G., Quéléver, L., Sarnela, N., Lehtipalo, K., Zannoni, N., Wu, C., Nie, W., Kangasluoma, J., Mohr, C., Kulmala, M., Zha, Q., Stolzenburg, D. and **Bianchi, F.** (2024) Elucidating the mechanisms of atmospheric new particle formation in the highly polluted Po Valley, Italy. *Atmospheric Chem. Phys.*, 24: 2423–2441. DOI: https://doi.org/10.5194/acp-24-2423-2024

Calderón, S.M., Tonttila, J., Buchholz, A., Joutsensaari, J., Komppula, M., Leskinen, A., Hao, L., Moisseev, D., Pullinen, I., Tiitta, P., Xu, J., Virtanen, A., Kokkola, H. and **Romakkaniemi, S.** (2022) Aerosol–stratocumulus interactions: towards a better process understanding using closures between observations and large eddy simulations. *Atmospheric Chem. Phys.*, 22: 12417–12441. DOI: https://doi.org/10.5194/acp-22-12417-2022

Capaldo, K.P., Pilinis, C. and **Pandis, S.N.** (2000) A computationally efficient hybrid approach for dynamic gas/aerosol transfer in air quality models. *Atmos. Environ.*,

34: 3617–3627. DOI: https://doi.org/10.1016/S1352-2310(00)00092-3

Carlton, A.G. and **Turpin, B.J.** (2013) Particle partitioning potential of organic compounds is highest in the Eastern US and driven by anthropogenic water. *Atmospheric Chem. Phys.*, 13: 10203–10214. DOI: https://doi.org/10.5194/acp-13-10203-2013

Carslaw, K. (ed.) (2022) Aerosols and Climate, Elsevier.

Carslaw, K.S., Lee, L.A., Reddington, C.L., Pringle, K.J., Rap, A., Forster, P.M., Mann, G.W., Spracklen, D.V., Woodhouse, M.T., Regayre, L.A. and **Pierce, J.R.** (2013) Large contribution of natural aerosols to uncertainty in indirect forcing. *Nature*, 503: 67–71. https://doi.org/10.1038/nature12674

Carter, T.S., Heald, C.L., Cappa, C.D., Kroll, J.H., Campos, T.L., Coe, H., Cotterell, M.I., Davies, N.W., Farmer, D.K., Fox, C., Garofalo, L.A., Hu, L., Langridge, J.M., Levin, E.J.T., Murphy, S.M., Pokhrel, R.P., Shen, Y., Szpek, K., Taylor, J.W. and **Wu, H.** (2021) Investigating Carbonaceous Aerosol and Its Absorption Properties From Fires in the Western United States (WE-CAN) and Southern Africa (ORACLES and CLARIFY). *J. Geophys. Res. Atmospheres*, 126: e2021JD034984. DOI: https://doi.org/10.1029/2021JD034984

Chakrabarty, R.K., Shetty, N.J., Thind, A.S., Beeler, P., Sumlin, B.J., Zhang, C., Liu, P., Idrobo, J.C., Adachi, K., Wagner, N.L., Schwarz, J.P., Ahern, A., Sedlacek, A.J., Lambe, A., Daube, C., Lyu, M., Liu, C., Herndon, S., Onasch, T.B. and **Mishra, R.** (2023) Shortwave absorption by wildfire smoke dominated by dark brown carbon. *Nat. Geosci.*, 16: 683–688. DOI: https://doi.org/10.1038/s41561-023-01237-9

Chandrakar, K.K., Cantrell, W., Chang, K., Ciochetto, D., Niedermeier, D., Ovchinnikov, M., Shaw, R.A. and **Yang, F.** (2016) Aerosol indirect effect from turbulence-induced broadening of cloud-droplet size distributions. *Proc. Natl. Acad. Sci.*, 113: 14243–14248. DOI: https://doi.org/10.1073/pnas.1612686113

Chatziparaschos, M., Daskalakis, N., Myriokefalitakis, S., Kalivitis, N., Nenes, A., Gonçalves Ageitos, M., Costa-Surós, M., Pérez García-Pando, C., Zanoli, M., Vrekoussis, M. and **Kanakidou, M.** (2023) Role of K-feldspar and quartz in global ice nucleation by mineral dust in mixed-phase clouds. *Atmospheric Chem. Phys.*, 23: 1785–1801. DOI: https://doi.org/10.5194/acp-23-1785-2023

Chatziparaschos, M., Myriokefalitakis, S., Kalivitis, N., Daskalakis, N., Nenes, A., Gonçalves Ageitos, M., Costa-Surós, M., Pérez García-Pando, C., Vrekoussis, M. and **Kanakidou, M.** (2025) Assessing the global contribution of marine aerosols, terrestrial bioaerosols, and desert dust to ice-nucleating particle concentrations. *Atmospheric Chem. Phys.*, 25: 9085–9111. DOI: https://doi.org/10.5194/acp-25-9085-2025

Chen, Y.-C., Christensen, M.W., Stephens, G.L. and **Seinfeld, J.H.** (2014) Satellite-based estimate of global aerosol–cloud radiative forcing by marine warm clouds. *Nat. Geosci.*, 7: 643–646. DOI: https://doi.org/10.1038/ngeo2214

Christensen, M.W., Gettelman, A., Cermak, J., Dagan, G., Diamond, M., Douglas, A., Feingold, G., Glassmeier, F., Goren, T., Grosvenor, D.P., Gryspeerdt, E., Kahn, R., Li, Z., Ma, P.-L., Malavelle, F., McCoy, I.L., McCoy, D.T., McFarquhar, G., Mülmenstädt, J., Pal, S., Possner, A., Povey, A., Quaas, J., Rosenfeld, D., Schmidt, A., Schrödner, R., Sorooshian, A., Stier, P., Toll, V., Watson-Parris, D., Wood, R., Yang, M. and **Yuan, T.** (2022) Opportunistic experiments to constrain aerosol effective radiative forcing. *Atmospheric Chem. Phys.*, 22: 641–674. DOI: https://doi.org/10.5194/acp-22-641-2022

Ciarelli, G., Aksoyoglu, S., Crippa, M., Jimenez, J.-L., Nemitz, E., Sellegri, K., Äijälä, M., Carbone, S., Mohr, C., O'Dowd, C., Poulain, L., Baltensperger, U. and **Prévôt, A.S.H.** (2016) Evaluation of European air quality modelled by CAMx including the volatility basis set scheme. *Atmospheric Chem. Phys.*, 16: 10313–10332. DOI: https://doi.org/10.5194/acp-16-10313-2016

Claquin, T., Schulz, M. and **Balkanski, Y.J.** (1999) Modeling the mineralogy of atmospheric dust sources. *J. Geophys. Res. Atmospheres*, 104: 22243–22256. DOI: https://doi.org/10.1029/1999JD900416

Clark, R.N., Swayze, G.A., Livo, K.E., Brodrick, P.G., Dobrea, E.N., Vijayarangan, S., Green, R.O., Wettergreen, D., Candela, A., Hendrix, A., García-Pando, C.P., Pearson, N.C., Lane, M.D., González-Romero, A., Querol, X. and **Teams, the EMIT and TREX.** (2024) Imaging Spectroscopy: Earth and Planetary Remote Sensing with the PSI Tetracorder and Expert Systems from Rovers to EMIT and Beyond. *Planet. Sci. J.*, 5: 276. DOI: https://doi.org/10.3847/PSJ/ad6c3a

Cremer, R.S., Kim, P., Blichner, S.M., Tovazzi, E., Johnson, B., Kipling, Z., Kühn, T., Watson-Parris, D., Neubauer, D., Stier, P., Sellar, A., Holopainen, E., Riipinen, I. and **Partridge, D.G.** (2024) Investigating the role of air mass history of Arctic black carbon in GCMs, EGU24. DOI: https://doi.org/10.5194/egusphere-egu24-18277

Curtius, J., Heinritzi, M., Beck, L.J., Lelieveld, J. *et al.* (2024) Isoprene nitrates drive new particle formation in Amazon's upper troposphere. *Nature*, 636: 124–130. DOI: https://doi.org/10.1038/s41586-024-08192-4

Dada, L., Lehtipalo, K., Kontkanen, J., Nieminen, T., Baalbaki, R., Ahonen, L., Duplissy, J., Yan, C., Chu, B., Petäjä, T., Lehtinen, K., Kerminen, V.-M., Kulmala, M. and **Kangasluoma, J.** (2020) Formation and growth of sub-3-nm aerosol particles in experimental chambers. *Nat. Protoc.*, 15: 1013–1040. DOI: https://doi.org/10.1038/s41596-019-0274-z

Dada, L., Okuljar, M., Shen, J., Olin, M., Wu, Y., Heimsch, L., Herlin, I., Kankaanrinta, S., Lampimäki, M., Kalliokoski, J., Baalbaki, R., Lohila, A., Petäjä, T., Maso, M.D., Duplissy, J., Kerminen, V.-M. and **Kulmala, M.** (2023b) The synergistic role of sulfuric acid, ammonia and organics in particle formation over an agricultural land. *Environ. Sci. Atmospheres*, 3: 1195–1211. DOI: https://doi.org/10.1039/D3EA00065F

Dada, L., Paasonen, P., Nieminen, T., Buenrostro Mazon, S., Kontkanen, J., Peräkylä, O., Lehtipalo, K., Hussein, T., Petäjä, T., Kerminen, V.M., Bäck, J. and **Kulmala, M.** (2017) Long-term analysis of clear-sky new particle formation events and nonevents in Hyytiälä. *Atmos. Chem. Phys.*, 17: 6227–6241. DOI: https://doi.org/10.5194/acp-17-6227-2017

Dada, L., Stolzenburg, D., Simon, M., Kulmala, M., *et al.* (2023a) Role of sesquiterpenes in biogenic new particle formation. *Sci. Adv.*, 9. DOI: https://doi.org/10.1126/sciadv.adi5297

Danabasoglu, G., Lamarque, J.-F., Bacmeister, J., Bailey, D.A., DuVivier, A.K., Edwards, J., Emmons, L.K., Fasullo, J., Garcia, R., Gettelman, A., Hannay, C., Holland, M.M., Large, W.G., Lauritzen, P.H., Lawrence, D.M., Lenaerts, J.T.M., Lindsay, K., Lipscomb, W.H., Mills, M.J., Neale, R., Oleson, K.W., Otto-Bliesner, B., Phillips, A.S., Sacks, W., Tilmes, S., van Kampenhout, L., Vertenstein, M., Bertini, A., Dennis, J., Deser, C., Fischer, C., Fox-Kemper, B., Kay, J.E., Kinnison, D., Kushner, P.J., Larson, V.E., Long, M.C., Mickelson, S., Moore, J.K., Nienhouse, E., Polvani, L., Rasch, P.J. and **Strand, W.G.** (2020) The Community Earth System Model Version 2 (CESM2). *J. Adv. Model. Earth Syst.*, 12: e2019MS001916. DOI: https://doi.org/10.1029/2019MS001916

Dedekind, Z., Proske, U., Ferrachat, S., Lohmann, U. and **Neubauer, D.** (2024) Simulating the seeder–feeder impacts on cloud ice and precipitation over the Alps. *Atmospheric Chem. Phys.*, 24: 5389–5404. DOI: https://doi.org/10.5194/acp-24-5389-2024

DeMott, P.J., Prenni, A.J., Liu, X., Kreidenweis, S.M., Petters, M.D., Twohy, C.H., Richardson, M.S., Eidhammer, T. and **Rogers, D.C.** (2010) Predicting global atmospheric ice nuclei distributions and their impacts on climate. *Proc. Natl. Acad. Sci.*, 107: 11217–11222. DOI: https://doi.org/10.1073/pnas.0910818107

Denier van der Gon, H. a. C., Bergström, R., Fountoukis, C., Johansson, C., Pandis, S.N., Simpson, D. and **Visschedijk, A.J.H.** (2015) Particulate emissions from residential wood combustion in Europe – revised estimates and an evaluation. *Atmospheric Chem. Phys.*, 15: 6503–6519. DOI: https://doi.org/10.5194/acp-15-6503-2015

Deshmukh, A., Phillips, V.T.J., Bansemer, A., Patade, S. and **Waman, D.** (2022) New Empirical Formulation for the Sublimational Breakup of Graupel and Dendritic Snow. *J. Atmos. Sci.*, 79: 317–336. DOI: https://doi.org/10.1175/JAS-D-20-0275.1

Di Biagio, C., Boucher, H., Caquineau, S., Chevaillier, S., Cuesta, J. and **Formenti, P.** (2014) Variability of the infrared complex refractive index of African mineral dust: experimental estimation and implications for radiative transfer and satellite remote sensing. *Atmospheric Chem. Phys.*, 14: 11093–11116. DOI: https://doi.org/10.5194/acp-14-11093-2014

Di Biagio, C., Formenti, P., Balkanski, Y., Caponi, L., Cazaunau, M., Pangui, E., Journet, E., Nowak, S., Andreae, M.O., Kandler, K., Saeed, T., Piketh, S., Seibert, D., Williams, E. and **Doussin, J.-F.** (2019) Complex refractive indices and single-scattering albedo of global dust aerosols in the shortwave spectrum and relationship to size and iron content. *Atmospheric Chem. Phys.*, 19: 15503–15531. DOI: https://doi.org/10.5194/acp-19-15503-2019

Di Biagio, C., Formenti, P., Balkanski, Y., Caponi, L., Cazaunau, M., Pangui, E., Journet, E., Nowak, S., Caquineau, S., Andreae, M.O., Kandler, K., Saeed, T., Piketh, S., Seibert, D., Williams, E. and **Doussin, J.-F.** (2017) Global scale variability of the mineral dust long-wave refractive index: a new dataset of in situ measurements for climate modeling and remote sensing. *Atmospheric Chem. Phys.*, 17: 1901–1929. DOI: https://doi.org/10.5194/acp-17-1901-2017

Digby, R.A.R., von Salzen, K., Monahan, A.H., Gillett, N.P. and **Li, J.** (2025) The impact of uncertainty in black carbon's refractive index on simulated optical depth and radiative forcing. *Atmospheric Chem. Phys.*, 25: 3109–3130. DOI: https://doi.org/10.5194/acp-25-3109-2025

Donahue, N.M., Epstein, S.A., Pandis, S.N. and **Robinson, A.L.** (2011) A two-dimensional volatility basis set: 1. organic-aerosol mixing thermodynamics. *Atmospheric Chem. Phys.*, 11: 3303–3318. DOI: https://doi.org/10.5194/acp-11-3303-2011

Donahue, N.M., Robinson, A.L., Stanier, C.O. and **Pandis, S.N.** (2006) Coupled Partitioning, Dilution, and Chemical Aging of Semivolatile Organics. *Environ. Sci. Technol.*, 40: 2635–2643. DOI: https://doi.org/10.1021/es052297c

Döscher, R., Acosta, M., Alessandri, A., Zhang, Q., *et al.* (2022) The EC-Earth3 Earth system model for the Coupled Model Intercomparison Project 6. *Geosci. Model Dev.*, 15: 2973–3020. DOI: https://doi.org/10.5194/gmd-15-2973-2022

Drugé, T., Nabat, P., Michou, M. and **Mallet, M.** (2025) Radiative and climate effects of aerosol scattering in long-wave radiation based on global climate modelling. *Atmospheric Chem. Phys.*, 25: 11651–11671. DOI: https://doi.org/10.5194/acp-25-11651-2025

Dunne, E.M., Gordon, H., Kürten, A., Carslaw, K.S., *et al.* (2016) Global atmospheric particle formation from CERN CLOUD measurements. *Science*, 354: 1119–1124. DOI: https://doi.org/10.1126/science.aaf2649

Dunne, E.M., Mikkonen, S., Kokkola, H. and **Korhonen, H.** (2014) A global process-based study of marine CCN trends and variability. *Atmospheric Chem. Phys.*, 14: 13631–13642. DOI: https://doi.org/10.5194/acp-14-13631-2014

Dusek, U., Frank, G.P., Hildebrandt, L., Curtius, J., Schneider, J., Walter, S., Chand, D., Drewnick, F., Hings, S., Jung, D., Borrmann, S. and **Andreae, M.O.** (2006) Size Matters More Than Chemistry for Cloud-Nucleating Ability of Aerosol Particles. *Science*, 312: 1375–1378. DOI: https://doi.org/10.1126/science.1125261

Ehn, M., Thornton, J.A., Kleist, E., Sipilä, M., Junninen, H., Pullinen, I., Springer, M., Rubach, F., Tillmann, R., Lee, B., Lopez-Hilfiker, F., Andres, S., Acir, I.-H., Rissanen, M., Jokinen, T., Schobesberger, S., Kangasluoma, J., Kontkanen, J., Nieminen, T., Kurtén, T., Nielsen, L.B.,

Jørgensen, S., Kjaergaard, H.G., Canagaratna, M., Maso, M.D., Berndt, T., Petäjä, T., Wahner, A., Kerminen, V.-M., Kulmala, M., Worsnop, D.R., Wildt, J. and **Mentel, T.F.** (2014) A large source of low-volatility secondary organic aerosol. *Nature*, 506: 476–479. DOI: https://doi.org/10.1038/nature13032

Engelbrecht, J.P., Moosmüller, H., Pincock, S., Jayanty, R.K.M., Lersch, T. and **Casuccio, G.** (2016) Technical note: Mineralogical, chemical, morphological, and optical interrelationships of mineral dust re-suspensions. *Atmospheric Chem. Phys.*, 16: 10809–10830. DOI: https://doi.org/10.5194/acp-16-10809-2016

Enghoff, M.B. and **Svensmark, H.** (2008) The role of atmospheric ions in aerosol nucleation – a review. *Atmospheric Chem. Phys.*, 8: 4911–4923. DOI: https://doi.org/10.5194/acp-8-4911-2008

Ervens, B. (2015) Modeling the Processing of Aerosol and Trace Gases in Clouds and Fogs. *Chem. Rev.*, 115: 4157–4198. DOI: https://doi.org/10.1021/cr5005887

Ervens, B., Turpin, B.J. and **Weber, R.J.** (2011) Secondary organic aerosol formation in cloud droplets and aqueous particles (aqSOA): a review of laboratory, field and model studies. *Atmospheric Chem. Phys.*, 11: 11069–11102. DOI: https://doi.org/10.5194/acp-11-11069-2011

Eyring, V., Bony, S., Meehl, G.A., Senior, C.A., Stevens, B., Stouffer, R.J. and **Taylor, K.E.** (2016) Overview of the Coupled Model Intercomparison Project Phase 6 (CMIP6) experimental design and organization. *Geosci. Model Dev.*, 9: 1937–1958. DOI: https://doi.org/10.5194/gmd-9-1937-2016

Faiola, C. and **Taipale, D.** (2020) Impact of insect herbivory on plant stress volatile emissions from trees: A synthesis of quantitative measurements and recommendations for future research. *Atmospheric Environ. X*, 5: 100060. DOI: https://doi.org/10.1016/j.aeaoa.2019.100060

Fairlie, T.D., Jacob, D.J., Dibb, J.E., Alexander, B., Avery, M.A., van Donkelaar, A. and **Zhang, L.** (2010) Impact of mineral dust on nitrate, sulfate, and ozone in transpacific Asian pollution plumes. *Atmospheric Chem. Phys.*, 10: 3999–4012. DOI: https://doi.org/10.5194/acp-10-3999-2010

Fan, X., Cai, F., Xu, C., Yu, X., Wang, Y., Xiao, X., Ji, W., Cao, T., Song, J. and **Peng, P.** (2021) Molecular weight-dependent abundance, absorption, and fluorescence characteristics of water-soluble organic matter in atmospheric aerosols. *Atmos. Environ.*, 247: 118159. DOI: https://doi.org/10.1016/j.atmosenv.2020.118159

Fanourgakis, G.S., Kanakidou, M., Nenes, A., Bauer, S.E., Bergman, T., Carslaw, K.S., Grini, A., Hamilton, D.S., Johnson, J.S., Karydis, V.A., Kirkevåg, A., Kodros, J.K., Lohmann, U., Luo, G., Makkonen, R., Matsui, H., Neubauer, D., Pierce, J.R., Schmale, J., Stier, P., Tsigaridis, K., van Noije, T., Wang, H., Watson-Parris, D., Westervelt, D.M., Yang, Y., Yoshioka, M., Daskalakis, N., Decesari, S., Gysel-Beer, M., Kalivitis, N., Liu, X., Mahowald, N.M., Myriokefalitakis, S., Schrödner, R., Sfakianaki, M., Tsimpidi, A.P., Wu, M. and **Yu, F.** (2019) Evaluation of global simulations of aerosol particle and cloud condensation nuclei number, with implications for cloud droplet formation. *Atmospheric Chem. Phys.*, 19: 8591–8617. DOI: https://doi.org/10.5194/acp-19-8591-2019

Farina, S.C., Adams, P.J. and **Pandis, S.N.** (2010) Modeling global secondary organic aerosol formation and processing with the volatility basis set: Implications for anthropogenic secondary organic aerosol. *J. Geophys. Res. Atmospheres*, 115. DOI: https://doi.org/10.1029/2009JD013046

Feichter, J., Kjellström, E., Rodhe, H., Dentener, F., Lelieveldi, J. and **Roelofs, G.-J.** (1996) Simulation of the tropospheric sulfur cycle in a global climate model. *Atmos. Environ.*, 30: 1693–1707. DOI: https://doi.org/10.1016/1352-2310(95)00394-0

Feingold, G. and **Kreidenweis, S.** (2000) Does cloud processing of aerosol enhance droplet concentrations? *J. Geophys. Res. Atmospheres*, 105: 24351–24361. DOI: https://doi.org/10.1029/2000JD900369

Feingold, G., McComiskey, A., Rosenfeld, D. and **Sorooshian, A.** (2013) On the relationship between cloud contact time and precipitation susceptibility to aerosol. *J. Geophys. Res. Atmospheres*, 118: 10,544–10,554. DOI: https://doi.org/10.1002/jgrd.50819

Feingold, G., Remer, L.A., Ramaprasad, J. and **Kaufman, Y.J.** (2001) Analysis of smoke impact on clouds in Brazilian biomass burning regions: An extension of Twomey's approach. *J. Geophys. Res. Atmospheres*, 106: 22907–22922. DOI: https://doi.org/10.1029/2001JD000732

Feng, Y., Ramanathan, V. and **Kotamarthi, V.R.** (2013) Brown carbon: a significant atmospheric absorber of solar radiation? *Atmospheric Chem. Phys.*, 13: 8607–8621. DOI: https://doi.org/10.5194/acp-13-8607-2013

Fenter, F.F., Caloz, F. and **Rossi, M.J.** (1995) Experimental evidence for the efficient "dry deposition" of nitric acid on calcite. *Atmos. Environ.*, 29: 3365–3372. DOI: https://doi.org/10.1016/1352-2310(95)00183-Y

Fiddes, S.L., Mallet, M.D., Protat, A., Woodhouse, M.T., Alexander, S.P. and **Furtado, K.** (2024) A machine learning approach for evaluating Southern Ocean cloud radiative biases in a global atmosphere model. *Geosci. Model Dev.*, 17: 2641–2662. DOI: https://doi.org/10.5194/gmd-17-2641-2024

Field, P.R., Lawson, R.P., Brown, P.R.A., Lloyd, G., Westbrook, C., Moisseev, D., Miltenberger, A., Nenes, A., Blyth, A., Choularton, T., Connolly, P., Buehl, J., Crosier, J., Cui, Z., Dearden, C., DeMott, P., Flossmann, A., Heymsfield, A., Huang, Y., Kalesse, H., Kanji, Z.A., Korolev, A., Kirchgaessner, A., Lasher-Trapp, S., Leisner, T., McFarquhar, G., Phillips, V., Stith, J. and **Sullivan, S.** (2017) Secondary Ice Production: Current State of the Science and Recommendations for the Future. *Meteorol. Monogr.*, 58: 7.1–7.20. DOI: https://doi.org/10.1175/AMSMONOGRAPHS-D-16-0014.1

Forrister, H., Liu, J., Scheuer, E., Dibb, J., Ziemba, L., Thornhill, K.L., Anderson, B., Diskin, G., Perring, A.E., Schwarz, J.P., Campuzano-Jost, P., Day, D.A., Palm, B.B., Jimenez, J.L., Nenes, A. and **Weber, R.J.** (2015) Evolution of brown

carbon in wildfire plumes. *Geophys. Res. Lett.*, 42: 4623–4630. DOI: https://doi.org/10.1002/2015GL063897

Forster, P., Storelvmo, T., Armour, K., Collins, W., Dufresne, J.-L., Frame, D., Lunt, D.J., Mauritsen, T., Palmer, M.D., Watanabe, M., Wild, M. and **Zhang, H.** (2021) The Earth's Energy Budget, Climate Feedbacks and Climate Sensitivity, in Masson-Delmotte, V., Zhai, P., Pirani, A., Connors, S.L., Péan, C., Berger, S., Caud, N., Chen, Y., Goldfarb, L., Gormis, M.I., Huang, M., Leitzell, K., Lonnoy, E., Matthews, J.B.R., Maycock, T.K., Waterfield, T., Yelekçi, O., Yu, R. and Zhou, B. (eds.) *Climate Change 2021 – The Physical Science Basis: Working Group I Contribution to the Sixth Assessment Report of the Intergovernmental Panel on Climate Change*. Cambridge: Cambridge University Press. pp. 923–1054. DOI: https://doi.org/10.1017/9781009157896.009

Fountoukis, C. and **Nenes, A.** (2005) Continued development of a cloud droplet formation parameterization for global climate models. *J. Geophys. Res. Atmospheres*, 110. DOI: https://doi.org/10.1029/2004JD005591

Fountoukis, C. and **Nenes, A.** (2007) ISORROPIA II: a computationally efficient thermodynamic equilibrium model for K^+–Ca^{2+}–Mg^{2+}–$NH4^+$–Na^+–SO_4^{2-}–NO_3^-–Cl^-–H_2O aerosols. *Atmospheric Chem. Phys.*, 7: 4639–4659. DOI: https://doi.org/10.5194/acp-7-4639-2007

Frey, L., Höpner, F., Kirkevåg, A. and **Bender, F. a.-M.** (2021) Absorbing aerosols over Asia – an inter-model and model-observation comparison study using CAM5.3-Oslo. *Tellus B Chem. Phys. Meteorol.*, 73: 1–25. DOI: https://doi.org/10.1080/16000889.2021.1909815

Fukuta, N. and **Schaller, R.C.** (1982) Ice Nucleation by Aerosol Particles. Theory of Condensation-Freezing Nucleation. *J. Atmos. Sci.*, 39: 648–655. DOI: https://doi.org/10.1175/1520-0469(1982)039<0648:INBAPT>2.0.CO;2

Fuzzi, S., Baltensperger, U., Carslaw, K., Decesari, S., Denier van der Gon, H., Facchini, M.C., Fowler, D., Koren, I., Langford, B., Lohmann, U., Nemitz, E., Pandis, S., Riipinen, I., Rudich, Y., Schaap, M., Slowik, J.G., Spracklen, D.V., Vignati, E., Wild, M., Williams, M. and **Gilardoni, S.** (2015) Particulate matter, air quality and climate: lessons learned and future needs. *Atmospheric Chem. Phys.*, 15: 8217–8299. DOI: https://doi.org/10.5194/acp-15-8217-2015

Geerts, B., Pokharel, B. and **Kristovich, D.A.R.** (2015) Blowing Snow as a Natural Glaciogenic Cloud Seeding Mechanism. *Mon. Weather Rev.*, 143: 5017–5033. DOI: https://doi.org/10.1175/MWR-D-15-0241.1

Georgakaki, P., Billault-Roux, A.-C., Foskinis, R., Gao, K., Sotiropoulou, G., Gini, M., Takahama, S., Eleftheriadis, K., Papayannis, A., Berne, A. and **Nenes, A.** (2024) Unraveling ice multiplication in winter orographic clouds via in-situ observations, remote sensing and modeling. *Npj Clim. Atmospheric Sci.*, 7: 1–13. DOI: https://doi.org/10.1038/s41612-024-00671-9

Georgakaki, P. and **Nenes, A.** (2024) RaFSIP: Parameterizing Ice Multiplication in Models Using a Machine Learning Approach. *J. Adv. Model. Earth Syst.*, 16: e2023MS003923. DOI: https://doi.org/10.1029/2023MS003923

Georgakaki, P., Sotiropoulou, G. and **Nenes, A.** (2024) Updated Morrison cloud microphysics scheme for WRF including ice multiplication processes. DOI: https://doi.org/10.5281/zenodo.13257172

Georgakaki, P., Sotiropoulou, G., Vignon, É., Billault-Roux, A.-C., Berne, A. and **Nenes, A.** (2022) Secondary ice production processes in wintertime alpine mixed-phase clouds. *Atmospheric Chem. Phys.*, 22: 1965–1988. DOI: https://doi.org/10.5194/acp-22-1965-2022

Gettelman, A., Mills, M.J., Kinnison, D.E., Garcia, R.R., Smith, A.K., Marsh, D.R., Tilmes, S., Vitt, F., Bardeen, C.G., McInerny, J., Liu, H.-L., Solomon, S.C., Polvani, L.M., Emmons, L.K., Lamarque, J.-F., Richter, J.H., Glanville, A.S., Bacmeister, J.T., Phillips, A.S., Neale, R.B., Simpson, I.R., DuVivier, A.K., Hodzic, A. and **Randel, W.J.** (2019) The Whole Atmosphere Community Climate Model Version 6 (WACCM6). *J. Geophys. Res. Atmospheres*, 124: 12380–12403. DOI: https://doi.org/10.1029/2019JD030943

Gettelman, A. and **Morrison, H.** (2015) Advanced Two-Moment Bulk Microphysics for Global Models. Part I: Off-Line Tests and Comparison with Other Schemes. *J. Climate*, 28: 1268–1287. DOI: https://doi.org/10.1175/JCLI-D-14-00102.1

Ghan, S.J., Abdul-Razzak, H., Nenes, A., Ming, Y., Liu, X., Ovchinnikov, M., Shipway, B., Meskhidze, N., Xu, J. and **Shi, X.** (2011) Droplet nucleation: Physically-based parameterizations and comparative evaluation. *J. Adv. Model. Earth Syst.*, 3. DOI: https://doi.org/10.1029/2011MS000074

Ghosh, P., Evans, K.J., Grosvenor, D.P., Kang, H.-G., Mahajan, S., Xu, M., Zhang, W. and **Gordon, H.** (2025) Assessing modifications to the Abdul-Razzak and Ghan aerosol activation parameterization (version ARG2000) to improve simulated aerosol–cloud radiative effects in the UK Met Office Unified Model (UM version 13.0). *Geosci. Model Dev.*, 18: 4899–4913. DOI: https://doi.org/10.5194/gmd-18-4899-2025

Gilardoni, S., Massoli, P., Giulianelli, L., Rinaldi, M., Paglione, M., Pollini, F., Lanconelli, C., Poluzzi, V., Carbone, S., Hillamo, R., Russell, L.M., Facchini, M.C. and **Fuzzi, S.** (2014) Fog scavenging of organic and inorganic aerosol in the Po Valley. *Atmospheric Chem. Phys.*, 14: 6967–6981. DOI: https://doi.org/10.5194/acp-14-6967-2014

Glassmeier, F. and **Lohmann, U.** (2016) Constraining Precipitation Susceptibility of Warm-, Ice-, and Mixed-Phase Clouds with Microphysical Equations. *J. Atmospheric Sci.*, 73: 5003–5023. DOI: https://doi.org/10.1175/JAS-D-16-0008.1

Gonçalves Ageitos, M., Obiso, V., Miller, R.L., Jorba, O., Klose, M., Dawson, M., Balkanski, Y., Perlwitz, J., Basart, S., Di Tomaso, E., Escribano, J., Macchia, F., Montané, G., Mahowald, N.M., Green, R.O., Thompson, D.R. and **Pérez García-Pando, C.** (2023) Modeling dust mineralogical composition: sensitivity to soil mineralogy atlases and their expected climate impacts. *Atmospheric Chem. Phys.*, 23: 8623–8657. DOI: https://doi.org/10.5194/acp-23-8623-2023

Goodman, A.L., Bernard, E.T. and **Grassian, V.H.** (2001) Spectroscopic Study of Nitric Acid and Water Adsorption on Oxide Particles: Enhanced Nitric Acid Uptake Kinetics in the Presence of Adsorbed Water. *J. Phys. Chem. A*, 105: 6443–6457. DOI: https://doi.org/10.1021/jp003722l

Gordon, H., Kirkby, J., Baltensperger, U., Bianchi, F., Breitenlechner, M., Curtius, J., Dias, A., Dommen, J., Donahue, N.M., Dunne, E.M., Duplissy, J., Ehrhart, S., Flagan, R.C., Frege, C., Fuchs, C., Hansel, A., Hoyle, C.R., Kulmala, M., Kürten, A., Lehtipalo, K., Makhmutov, V., Molteni, U., Rissanen, M.P., Stozkhov, Y., Tröstl, J., Tsagkogeorgas, G., Wagner, R., Williamson, C., Wimmer, D., Winkler, P.M., Yan, C. and **Carslaw, K.S.** (2017) Causes and importance of new particle formation in the present-day and preindustrial atmospheres. *J. Geophys. Res. Atmospheres*, 122: 8739–8760. DOI: https://doi.org/10.1002/2017JD026844

Gordon, H., Sengupta, K., Rap, A., Carslaw, K.S. *et al.* (2016) Reduced anthropogenic aerosol radiative forcing caused by biogenic new particle formation. *Proc. Natl. Acad. Sci.*, 113: 12053–12058. DOI: https://doi.org/10.1073/pnas.1602360113

Graham, E.L., Wu, C., Bell, D.M., Bertrand, A., Haslett, S.L., Baltensperger, U., El Haddad, I., Krejci, R., Riipinen, I. and **Mohr, C.** (2023) Volatility of aerosol particles from NO_3 oxidation of various biogenic organic precursors. *Atmospheric Chem. Phys.*, 23: 7347–7362. DOI: https://doi.org/10.5194/acp-23-7347-2023

Graham, E.L., Zieger, P., Mohr, C., Wideqvist, U., Hennig, T., Ekman, A.M.L., Krejci, R., Ström, J. and **Riipinen, I.** (2020) Physical and chemical properties of aerosol particles and cloud residuals on Mt. Åreskutan in Central Sweden during summer 2014. *Tellus B Chem. Phys. Meteorol.*, 72: 1776080. DOI: https://doi.org/10.1080/16000889.2020.1776080

Gramlich, Y., Siegel, K., Haslett, S.L., Freitas, G., Krejci, R., Zieger, P. and **Mohr, C.** (2023) Revealing the chemical characteristics of Arctic low-level cloud residuals – in situ observations from a mountain site. *Atmospheric Chem. Phys.*, 23: 6813–6834. DOI: https://doi.org/10.5194/acp-23-6813-2023

Green, R.O., Mahowald, N., Thompson, D.R., Ung, C., Brodrick, P., Pollock, R., Bennett, M., Lundeen, S., Joyce, M., Olson- Duvall, W., Oaida, B., Bradley, C., Diaz, E., Clark, R., Vannan, S., Swayze, G., Kokaly, R., Ginoux, P., Miller, R., Okin, G., Garcia-Pando, C.P., Ehlmann, B., Kalashnikova, O., Painter, T.H., Realmuto, V., Chadwick, D., Ben-Dor, E., Pearlshtien, D.H., Guanter, L., Phillips, B., Reath, K., Thorpe, A., Shaw, L., Keebler, A., Ochoa, F., Grant, K., Sen, A., Duren, R., Obiso, V., Gonçalves-Ageitos, M. and **Huang, Y.** (2023) Performance and Early Results from the Earth Surface Mineral Dust Source Investigation (EMIT) Imaging Spectroscopy Mission. In: *2023 IEEE Aerospace Conference, 2023 IEEE Aerospace Conference*, pp. 1–10. DOI: https://doi.org/10.1109/AERO55745.2023.10115851

Griesche, H.J., Barrientos-Velasco, C., Deneke, H., Hünerbein, A., Seifert, P. and **Macke, A.** (2024) Low-level Arctic clouds: a blind zone in our knowledge of the radiation budget. *Atmospheric Chem. Phys.*, 24: 597–612. DOI: https://doi.org/10.5194/acp-24-597-2024

Griffin, R.J., Cocker III, D.R., Flagan, R.C. and **Seinfeld, J.H.** (1999) Organic aerosol formation from the oxidation of biogenic hydrocarbons. *J. Geophys. Res. Atmospheres*, 104: 3555–3567. DOI: https://doi.org/10.1029/1998JD100049

Gryspeerdt, E., Goren, T. and **Smith, T.W.P.** (2021) Observing the timescales of aerosol–cloud interactions in snapshot satellite images. *Atmospheric Chem. Phys.*, 21: 6093–6109. DOI: https://doi.org/10.5194/acp-21-6093-2021

Gryspeerdt, E., Goren, T., Sourdeval, O., Quaas, J., Mülmenstädt, J., Dipu, S., Unglaub, C., Gettelman, A. and **Christensen, M.** (2019) Constraining the aerosol influence on cloud liquid water path. *Atmospheric Chem. Phys.*, 19: 5331–5347. DOI: https://doi.org/10.5194/acp-19-5331-2019

Gryspeerdt, E., Quaas, J. and **Bellouin, N.** (2016) Constraining the aerosol influence on cloud fraction. *J. Geophys. Res. Atmospheres*, 121: 3566–3583. DOI: https://doi.org/10.1002/2015JD023744

Grzegorczyk, P., Yadav, S., Zanger, F., Theis, A., Mitra, S.K., Borrmann, S. and **Szakáll, M.** (2023) Fragmentation of ice particles: laboratory experiments on graupel–graupel and graupel–snowflake collisions. *Atmospheric Chem. Phys.*, 23: 13505–13521. DOI: https://doi.org/10.5194/acp-23-13505-2023

Guenther, A.B., Jiang, X., Heald, C.L., Sakulyanontvittaya, T., Duhl, T., Emmons, L.K. and **Wang, X.** (2012) The Model of Emissions of Gases and Aerosols from Nature version 2.1 (MEGAN2.1): an extended and updated framework for modeling biogenic emissions. *Geosci. Model Dev.*, 5: 1471–1492. DOI: https://doi.org/10.5194/gmd-5-1471-2012

Guo, H., Otjes, R., Schlag, P., Kiendler-Scharr, A., Nenes, A. and **Weber, R.J.** (2018) Effectiveness of ammonia reduction on control of fine particle nitrate. *Atmospheric Chem. Phys.*, 18: 12241–12256. DOI: https://doi.org/10.5194/acp-18-12241-2018

Guo, H., Xu, L., Bougiatioti, A., Cerully, K.M., Capps, S.L., Hite, J.R.J., Carlton, A.G., Lee, S.-H., Bergin, M.H., Ng, N.L., Nenes, A. and **Weber, R.J.** (2015) Fine-particle water and pH in the southeastern United States. *Atmospheric Chem. Phys.*, 15: 5211–5228. DOI: https://doi.org/10.5194/acp-15-5211-2015

Hallett, J. and **Mossop, S.C.** (1974) Production of secondary ice particles during the riming process. *Nature*, 249: 26–28. DOI: https://doi.org/10.1038/249026a0

Harrison, A.D., Lever, K., Sanchez-Marroquin, A., Holden, M.A., Whale, T.F., Tarn, M.D., McQuaid, J.B. and **Murray, B.J.** (2019) The ice-nucleating ability of quartz immersed in water and its atmospheric importance compared to K-feldspar. *Atmospheric Chem. Phys.*, 19: 11343–11361. DOI: https://doi.org/10.5194/acp-19-11343-2019

Harrison, A.D., Whale, T.F., Carpenter, M.A., Holden, M.A., Neve, L., O'Sullivan, D., Vergara Temprado, J. and **Murray, B.J.** (2016) Not all feldspars are equal: a survey of ice nucleating properties across the feldspar group of minerals. *Atmospheric Chem. Phys.*, 16: 10927–10940. DOI: https://doi.org/10.5194/acp-16-10927-2016

Hauglustaine, D.A., Balkanski, Y. and **Schulz, M.** (2014) A global model simulation of present and future nitrate aerosols and their direct radiative forcing of climate. *Atmospheric Chem. Phys.*, 14: 11031–11063. DOI: https://doi.org/10.5194/acp-14-11031-2014

Haugvaldstad, O.W., Olivié, D., Storelvmo, T. and **Schulz, M.** (2025) Dust radiative forcing in CMIP6 Earth System models: insights from the AerChemMIP piClim-2xdust experiment. *Atmospheric Chem. Phys.*, 25: 13199–13219. DOI: https://doi.org/10.5194/acp-25-13199-2025

He, X.-C., Simon, M., Iyer, S., Kulmala, M., *et al.* (2023) Iodine oxoacids enhance nucleation of sulfuric acid particles in the atmosphere. *Science*, 382: 1308–1314. DOI: https://doi.org/10.1126/science.adh2526

He, X.-C., Tham, Y.J., Dada, L., Sipilä, M., *et al.* (2021a) Role of iodine oxoacids in atmospheric aerosol nucleation. *Science*, 371: 589–595. DOI: https://doi.org/10.1126/science.abe0298

He, Y., Akherati, A., Nah, T., Ng, N.L., Garofalo, L.A., Farmer, D.K., Shiraiwa, M., Zaveri, R.A., Cappa, C.D., Pierce, J.R. and **Jathar, S.H.** (2021b) Particle Size Distribution Dynamics Can Help Constrain the Phase State of Secondary Organic Aerosol. *Environ. Sci. Technol.*, 55: 1466–1476. DOI: https://doi.org/10.1021/acs.est.0c05796

Heikkinen, L., Partridge, D.G., Blichner, S., Huang, W., Ranjan, R., Bowen, P., Tovazzi, E., Petäjä, T., Mohr, C. and **Riipinen, I.** (2024) Cloud response to co-condensation of water and organic vapors over the boreal forest. *Atmospheric Chem. Phys.*, 24: 5117–5147. DOI: https://doi.org/10.5194/acp-24-5117-2024

Heinritzi, M., Dada, L., Simon, M., Curtius, J., *et al.* (2020) Molecular understanding of the suppression of new-particle formation by isoprene. *Atmospheric Chem. Phys.*, 20: 11809–11821. DOI: https://doi.org/10.5194/acp-20-11809-2020

Henze, D.K. and **Seinfeld, J.H.** (2006) Global secondary organic aerosol from isoprene oxidation. *Geophys. Res. Lett.*, 33. DOI: https://doi.org/10.1029/2006GL025976

Herbert, R.J., Sanchez-Marroquin, A., Grosvenor, D.P., Pringle, K.J., Arnold, S.R., Murray, B.J. and **Carslaw, K.S.** (2025) Gaps in our understanding of ice-nucleating particle sources exposed by global simulation of the UK Earth System Model. *Atmospheric Chem. Phys.*, 25: 291–325. DOI: https://doi.org/10.5194/acp-25-291-2025

Heslin-Rees, D., Tunved, P., Ström, J., Cremer, R., Zieger, P., Riipinen, I., Ekman, A.M.L., Eleftheriadis, K. and **Krejci, R.** (2024) Increase in precipitation scavenging contributes to long-term reductions of light-absorbing aerosol in the Arctic. *Atmospheric Chem. Phys.*, 24: 2059–2075. DOI: https://doi.org/10.5194/acp-24-2059-2024

Hess, M., Koepke, P. and **Schult, I.** (1998) Optical Properties of Aerosols and Clouds: The Software Package OPAC, *Bull. Amer. Meteor. Soc.*, 79: 831–844. DOI: https://doi.org/10.1175/1520-0477(1998)079<0831:OPOAAC>2.0.CO;2

Heymsfield, A.J. and **Sabin, R.M.** (1989) Cirrus Crystal Nucleation by Homogeneous Freezing of Solution Droplets. *J. Atmos. Sci.*, 46: 2252–2264. DOI: https://doi.org/10.1175/1520-0469(1989)046<2252:CCNBHF>2.0.CO;2

Highwood, E.J., Northway, M.J., McMeeking, G.R., Morgan, W.T., Liu, D., Osborne, S., Bower, K., Coe, H., Ryder, C. and **Williams, P.** (2012) Aerosol scattering and absorption during the EUCAARI-LONGREX flights of the Facility for Airborne Atmospheric Measurements (FAAM) BAe-146: can measurements and models agree? *Atmospheric Chem. Phys.*, 12: 7251–7267. DOI: https://doi.org/10.5194/acp-12-7251-2012

Hodzic, A., Bessagnet, B. and **Vautard, R.** (2006) A model evaluation of coarse-mode nitrate heterogeneous formation on dust particles. *Atmos. Environ.*, 40: 4158–4171. DOI: https://doi.org/10.1016/j.atmosenv.2006.02.015

Hodzic, A., Campuzano-Jost, P., Bian, H., Chin, M., Colarco, P.R., Day, D.A., Froyd, K.D., Heinold, B., Jo, D.S., Katich, J.M., Kodros, J.K., Nault, B.A., Pierce, J.R., Ray, E., Schacht, J., Schill, G.P., Schroder, J.C., Schwarz, J.P., Sueper, D.T., Tegen, I., Tilmes, S., Tsigaridis, K., Yu, P. and **Jimenez, J.L.** (2020) Characterization of organic aerosol across the global remote troposphere: a comparison of ATom measurements and global chemistry models. *Atmospheric Chem. Phys.*, 20: 4607–4635. DOI: https://doi.org/10.5194/acp-20-4607-2020

Hodzic, A., Kasibhatla, P.S., Jo, D.S., Cappa, C.D., Jimenez, J.L., Madronich, S. and **Park, R.J.** (2016) Rethinking the global secondary organic aerosol (SOA) budget: stronger production, faster removal, shorter lifetime. *Atmospheric Chem. Phys.*, 16: 7917–7941. DOI: https://doi.org/10.5194/acp-16-7917-2016

Hoesly, R.M., Smith, S.J., Feng, L., Klimont, Z., Janssens-Maenhout, G., Pitkanen, T., Seibert, J.J., Vu, L., Andres, R.J., Bolt, R.M., Bond, T.C., Dawidowski, L., Kholod, N., Kurokawa, J., Li, M., Liu, L., Lu, Z., Moura, M.C.P., O'Rourke, P.R. and **Zhang, Q.** (2018) Historical (1750–2014) anthropogenic emissions of reactive gases and aerosols from the Community Emissions Data System (CEDS). *Geosci. Model Dev.*, 11: 369–408. DOI: https://doi.org/10.5194/gmd-11-369-2018

Holopainen, E., Kokkola, H., Faiola, C., Laakso, A. and **Kühn, T.** (2022) Insect Herbivory Caused Plant Stress Emissions Increases the Negative Radiative Forcing of Aerosols. *J. Geophys. Res. Atmospheres*, 127: e2022JD036733. DOI: https://doi.org/10.1029/2022JD036733

Holopainen, E., Kokkola, H., Laakso, A. and **Kühn, T.** (2020) In-cloud scavenging scheme for sectional aerosol modules – implementation in the framework of the Sectional Aerosol module for Large Scale Applications

version 2.0 (SALSA2.0) global aerosol module. *Geosci. Model Dev.*, 13: 6215–6235. DOI: https://doi.org/10.5194/gmd-13-6215-2020

Holopainen, J.K. and **Gershenzon, J.** (2010) Multiple stress factors and the emission of plant VOCs. *Trends Plant Sci.*, 15: 176–184. DOI: https://doi.org/10.1016/j.tplants.2010.01.006

Hoose, C. (2022) Another Piece of Evidence for Important but Uncertain Ice Multiplication Processes. *AGU Adv.*, 3: e2022AV000669. DOI: https://doi.org/10.1029/2022AV000669

Hoose, C., Kristjánsson, J.E., Chen, J.-P. and **Hazra, A.** (2010) A Classical-Theory-Based Parameterization of Heterogeneous Ice Nucleation by Mineral Dust, Soot, and Biological Particles in a Global Climate Model. *J. Atmospheric Sci.*, 67: 2483–2503. DOI: https://doi.org/10.1175/2010JAS3425.1

Hoose, C., Lohmann, U., Erdin, R. and **Tegen, I.** (2008) The global influence of dust mineralogical composition on heterogeneous ice nucleation in mixed-phase clouds. *Environ. Res. Lett.*, 3: 025003. DOI: https://doi.org/10.1088/1748-9326/3/2/025003

Hoose, C. and **Möhler, O.** (2012) Heterogeneous ice nucleation on atmospheric aerosols: a review of results from laboratory experiments. *Atmospheric Chem. Phys.*, 12: 9817–9854. DOI: https://doi.org/10.5194/acp-12-9817-2012

Hoppel, W.A., Frick, G.M. and **Larson, R.E.** (1986) Effect of nonprecipitating clouds on the aerosol size distribution in the marine boundary layer. *Geophys. Res. Lett.*, 13: 125–128. DOI: https://doi.org/10.1029/GL013i002p00125

Howell, W.E. (1949) The Growth of Cloud Drops in Uniformly Cooled Air. *Journal of Atmospheric Sciences*, 6(2): 134–149. DOI: https://doi.org/10.1175/1520-0469(1949)006<0134:TGOCDI>2.0.CO;2

Hsieh, W.C., Jonsson, H., Wang, L.-P., Buzorius, G., Flagan, R.C., Seinfeld, J.H. and **Nenes, A.** (2009) On the representation of droplet coalescence and autoconversion: Evaluation using ambient cloud droplet size distributions. *J. Geophys. Res. Atmospheres*, 114. DOI: https://doi.org/10.1029/2008JD010502

Hudson, J.G., Noble, S. and **Tabor, S.** (2015) Cloud supersaturations from CCN spectra Hoppel minima. *J. Geophys. Res. Atmospheres*, 120: 3436–3452. DOI: https://doi.org/10.1002/2014JD022669

Huijnen, V., Williams, J., van Weele, M., van Noije, T., Krol, M., Dentener, F., Segers, A., Houweling, S., Peters, W., de Laat, J., Boersma, F., Bergamaschi, P., van Velthoven, P., Le Sager, P., Eskes, H., Alkemade, F., Scheele, R., Nédélec, P. and **Pätz, H.-W.** (2010) The global chemistry transport model TM5: description and evaluation of the tropospheric chemistry version 3.0. *Geosci. Model Dev.*, 3: 445–473. DOI: https://doi.org/10.5194/gmd-3-445-2010

Ickes, L., Frostenberg, H., Surós, M.C., Georgakaki, P., Proske, U., Sotiropoulou, G., May, E., Ageitos, M.G., Eriksson, P., Lewinschall, A., Nenes, A., Neubauer, D., García-Pando, C.P. and **Sedland, Ø.** (2025) Dominant microphysical processes for mixed-phase clouds across climate models, EGU25, EGU General Assembly 2025, Vienna, Austria, 27 Apr–2 May 2025, EGU25–20620. DOI: https://doi.org/10.5194/egusphere-egu25-20620

Im, U., Tsigaridis, K., Faluvegi, G., Langen, P.L., French, J.P., Mahmood, R., Thomas, M.A., von Salzen, K., Thomas, D.C., Whaley, C.H., Klimont, Z., Skov, H. and **Brandt, J.** (2021) Present and future aerosol impacts on Arctic climate change in the GISS-E2.1 Earth system model. *Atmospheric Chem. Phys.*, 21: 10413–10438. DOI: https://doi.org/10.5194/acp-21-10413-2021

Irfan, M., Kühn, T., Yli-Juuti, T., Laakso, A., Holopainen, E., Worsnop, D.R., Virtanen, A. and **Kokkola, H.** (2024) A model study investigating the sensitivity of aerosol forcing to the volatilities of semi-volatile organic compounds. *Atmospheric Chem. Phys.*, 24: 8489–8506. DOI: https://doi.org/10.5194/acp-24-8489-2024

Isokääntä, S., Kim, P., Mikkonen, S., Kühn, T., Kokkola, H., Yli-Juuti, T., Heikkinen, L., Luoma, K., Petäjä, T., Kipling, Z., Partridge, D. and **Virtanen, A.** (2022) The effect of clouds and precipitation on the aerosol concentrations and composition in a boreal forest environment. *Atmospheric Chem. Phys.*, 22: 11823–11843. DOI: https://doi.org/10.5194/acp-22-11823-2022

James, R.L., Phillips, V.T.J. and **Connolly, P.J.** (2021) Secondary ice production during the break-up of freezing water drops on impact with ice particles. *Atmospheric Chem. Phys.*, 21: 18519–18530. DOI: https://doi.org/10.5194/acp-21-18519-2021

Järvinen, E., McCluskey, C.S., Waitz, F., Schnaiter, M., Bansemer, A., Bardeen, C.G., Gettelman, A., Heymsfield, A., Stith, J.L., Wu, W., D'Alessandro, J.J., McFarquhar, G.M., Diao, M., Finlon, J.A., Hill, T.C.J., Levin, E.J.T., Moore, K.A. and **DeMott, P.J.** (2022) Evidence for Secondary Ice Production in Southern Ocean Maritime Boundary Layer Clouds. *J. Geophys. Res. Atmospheres*, 127: e2021JD036411. DOI: https://doi.org/10.1029/2021JD036411

Jensen, J.B. and **Lee, S.** (2008) Giant Sea-Salt Aerosols and Warm Rain Formation in Marine Stratocumulus. *J. Atmos. Sci.*, 65: 3678–3694. DOI: https://doi.org/10.1175/2008JAS2617.1

Jensen, J.B. and **Nugent, A.D.** (2017) Condensational Growth of Drops Formed on Giant Sea-Salt Aerosol Particles. *J. Atmos. Sci.*, 74: 679–697. DOI: https://doi.org/10.1175/JAS-D-15-0370.1

Jeuken, A., Veefkind, J.P., Dentener, F., Metzger, S. and **Gonzalez, C.R.** (2001) Simulation of the aerosol optical depth over Europe for August 1997 and a comparison with observations. *J. Geophys. Res. Atmospheres*, 106: 28295–28311. DOI: https://doi.org/10.1029/2001JD900063

Jia, H., Ma, X., Yu, F. and **Quaas, J.** (2021) Significant underestimation of radiative forcing by aerosol–cloud interactions derived from satellite-based methods. *Nat. Commun.*, 12: 3649. DOI: https://doi.org/10.1038/s41467-021-23888-1

Jia, H., Quaas, J., Gryspeerdt, E., Böhm, C. and **Sourdeval, O.** (2022) Addressing the difficulties in quantifying droplet number response to aerosol from satellite observations. *Atmospheric Chem. Phys.*, 22: 7353–7372. DOI: https://doi.org/10.5194/acp-22-7353-2022

Jia, Y., Andersen, H. and **Cermak, J.** (2024) Analysis of the cloud fraction adjustment to aerosols and its dependence on meteorological controls using explainable machine learning. *Atmospheric Chem. Phys.*, 24: 13025–13045. DOI: https://doi.org/10.5194/acp-24-13025-2024

Jiang, J., Aksoyoglu, S., El-Haddad, I., Ciarelli, G., Denier van der Gon, H.A.C., Canonaco, F., Gilardoni, S., Paglione, M., Minguillón, M.C., Favez, O., Zhang, Y., Marchand, N., Hao, L., Virtanen, A., Florou, K., O'Dowd, C., Ovadnevaite, J., Baltensperger, U. and **Prévôt, A.S.H.** (2019) Sources of organic aerosols in Europe: a modeling study using CAMx with modified volatility basis set scheme. *Atmospheric Chem. Phys.*, 19: 15247–15270. DOI: https://doi.org/10.5194/acp-19-15247-2019

Jing, X., Suzuki, K. and **Michibata, T.** (2019) The Key Role of Warm Rain Parameterization in Determining the Aerosol Indirect Effect in a Global Climate Model. *J. Clim.*, 32: 4409–4430. DOI: https://doi.org/10.1175/JCLI-D-18-0789.1

Jo, D.S., Park, R.J., Lee, S., Kim, S.-W. and **Zhang, X.** (2016) A global simulation of brown carbon: implications for photochemistry and direct radiative effect. *Atmospheric Chem. Phys.*, 16: 3413–3432. DOI: https://doi.org/10.5194/acp-16-3413-2016

Jöckel, P., Tost, H., Pozzer, A., Brühl, C., Buchholz, J., Ganzeveld, L., Hoor, P., Kerkweg, A., Lawrence, M.G., Sander, R., Steil, B., Stiller, G., Tanarhte, M., Taraborrelli, D., van Aardenne, J. and **Lelieveld, J.** (2006) The atmospheric chemistry general circulation model ECHAM5/MESSy1: consistent simulation of ozone from the surface to the mesosphere. *Atmospheric Chem. Phys.*, 6: 5067–5104. DOI: https://doi.org/10.5194/acp-6-5067-2006

Johnson, D. (1982) The Role of Giant and Ultra-Giant Aerosol-Particles in Warm Rain Initiation. *J. Atmospheric Sci.*, 39: 448–460. DOI: https://doi.org/10.1175/1520-0469(1982)039<0448:TROGAU>2.0.CO;2

Journet, E., Balkanski, Y. and **Harrison, S.P.** (2014) A new data set of soil mineralogy for dust-cycle modeling. *Atmospheric Chem. Phys.*, 14: 3801–3816. DOI: https://doi.org/10.5194/acp-14-3801-2014

Kahn, R.A., Andrews, E., Brock, C.A., Chin, M., Feingold, G., Gettelman, A., Levy, R.C., Murphy, D.M., Nenes, A., Pierce, J.R., Popp, T., Redemann, J., Sayer, A.M., da Silva, A.M., Sogacheva, L. and **Stier, P.** (2023) Reducing Aerosol Forcing Uncertainty by Combining Models With Satellite and Within-The-Atmosphere Observations: A Three-Way Street. *Rev. Geophys.*, 61: e2022RG000796. DOI: https://doi.org/10.1029/2022RG000796

Kakavas, S. and **Pandis, S.N.** (2021) Effects of urban dust emissions on fine and coarse PM levels and composition. *Atmos. Environ.*, 246: 118006. DOI: https://doi.org/10.1016/j.atmosenv.2020.118006

Kakavas, S., Pandis, S.N. and **Nenes, A.** (2022) ISORROPIA-Lite: A Comprehensive Atmospheric Aerosol Thermodynamics Module for Earth System Models. *Tellus B Chem. Phys. Meteorol.*, 74: 1–23. DOI: https://doi.org/10.16993/tellusb.33

Kanakidou, M., Seinfeld, J.H., Pandis, S.N., Barnes, I., Dentener, F.J., Facchini, M.C., Van Dingenen, R., Ervens, B., Nenes, A., Nielsen, C.J., Swietlicki, E., Putaud, J.P., Balkanski, Y., Fuzzi, S., Horth, J., Moortgat, G.K., Winterhalter, R., Myhre, C.E.L., Tsigaridis, K., Vignati, E., Stephanou, E.G. and **Wilson, J.** (2005) Organic aerosol and global climate modelling: a review. *Atmospheric Chem. Phys.*, 5: 1053–1123. DOI: https://doi.org/10.5194/acp-5-1053-2005

Kanji, Z.A., Ladino, L.A., Wex, H., Boose, Y., Burkert-Kohn, M., Cziczo, D.J. and **Krämer, M.** (2017) Overview of Ice Nucleating Particles. *Meteor. Monogr.*, 58: 1.1–1.33. DOI: https://doi.org/10.1175/AMSMONOGRAPHS-D-16-0006.1

Karlsson, L., Krejci, R., Koike, M., Ebell, K. and **Zieger, P.** (2021) A long-term study of cloud residuals from low-level Arctic clouds. *Atmospheric Chem. Phys.*, 21: 8933–8959. DOI: https://doi.org/10.5194/acp-21-8933-2021

Karydis, V.A., Capps, S.L., Russell, A.G. and **Nenes, A.** (2012) Adjoint sensitivity of global cloud droplet number to aerosol and dynamical parameters. *Atmospheric Chem. Phys.*, 12: 9041–9055. DOI: https://doi.org/10.5194/acp-12-9041-2012

Karydis, V.A., Tsimpidi, A.P., Lei, W., Molina, L.T. and **Pandis, S.N.** (2011) Formation of semivolatile inorganic aerosols in the Mexico City Metropolitan Area during the MILAGRO campaign. *Atmospheric Chem. Phys.*, 11: 13305–13323. DOI: https://doi.org/10.5194/acp-11-13305-2011

Karydis, V.A., Tsimpidi, A.P., Pozzer, A., Astitha, M. and **Lelieveld, J.** (2016) Effects of mineral dust on global atmospheric nitrate concentrations. *Atmospheric Chem. Phys.*, 16: 1491–1509. DOI: https://doi.org/10.5194/acp-16-1491-2016

Karydis, V.A., Tsimpidi, A.P., Pozzer, A. and **Lelieveld, J.** (2021) How alkaline compounds control atmospheric aerosol particle acidity. *Atmospheric Chem. Phys.*, 21: 14983–15001. DOI: https://doi.org/10.5194/acp-21-14983-2021

Kazil, J. and **Lovejoy, E.R.** (2007) A semi-analytical method for calculating rates of new sulfate aerosol formation from the gas phase. *Atmospheric Chem. Phys.*, 7: 3447–3459. DOI: https://doi.org/10.5194/acp-7-3447-2007

Kazil, J., Stier, P., Zhang, K., Quaas, J., Kinne, S., O'Donnell, D., Rast, S., Esch, M., Ferrachat, S., Lohmann, U. and **Feichter, J.** (2010) Aerosol nucleation and its role for clouds and Earth's radiative forcing in the aerosol-climate model ECHAM5-HAM. *Atmospheric Chem. Phys.*, 10: 10733–10752. DOI: https://doi.org/10.5194/acp-10-10733-2010

Kecorius, S., Vogl, T., Paasonen, P., Lampilahti, J., Rothenberg, D., Wex, H., Zeppenfeld, S., van Pinxteren, M., Hartmann, M., Henning, S., Gong, X., Welti, A., Kulmala, M., Stratmann, F., Herrmann, H. and **Wiedensohler, A.** (2019) New particle formation and its effect on cloud condensation nuclei abundance in the summer Arctic: a case study in the Fram

Strait and Barents Sea. *Atmospheric Chem. Phys.*, 19: 14339–14364. DOI: https://doi.org/10.5194/acp-19-14339-2019

Kelesidis, G.A., Neubauer, D., Fan, L.-S., Lohmann, U. and **Pratsinis, S.E.** (2022) Enhanced Light Absorption and Radiative Forcing by Black Carbon Agglomerates. *Environ. Sci. Technol.*, 56: 8610–8618. DOI: https://doi.org/10.1021/acs.est.2c00428

Kerminen, V.-M., Chen, X., Vakkari, V., Petäjä, T., Kulmala, M. and **Bianchi, F.** (2018) Atmospheric new particle formation and growth: review of field observations. *Environ. Res. Lett.*, 13: 103003. DOI: https://doi.org/10.1088/1748-9326/aadf3c

Khairoutdinov, M. and **Kogan, Y.** (2000) *A New Cloud Physics Parameterization in a Large-Eddy Simulation Model of Marine Stratocumulus*.

Kiendler-Scharr, A., Wildt, J., Maso, M.D., Hohaus, T., Kleist, E., Mentel, T.F., Tillmann, R., Uerlings, R., Schurr, U. and **Wahner, A.** (2009) New particle formation in forests inhibited by isoprene emissions. *Nature*, 461: 381–384. DOI: https://doi.org/10.1038/nature08292

Kirkby, J., Amorim, A., Baltensperger, U., Carslaw, K.S., Christoudias, T., Curtius, J., Donahue, N.M., Haddad, I.E., Flagan, R.C., Gordon, H., Hansel, A., Harder, H., Junninen, H., Kulmala, M., Kürten, A., Laaksonen, A., Lehtipalo, K., Lelieveld, J., Möhler, O., Riipinen, I., Stratmann, F., Tomé, A., Virtanen, A., Volkamer, R., Winkler, P.M. and **Worsnop, D.R.** (2023) Atmospheric new particle formation from the CERN CLOUD experiment. *Nat. Geosci.*, 16: 948–957. DOI: https://doi.org/10.1038/s41561-023-01305-0

Kirkby, J., Curtius, J., Almeida, J., Kulmala, M., *et al.* (2011) Role of sulphuric acid, ammonia and galactic cosmic rays in atmospheric aerosol nucleation. *Nature*, 476: 429–433. DOI: https://doi.org/10.1038/nature10343

Kirkby, J., Duplissy, J., Sengupta, K., Curtius, J., *et al.* (2016) Ion-induced nucleation of pure biogenic particles. *Nature*, 533: 521–526. DOI: https://doi.org/10.1038/nature17953

Kirkevåg, A., Grini, A., Olivié, D., Seland, Ø., Alterskjær, K., Hummel, M., Karset, I.H.H., Lewinschal, A., Liu, X., Makkonen, R., Bethke, I., Griesfeller, J., Schulz, M. and **Iversen, T.** (2018) A production-tagged aerosol module for Earth system models, OsloAero5.3 – extensions and updates for CAM5.3-Oslo. *Geosci. Model Dev.*, 11: 3945–3982. DOI: https://doi.org/10.5194/gmd-11-3945-2018

Kirkevåg, A., Iversen, T., Seland, Ø., Hoose, C., Kristjánsson, J.E., Struthers, H., Ekman, A.M.L., Ghan, S., Griesfeller, J., Nilsson, E.D. and **Schulz, M.** (2013) Aerosol–climate interactions in the Norwegian Earth System Model – NorESM1-M. *Geosci. Model Dev.*, 6: 207–244. DOI: https://doi.org/10.5194/gmd-6-207-2013

Kittelson, D., Khalek, I., McDonald, J., Stevens, J. and **Giannelli, R.** (2022) Particle emissions from mobile sources: Discussion of ultrafine particle emissions and definition. *J. Aerosol Sci.*, 159: 105881. DOI: https://doi.org/10.1016/j.jaerosci.2021.105881

Kleinheins, J., Kiselev, A., Keinert, A., Kind, M. and **Leisner, T.** (2021) Thermal Imaging of Freezing Drizzle Droplets: Pressure Release Events as a Source of Secondary Ice Particles, *J. Atmos. Sci.*, 78: 1703–1713. DOI: https://doi.org/10.1175/JAS-D-20-0323.1

Klingmüller, K., Metzger, S., Abdelkader, M., Karydis, V.A., Stenchikov, G.L., Pozzer, A. and **Lelieveld, J.** (2018) Revised mineral dust emissions in the atmospheric chemistry–climate model EMAC (MESSy 2.52 DU_Astitha1 KKDU2017 patch). *Geosci. Model Dev.*, 11: 989–1008. DOI: https://doi.org/10.5194/gmd-11-989-2018

Knutti, R., Rugenstein, M.A.A. and **Hegerl, G.C.** (2017) Beyond equilibrium climate sensitivity. *Nat. Geosci.*, 10: 727–736. DOI: https://doi.org/10.1038/ngeo3017

Kodros, J.K., Papanastasiou, D.K., Paglione, M., Masiol, M., Squizzato, S., Florou, K., Skyllakou, K., Kaltsonoudis, C., Nenes, A. and **Pandis, S.N.** (2020) Rapid dark aging of biomass burning as an overlooked source of oxidized organic aerosol. *Proc. Natl. Acad. Sci.*, 117: 33028–33033. DOI: https://doi.org/10.1073/pnas.2010365117

Köhler, H. (1936) The nucleus in and the growth of hygroscopic droplets. *Trans. Faraday Soc.*, 32: 1152–1161. DOI: https://doi.org/10.1039/tf9363201152

Koike, M., Ukita, J., Ström, J., Tunved, P., Shiobara, M., Vitale, V., Lupi, A., Baumgardner, D., Ritter, C., Hermansen, O., Yamada, K. and **Pedersen, C.A.** (2019) Year-Round In Situ Measurements of Arctic Low-Level Clouds: Microphysical Properties and Their Relationships With Aerosols. *J. Geophys. Res. Atmospheres*, 124: 1798–1822. DOI: https://doi.org/10.1029/2018JD029802

Kok, J.F., Adebiyi, A.A., Albani, S., Balkanski, Y., Checa-Garcia, R., Chin, M., Colarco, P.R., Hamilton, D.S., Huang, Y., Ito, A., Klose, M., Li, L., Mahowald, N.M., Miller, R.L., Obiso, V., Pérez García-Pando, C., Rocha-Lima, A. and **Wan, J.S.** (2021) Contribution of the world's main dust source regions to the global cycle of desert dust. *Atmospheric Chem. Phys.*, 21: 8169–8193. DOI: https://doi.org/10.5194/acp-21-8169-2021

Kok, J.F., Gupta, A.K., Adebiyi, A.A., Albani, S., Balkanski, Y., Checa-Garcia, R., Colarco, P.R., Evan, A.T., Hamilton, D., Huang, Y., Ito, A., Klose, M., Li, L., Mahowald, N.M., Miller, R.L., Obiso, V., Garcia-Pando, C.P., Lima, A.R. and **Wan, J.** (2025) The longwave direct radiative forcing of desert dust. *105th AMS Annual Meeting*.

Kok, J.F., Ridley, D.A., Zhou, Q., Miller, R.L., Zhao, C., Heald, C.L., Ward, D.S., Albani, S. and **Haustein, K.** (2017) Smaller desert dust cooling effect estimated from analysis of dust size and abundance. *Nat. Geosci.*, 10: 274–278. DOI: https://doi.org/10.1038/ngeo2912

Kok, J.F., Storelvmo, T., Karydis, V.A., Adebiyi, A.A., Mahowald, N.M., Evan, A.T., He, C. and **Leung, D.M.** (2023) Mineral dust aerosol impacts on global climate and climate change. *Nat. Rev. Earth Environ.*, 4: 71–86. DOI: https://doi.org/10.1038/s43017-022-00379-5

Kokkola, H., Korhonen, H., Lehtinen, K.E.J., Makkonen, R., Asmi, A., Järvenoja, S., Anttila, T., Partanen, A.-I., Kulmala, M., Järvinen, H., Laaksonen, A. and **Kerminen, V.-M.** (2008) SALSA – a Sectional Aerosol module for Large

Scale Applications. *Atmospheric Chem. Phys.*, 8: 2469–2483. DOI: https://doi.org/10.5194/acp-8-2469-2008

Kokkola, H., Kühn, T., Laakso, A., Bergman, T., Lehtinen, K.E.J., Mielonen, T., Arola, A., Stadtler, S., Korhonen, H., Ferrachat, S., Lohmann, U., Neubauer, D., Tegen, I., Siegenthaler-Le Drian, C., Schultz, M.G., Bey, I., Stier, P., Daskalakis, N., Heald, C.L. and **Romakkaniemi, S.** (2018) SALSA2.0: The sectional aerosol module of the aerosol–chemistry–climate model ECHAM6.3.0-HAM2.3-MOZ1.0. *Geosci. Model Dev.*, 11: 3833–3863. DOI: https://doi.org/10.5194/gmd-11-3833-2018

Kokkola, H., Tonttila, J., Calderón, S.M., Romakkaniemi, S., Lipponen, A., Peräkorpi, A., Mielonen, T., Gryspeerdt, E., Virtanen, T.H., Kolmonen, P. and **Arola, A.** (2025) Model analysis of biases in the satellite-diagnosed aerosol effect on the cloud liquid water path. *Atmospheric Chem. Phys.*, 25: 1533–1543. DOI: https://doi.org/10.5194/acp-25-1533-2025

Kommula, S.M., Buchholz, A., Gramlich, Y., Mielonen, T., Hao, L., Pullinen, I., Vettikkat, L., Ylisirniö, A., Joutsensaari, J., Schobesberger, S., Tiitta, P., Leskinen, A., Rees, D.H., Haslett, S.L., Siegel, K., Lunder, C., Zieger, P., Krejci, R., Romakkaniemi, S., Mohr, C. and **Virtanen, A.** (2024) Effect of Long-Range Transported Fire Aerosols on Cloud Condensation Nuclei Concentrations and Cloud Properties at High Latitudes. *Geophys. Res. Lett.*, 51: e2023GL107134. DOI: https://doi.org/10.1029/2023GL107134

Korolev, A., DeMott, P.J., Heckman, I., Wolde, M., Williams, E., Smalley, D.J. and **Donovan, M.F.** (2022) Observation of secondary ice production in clouds at low temperatures. *Atmospheric Chem. Phys.*, 22: 13103–13113. DOI: https://doi.org/10.5194/acp-22-13103-2022

Korolev, A. and **Leisner, T.** (2020) Review of experimental studies of secondary ice production. *Atmospheric Chem. Phys.*, 20: 11767–11797. DOI: https://doi.org/10.5194/acp-20-11767-2020

Korolev, A. and **Milbrandt, J.** (2022) How Are Mixed-Phase Clouds Mixed? *Geophys. Res. Lett.*, 49: e2022GL099578. DOI: https://doi.org/10.1029/2022GL099578

Kostenidou, E., Karnezi, E., Hite Jr., J.R., Bougiatioti, A., Cerully, K., Xu, L., Ng, N.L., Nenes, A. and **Pandis, S.N.** (2018) Organic aerosol in the summertime southeastern United States: components and their link to volatility distribution, oxidation state and hygroscopicity. *Atmospheric Chem. Phys.*, 18: 5799–5819. DOI: https://doi.org/10.5194/acp-18-5799-2018

Kostinski, A.B. and **Shaw, R.A.** (2005) Fluctuations and Luck in Droplet Growth by Coalescence, *Bull. Amer. Meteor. Soc.*, 86: 235–244. DOI: https://doi.org/10.1175/BAMS-86-2-235

Kroll, J.H. and **Seinfeld, J.H.** (2008) Chemistry of secondary organic aerosol: Formation and evolution of low-volatility organics in the atmosphere. *Atmos. Environ.*, 42: 3593–3624. DOI: https://doi.org/10.1016/j.atmosenv.2008.01.003

Krueger, B.J., Grassian, V.H., Cowin, J.P. and **Laskin, A.** (2004) Heterogeneous chemistry of individual mineral dust particles from different dust source regions: the importance of particle mineralogy. *Atmos. Environ.*, 38: 6253–6261. DOI: https://doi.org/10.1016/j.atmosenv.2004.07.010

Kulkarni, G. and **Dobbie, S.** (2010) Ice nucleation properties of mineral dust particles: determination of onset RH_i, IN active fraction, nucleation time-lag, and the effect of active sites on contact angles. *Atmospheric Chem. Phys.*, 10: 95–105. DOI: https://doi.org/10.5194/acp-10-95-2010

Kulmala, M. (2003) How Particles Nucleate and Grow. *Science*, 302: 1000–1001. DOI: https://doi.org/10.1126/science.1090848

Kulmala, M., Asmi, A., Lappalainen, H.K., Pandis, S.N. *et al.* (2011) General overview: European Integrated project on Aerosol Cloud Climate and Air Quality interactions (EUCAARI) – integrating aerosol research from nano to global scales. *Atmospheric Chem. Phys.*, 11: 13061–13143. https://doi.org/10.5194/acp-11-13061-2011

Kulmala, M., Junninen, H., Dada, L., Salma, I., Weidinger, T., Thén, W., Vörösmarty, M., Komsaare, K., Stolzenburg, D., Cai, R., Yan, C., Li, X., Deng, C., Jiang, J., Petäjä, T., Nieminen, T. and **Kerminen, V.-M.** (2022) Quiet New Particle Formation in the Atmosphere. *Front. Environ. Sci.*, 10. DOI: https://doi.org/10.3389/fenvs.2022.912385

Kulmala, M., Lehtinen, K.E.J. and **Laaksonen, A.** (2006) Cluster activation theory as an explanation of the linear dependence between formation rate of 3nm particles and sulphuric acid concentration. *Atmospheric Chem. Phys.*, 6: 787–793. DOI: https://doi.org/10.5194/acp-6-787-2006

Kulmala, M., Vehkamäki, H., Petäjä, T., Dal Maso, M., Lauri, A., Kerminen, V.M., Birmili, W. and **McMurry, P.H.** (2004) Formation and growth rates of ultrafine atmospheric particles: a review of observations. *J. Aerosol Sci.*, 35: 143–176. DOI: https://doi.org/10.1016/j.jaerosci.2003.10.003

Kupc, A., Williamson, C.J., Hodshire, A.L., Kazil, J., Ray, E., Bui, T.P., Dollner, M., Froyd, K.D., McKain, K., Rollins, A., Schill, G.P., Thames, A., Weinzierl, B.B., Pierce, J.R. and **Brock, C.A.** (2020) The potential role of organics in new particle formation and initial growth in the remote tropical upper troposphere. *Atmospheric Chem. Phys.*, 20: 15037–15060. DOI: https://doi.org/10.5194/acp-20-15037-2020

Kuwata, M., Shao, W., Lebouteiller, R. and **Martin, S.T.** (2013) Classifying organic materials by oxygen-to-carbon elemental ratio to predict the activation regime of Cloud Condensation Nuclei (CCN). *Atmospheric Chem. Phys.*, 13: 5309–5324. DOI: https://doi.org/10.5194/acp-13-5309-2013

Kwon, H.-S., Ryu, M.H. and **Carlsten, C.** (2020) Ultrafine particles: unique physicochemical properties relevant to health and disease. *Exp. Mol. Med.*, 52: 318–328. DOI: https://doi.org/10.1038/s12276-020-0405-1

Laskin, A., Laskin, J. and **Nizkorodov, S.A.** (2015) Chemistry of Atmospheric Brown Carbon. *Chem. Rev.*, 115: 4335–4382. DOI: https://doi.org/10.1021/cr5006167

Lauber, A., Kiselev, A., Pander, T., Handmann, P. and **Leisner, T.** (2018) Secondary Ice Formation during Freezing of Levitated Droplets. *J. Atmos. Sci.*, 75: 2815–2826. DOI: https://doi.org/10.1175/JAS-D-18-0052.1

Lehtipalo, K., Yan, C., Dada, L., Worsnop, D.R. *et al.* (2018) Multicomponent new particle formation from sulfuric acid, ammonia, and biogenic vapors. *Sci. Adv.*, 4: eaau5363. DOI: https://doi.org/10.1126/sciadv.aau5363

Leskinen, A., Portin, H., Komppula, M., Miettinen, P., Arola, A., Lihavainen, H., Hatakka, J., Laaksonen, A. and **Lehtinen, K.** (2009) Overview of the research activities and results at Puijo semi-urban measurement station. *Boreal Environ. Res.*, 14: 576–590.

Li, G., Wieder, J., Pasquier, J.T., Henneberger, J. and **Kanji, Z.A.** (2022a) Predicting atmospheric background number concentration of ice-nucleating particles in the Arctic. *Atmospheric Chem. Phys.*, 22: 14441–14454. DOI: https://doi.org/10.5194/acp-22-14441-2022

Li, J., Carlson, B.E., Yung, Y.L., Lv, D., Hansen, J., Penner, J.E., Liao, H., Ramaswamy, V., Kahn, R.A., Zhang, P., Dubovik, O., Ding, A., Lacis, A.A., Zhang, L. and **Dong, Y.** (2022b) Scattering and absorbing aerosols in the climate system. *Nat. Rev. Earth Environ.*, 3: 363–379. DOI: https://doi.org/10.1038/s43017-022-00296-7

Li, L., Mahowald, N., Pérez García-Pando, C., Ginoux, P., Brodrick, P., Clark, R., Okin, G., Kokaly, R.F., Green, R.O., Miller, R., Gonçalves Ageitos, M., Obiso, V., Keebler, A., Ehlmann, B., Swayze, G. and **Thompson, D.R.** (2024b) Improved quantification of mineral dust direct radiative impacts using new source mineralogy from EMIT imaging spectroscopy. *American Geophysical Union Fall Meeting 2024*.

Li, L., Mahowald, N.M., Gonçalves Ageitos, M., Obiso, V., Miller, R.L., Pérez García-Pando, C., Di Biagio, C., Formenti, P., Brodrick, P.G., Clark, R.N., Green, R.O., Kokaly, R., Swayze, G. and **Thompson, D.R.** (2024a) Improved constraints on hematite refractive index for estimating climatic effects of dust aerosols. *Commun. Earth Environ.*, 5: 1–12. DOI: https://doi.org/10.1038/s43247-024-01441-4

Li, L., Mahowald, N.M., Miller, R.L., Pérez García-Pando, C., Klose, M., Hamilton, D.S., Gonçalves Ageitos, M., Ginoux, P., Balkanski, Y., Green, R.O., Kalashnikova, O., Kok, J.F., Obiso, V., Paynter, D. and **Thompson, D.R.** (2021a) Quantifying the range of the dust direct radiative effect due to source mineralogy uncertainty. *Atmospheric Chem. Phys.*, 21: 3973–4005. DOI: https://doi.org/10.5194/acp-21-3973-2021

Li, W., Liu, L., Zhang, J., Xu, L., Wang, Y., Sun, Y. and **Shi, Z.** (2021b) Microscopic Evidence for Phase Separation of Organic Species and Inorganic Salts in Fine Ambient Aerosol Particles. *Environ. Sci. Technol.*, 55: 2234–2242. DOI: https://doi.org/10.1021/acs.est.0c02333

Li, X., Li, H., Yao, L., Stolzenburg, D., Sarnela, N., Vettikkat, L., Wollesen de Jonge, R., Baalbaki, R., Uusitalo, H., Kontkanen, J., Lehtipalo, K., Daellenbach, K.R., Jokinen, T., Aalto, J., Keronen, P., Schobesberger, S., Nieminen, T., Petäjä, T., Kerminen, V.-M., Bianchi, F., Kulmala, M. and **Dada, L.** (2024c) Over 20 years of observations in the boreal forest reveal a decreasing trend of atmospheric new particle formation. *Boreal Environ. Res.*, 29: 35–52.

Li, X., Nieminen, T., Baalbaki, R., Zhou, P., Paasonen, P., Makkonen, R., Zaidan, M.A., Sarnela, N., Yan, C., Jokinen, T., Salma, I., Vörösmarty, M., Petäjä, T., Kerminen, V.-M., Kulmala, M. and **Dada, L.** (2025) Parameterization of particle formation rates in distinct atmospheric environments. *Aerosol Res. Discuss.*, 3: 271–291. DOI: https://doi.org/10.5194/ar-2025-3

Lin, H. and **Leaitch, W.R.** (1997) Development of an in-cloud aerosol activation parametrization for climate modelling. In: *WMO Workshop on Measurement of Cloud Properties for Forecasts of Weather, Air Quality and Climate*. Mexico City, 328–335.

Liu, F., Yon, J., Fuentes, A., Lobo, P., Smallwood, G.J. and **Corbin, J.C.** (2020) Review of recent literature on the light absorption properties of black carbon: Refractive index, mass absorption cross section, and absorption function. *Aerosol Sci. Technol.*, 54: 33–51. DOI: https://doi.org/10.1080/02786826.2019.1676878

Liu, S., Aiken, A.C., Gorkowski, K., Dubey, M.K., Cappa, C.D., Williams, L.R., Herndon, S.C., Massoli, P., Fortner, E.C., Chhabra, P.S., Brooks, W.A., Onasch, T.B., Jayne, J.T., Worsnop, D.R., China, S., Sharma, N., Mazzoleni, C., Xu, L., Ng, N.L., Liu, D., Allan, J.D., Lee, J.D., Fleming, Z.L., Mohr, C., Zotter, P., Szidat, S. and **Prévôt, A.S.H.** (2015) Enhanced light absorption by mixed source black and brown carbon particles in UK winter. *Nat. Commun.*, 6: 8435. DOI: https://doi.org/10.1038/ncomms9435

Liu, Y., Dong, X., Wang, M., Emmons, L.K., Liu, Y., Liang, Y., Li, X. and **Shrivastava, M.** (2021) Analysis of secondary organic aerosol simulation bias in the Community Earth System Model (CESM2.1). *Atmospheric Chem. Phys.*, 21: 8003–8021. DOI: https://doi.org/10.5194/acp-21-8003-2021

Lohmann, U. (2017) Anthropogenic Aerosol Influences on Mixed-Phase Clouds. *Curr. Clim. Change Rep.*, 3: 32–44. DOI: https://doi.org/10.1007/s40641-017-0059-9

Lohmann, U. and **Diehl, K.** (2006) Sensitivity Studies of the Importance of Dust Ice Nuclei for the Indirect Aerosol Effect on Stratiform Mixed-Phase Clouds. *J. Atmospheric Sci.*, 63: 968–982. DOI: https://doi.org/10.1175/JAS3662.1

Lohmann, U., Mahrt, F. and **Lüönd, F.** (eds.) (2016) Clouds. In: *An Introduction to Clouds: From the Microscale to Climate*. Cambridge University Press, Cambridge, pp. 1–25. DOI: https://doi.org/10.1017/CBO9781139087513.002

Lohmann, U. and **Neubauer, D.** (2018) The importance of mixed-phase and ice clouds for climate sensitivity in the global aerosol–climate model ECHAM6-HAM2. *Atmospheric Chem. Phys.*, 18: 8807–8828. DOI: https://doi.org/10.5194/acp-18-8807-2018

Lohmann, U., Stier, P., Hoose, C., Ferrachat, S., Kloster, S., Roeckner, E. and **Zhang, J.** (2007) Cloud microphysics

and aerosol indirect effects in the global climate model ECHAM5-HAM. *Atmos. Chem. Phys.*, 7: 3425–3446. DOI: https://doi.org/10.5194/acp-7-3425-2007

Lowe, S.J., Partridge, D.G., Davies, J.F., Wilson, K.R., Topping, D. and **Riipinen, I.** (2019) Key drivers of cloud response to surface-active organics. *Nat. Commun.*, 10: 5214. DOI: https://doi.org/10.1038/s41467-019-12982-0

Lowenthal, D.H., Hallar, A.G., David, R.O., McCubbin, I.B., Borys, R.D. and **Mace, G.G.** (2019) Mixed-phase orographic cloud microphysics during StormVEx and IFRACS. *Atmospheric Chem. Phys.*, 19: 5387–5401. DOI: https://doi.org/10.5194/acp-19-5387-2019

Luke, E.P., Yang, F., Kollias, P., Vogelmann, A.M. and **Maahn, M.** (2021) New insights into ice multiplication using remote-sensing observations of slightly supercooled mixed-phase clouds in the Arctic. *Proc. Natl. Acad. Sci.*, 118: e2021387118. DOI: https://doi.org/10.1073/pnas.2021387118

Magaritz-Ronen, L., Pinsky, M. and **Khain, A.** (2016) Drizzle formation in stratocumulus clouds: effects of turbulent mixing. *Atmospheric Chem. Phys.*, 16: 1849–1862. DOI: https://doi.org/10.5194/acp-16-1849-2016

Mahowald, N.M., Li, L., Albani, S., Hamilton, D.S. and **Kok, J.F.** (2024) Opinion: The importance of historical and paleoclimate aerosol radiative effects. *Atmospheric Chem. Phys.*, 24: 533–551. DOI: https://doi.org/10.5194/acp-24-533-2024

Malavelle, F.F., Haywood, J.M., Jones, A., Gettelman, A., Clarisse, L., Bauduin, S., Allan, R.P., Karset, I.H.H., Kristjánsson, J.E., Oreopoulos, L., Cho, N., Lee, D., Bellouin, N., Boucher, O., Grosvenor, D.P., Carslaw, K.S., Dhomse, S., Mann, G.W., Schmidt, A., Coe, H., Hartley, M.E., Dalvi, M., Hill, A.A., Johnson, B.T., Johnson, C.E., Knight, J.R., O'Connor, F.M., Partridge, D.G., Stier, P., Myhre, G., Platnick, S., Stephens, G.L., Takahashi, H. and **Thordarson, T.** (2017) Strong constraints on aerosol–cloud interactions from volcanic eruptions. *Nature*, 546: 485–491. DOI: https://doi.org/10.1038/nature22974

Mandariya, A.K., Ahlawat, A., Haneef, M., Baig, N.A., Patel, K., Apte, J., Hildebrandt Ruiz, L., Wiedensohler, A. and **Habib, G.** (2024) Measurement report: Hygroscopicity of size-selected aerosol particles in the heavily polluted urban atmosphere of Delhi: impacts of chloride aerosol. *Atmospheric Chem. Phys.*, 24: 3627–3647. DOI: https://doi.org/10.5194/acp-24-3627-2024

Manshausen, P., Watson-Parris, D., Christensen, M.W., Jalkanen, J.-P. and **Stier, P.** (2022) Invisible ship tracks show large cloud sensitivity to aerosol. *Nature*, 610: 101–106. DOI: https://doi.org/10.1038/s41586-022-05122-0

Mao, J., Carlton, A., Cohen, R.C., Brune, W.H., Brown, S.S., Wolfe, G.M., Jimenez, J.L., Pye, H.O.T., Lee Ng, N., Xu, L., McNeill, V.F., Tsigaridis, K., McDonald, B.C., Warneke, C., Guenther, A., Alvarado, M.J., de Gouw, J., Mickley, L.J., Leibensperger, E.M., Mathur, R., Nolte, C.G., Portmann, R.W., Unger, N., Tosca, M. and **Horowitz, L.W.** (2018) Southeast Atmosphere Studies: learning from model-observation syntheses. *Atmospheric Chem. Phys.*, 18: 2615–2651. DOI: https://doi.org/10.5194/acp-18-2615-2018

Marais, E.A., Jacob, D.J., Jimenez, J.L., Campuzano-Jost, P., Day, D.A., Hu, W., Krechmer, J., Zhu, L., Kim, P.S., Miller, C.C., Fisher, J.A., Travis, K., Yu, K., Hanisco, T.F., Wolfe, G.M., Arkinson, H.L., Pye, H.O.T., Froyd, K.D., Liao, J. and **McNeill, V.F.** (2016) Aqueous-phase mechanism for secondary organic aerosol formation from isoprene: application to the southeast United States and co-benefit of SO_2 emission controls. *Atmospheric Chem. Phys.*, 16: 1603–1618. DOI: https://doi.org/10.5194/acp-16-1603-2016

Martinez-Villalobos, C., Neelin, J.D. and **Pendergrass, A.G.** (2022) Metrics for Evaluating CMIP6 Representation of Daily Precipitation Probability Distributions. DOI: https://doi.org/10.1175/JCLI-D-21-0617.1

Mauritsen, T., Bader, J., Becker, T., Roeckner, E., *et al.* (2019) Developments in the MPI-M Earth System Model version 1.2 (MPI-ESM1.2) and Its Response to Increasing CO_2. *J. Adv. Model. Earth Syst.*, 11: 998–1038. DOI: https://doi.org/10.1029/2018MS001400

McCluskey, C.S., DeMott, P.J., Ma, P.-L. and **Burrows, S.M.** (2019) Numerical Representations of Marine Ice-Nucleating Particles in Remote Marine Environments Evaluated Against Observations. *Geophys. Res. Lett.*, 46: 7838–7847. https://doi.org/10.1029/2018GL081861

McCoy, D.T., Bender, F. a.-M., Mohrmann, J.K.C., Hartmann, D.L., Wood, R. and **Grosvenor, D.P.** (2017) The global aerosol-cloud first indirect effect estimated using MODIS, MERRA, and AeroCom. *J. Geophys. Res. Atmospheres*, 122: 1779–1796. DOI: https://doi.org/10.1002/2016JD026141

McCrystall, M.R., Stroeve, J., Serreze, M., Forbes, B.C. and **Screen, J.A.** (2021) New climate models reveal faster and larger increases in Arctic precipitation than previously projected. *Nat. Commun.*, 12: 6765. DOI: https://doi.org/10.1038/s41467-021-27031-y

McFiggans, G., Mentel, T.F., Wildt, J., Pullinen, I., Kang, S., Kleist, E., Schmitt, S., Springer, M., Tillmann, R., Wu, C., Zhao, D., Hallquist, M., Faxon, C., Le Breton, M., Hallquist, Å.M., Simpson, D., Bergström, R., Jenkin, M.E., Ehn, M., Thornton, J.A., Alfarra, M.R., Bannan, T.J., Percival, C.J., Priestley, M., Topping, D. and **Kiendler-Scharr, A.** (2019) Secondary organic aerosol reduced by mixture of atmospheric vapours. *Nature*, 565: 587–593. DOI: https://doi.org/10.1038/s41586-018-0871-y

McGrath, M.J., Olenius, T., Ortega, I.K., Loukonen, V., Paasonen, P., Kurtén, T., Kulmala, M. and **Vehkamäki, H.** (2012) Atmospheric Cluster Dynamics Code: a flexible method for solution of the birth-death equations. *Atmospheric Chem. Phys.*, 12: 2345–2355. DOI: https://doi.org/10.5194/acp-12-2345-2012

McMurry, P.H., Woo, K.S., Weber, R., Chen, D.-R. and **Pui, D.Y.H.** (2000) Size distributions of 3–10 nm atmospheric particles: Implications for nucleation mechanisms. *Philos. Trans. R. Soc. Math. Phys. Eng. Sci.*, 358: 2625–2642. DOI: https://doi.org/10.1098/rsta.2000.0673

Mentel, T.F., Kleist, E., Andres, S., Dal Maso, M., Hohaus, T., Kiendler-Scharr, A., Rudich, Y., Springer, M., Tillmann, R., Uerlings, R., Wahner, A. and **Wildt, J.** (2013) Secondary aerosol formation from stress-induced biogenic emissions and possible climate feedbacks. *Atmospheric Chem. Phys.*, 13: 8755–8770. DOI: https://doi.org/10.5194/acp-13-8755-2013

Merikanto, J., Spracklen, D.V., Mann, G.W., Pickering, S.J. and **Carslaw, K.S.** (2009) Impact of nucleation on global CCN. *Atmospheric Chem. Phys.*, 9: 8601–8616. DOI: https://doi.org/10.5194/acp-9-8601-2009

Metzger, A., Verheggen, B., Dommen, J., Duplissy, J., Prevot, A.S.H., Weingartner, E., Riipinen, I., Kulmala, M., Spracklen, D.V., Carslaw, K.S. and **Baltensperger, U.** (2010) Evidence for the role of organics in aerosol particle formation under atmospheric conditions. *Proc. Natl. Acad. Sci.*, 107: 6646–6651. DOI: https://doi.org/10.1073/pnas.0911330107

Metzger, S., Dentener, F., Pandis, S. and **Lelieveld, J.** (2002) Gas/aerosol partitioning: 1. A computationally efficient model. *J. Geophys. Res. Atmospheres*, 107: ACH 16-1–ACH 16-24. DOI: https://doi.org/10.1029/2001JD001102

Meyers, M.P., DeMott, P.J. and **Cotton, W.R.** (1992) New Primary Ice-Nucleation Parameterizations in an Explicit Cloud Model. *J. Appl. Meteorol. Climatol.*, 31: 708–721. DOI: https://doi.org/10.1175/1520-0450(1992)031<0708:NPINPI>2.0.CO;2

Michibata, T., Suzuki, K., Sato, Y. and **Takemura, T.** (2016) The source of discrepancies in aerosol–cloud–precipitation interactions between GCM and A-Train retrievals. *Atmospheric Chem. Phys.*, 16: 15413–15424. DOI: https://doi.org/10.5194/acp-16-15413-2016

Midzi, J., Jeffery, D.W., Baumann, U., Rogiers, S., Tyerman, S.D. and **Pagay, V.** (2022) Stress-Induced Volatile Emissions and Signalling in Inter-Plant Communication. *Plants*, 11: 2566. DOI: https://doi.org/10.3390/plants11192566

Mignani, C., Creamean, J.M., Zimmermann, L., Alewell, C. and **Conen, F.** (2019) New type of evidence for secondary ice formation at around −15°C in mixed-phase clouds. *Atmospheric Chem. Phys.*, 19: 877–886. DOI: https://doi.org/10.5194/acp-19-877-2019

Milbrandt, J.A. and **Yau, M.K.** (2005) A Multimoment Bulk Microphysics Parameterization. Part II: A Proposed Three-Moment Closure and Scheme Description. *J. Atmos. Sci.*, 62: 3065–3081. DOI: https://doi.org/10.1175/JAS3535.1

Milousis, A., Klingmüller, K., Tsimpidi, A.P., Kok, J.F., Kanakidou, M., Nenes, A. and **Karydis, V.A.** (2025b) Impact of mineral dust on the global nitrate aerosol direct and indirect radiative effect. *Atmospheric Chem. Phys.*, 25: 1333–1351. DOI: https://doi.org/10.5194/acp-25-1333-2025

Milousis, A., Scholz, S.M.C., Fuchs, H., Tsimpidi, A.P. and **Karydis, V.A.** (2025a) Global Perspectives on Nitrate Aerosol Dynamics: A Comprehensive Sensitivity Analysis. *EGUsphere*, 1–42. DOI: https://doi.org/10.5194/egusphere-2025-313

Milousis, A., Tsimpidi, A.P., Tost, H., Pandis, S.N., Nenes, A., Kiendler-Scharr, A. and **Karydis, V.A.** (2024) Implementation of the ISORROPIA-lite aerosol thermodynamics model into the EMAC chemistry climate model (based on MESSy v2.55): implications for aerosol composition and acidity. *Geosci. Model Dev.*, 17: 1111–1131. DOI: https://doi.org/10.5194/gmd-17-1111-2024

Mohr, C., Thornton, J.A., Heitto, A., Lopez-Hilfiker, F.D., Lutz, A., Riipinen, I., Hong, J., Donahue, N.M., Hallquist, M., Petäjä, T., Kulmala, M. and **Yli-Juuti, T.** (2019) Molecular identification of organic vapors driving atmospheric nanoparticle growth. *Nat. Commun.*, 10: 4442. DOI: https://doi.org/10.1038/s41467-019-12473-2

Mok, J., Krotkov, N.A., Arola, A., Torres, O., Jethva, H., Andrade, M., Labow, G., Eck, T.F., Li, Z., Dickerson, R.R., Stenchikov, G.L., Osipov, S. and **Ren, X.** (2016) Impacts of brown carbon from biomass burning on surface UV and ozone photochemistry in the Amazon Basin. *Sci. Rep.*, 6: 36940. DOI: https://doi.org/10.1038/srep36940

Moosmüller, H., Engelbrecht, J.P., Skiba, M., Frey, G., Chakrabarty, R.K. and **Arnott, W.P.** (2012) Single scattering albedo of fine mineral dust aerosols controlled by iron concentration. *J. Geophys. Res. Atmospheres*, 117: D11. DOI: https://doi.org/10.1029/2011JD016909

Morales Betancourt, R. and **Nenes, A.** (2014) Droplet activation parameterization: the population-splitting concept revisited. *Geosci. Model Dev.*, 7: 2345–2357. DOI: https://doi.org/10.5194/gmd-7-2345-2014

Morgan, W.T., Allan, J.D., Bower, K.N., Esselborn, M., Harris, B., Henzing, J.S., Highwood, E.J., Kiendler-Scharr, A., McMeeking, G.R., Mensah, A.A., Northway, M.J., Osborne, S., Williams, P.I., Krejci, R. and **Coe, H.** (2010) Enhancement of the aerosol direct radiative effect by semi-volatile aerosol components: airborne measurements in North-Western Europe. *Atmospheric Chem. Phys.*, 10: 8151–8171. DOI: https://doi.org/10.5194/acp-10-8151-2010

Morrison, H., de Boer, G., Feingold, G., Harrington, J., Shupe, M.D. and **Sulia, K.** (2012) Resilience of persistent Arctic mixed-phase clouds. *Nat. Geosci.*, 5: 11–17. DOI: https://doi.org/10.1038/ngeo1332

Morrison, H. and **Gettelman, A.** (2008) A New Two-Moment Bulk Stratiform Cloud Microphysics Scheme in the Community Atmosphere Model, Version 3 (CAM3). Part I: Description and Numerical Tests. *J. Climate*, 21: 3642–3659. DOI: https://doi.org/10.1175/2008JCLI2105.1

Morrison, H., Thompson, G. and **Tatarskii, V.** (2009) Impact of Cloud Microphysics on the Development of Trailing Stratiform Precipitation in a Simulated Squall Line: Comparison of One- and Two-Moment Schemes. *Mon. Wea. Rev.*, 137: 991–1007. DOI: https://doi.org/10.1175/2008MWR2556.1

Motos, G., Freitas, G., Georgakaki, P., Wieder, J., Li, G., Aas, W., Lunder, C., Krejci, R., Pasquier, J.T., Henneberger, J., David, R.O., Ritter, C., Mohr, C., Zieger, P. and **Nenes, A.** (2023) Aerosol and dynamical contributions to cloud

droplet formation in Arctic low-level clouds. *Atmospheric Chem. Phys.*, 23: 13941–13956. DOI: https://doi.org/10.5194/acp-23-13941-2023

Mulcahy, J.P., Johnson, C., Jones, C.G., Povey, A.C., Scott, C.E., Sellar, A., Turnock, S.T., Woodhouse, M.T., Abraham, N.L., Andrews, M.B., Bellouin, N., Browse, J., Carslaw, K.S., Dalvi, M., Folberth, G.A., Glover, M., Grosvenor, D.P., Hardacre, C., Hill, R., Johnson, B., Jones, A., Kipling, Z., Mann, G., Mollard, J., O'Connor, F.M., Palmiéri, J., Reddington, C., Rumbold, S.T., Richardson, M., Schutgens, N.A.J., Stier, P., Stringer, M., Tang, Y., Walton, J., Woodward, S. and **Yool, A.** (2020) Description and evaluation of aerosol in UKESM1 and HadGEM3-GC3.1 CMIP6 historical simulations. *Geosci. Model Dev.*, 13: 6383–6423. DOI: https://doi.org/10.5194/gmd-13-6383-2020

Mülmenstädt, J., Ackerman, A.S., Fridlind, A.M., Huang, M., Ma, P.-L., Mahfouz, N., Bauer, S.E., Burrows, S.M., Christensen, M.W., Dipu, S., Gettelman, A., Leung, L.R., Tornow, F., Quaas, J., Varble, A.C., Wang, H., Zhang, K. and **Zheng, Y.** (2024) Can general circulation models (GCMs) represent cloud liquid water path adjustments to aerosol–cloud interactions? *Atmospheric Chem. Phys.*, 24: 13633–13652. DOI: https://doi.org/10.5194/acp-24-13633-2024

Mülmenstädt, J., Nam, C., Salzmann, M., Kretzschmar, J., L'Ecuyer, T.S., Lohmann, U., Ma, P.-L., Myhre, G., Neubauer, D., Stier, P., Suzuki, K., Wang, M. and **Quaas, J.** (2020) Reducing the aerosol forcing uncertainty using observational constraints on warm rain processes. *Sci. Adv.*, 6: eaaz6433. DOI: https://doi.org/10.1126/sciadv.aaz6433

Murray, B.J., Carslaw, K.S. and **Field, P.R.** (2021) Opinion: Cloud-phase climate feedback and the importance of ice-nucleating particles. *Atmospheric Chem. Phys.*, 21: 665–679. DOI: https://doi.org/10.5194/acp-21-665-2021

Murray, B.J., Knopf, D.A. and **Bertram, A.K.** (2005) The formation of cubic ice under conditions relevant to Earth's atmosphere. *Nature*, 434: 202–205. DOI: https://doi.org/10.1038/nature03403

Murray, B.J., O'Sullivan, D., Atkinson, J.D. and **Webb, M.E.** (2012) Ice nucleation by particles immersed in supercooled cloud droplets. *Chem. Soc. Rev.*, 41: 6519–6554. DOI: https://doi.org/10.1039/c2cs35200a

Myriokefalitakis, S., Bergas-Massó, E., Gonçalves-Ageitos, M., Pérez García-Pando, C., van Noije, T., Le Sager, P., Ito, A., Athanasopoulou, E., Nenes, A., Kanakidou, M., Krol, M.C. and **Gerasopoulos, E.** (2022) Multiphase processes in the EC-Earth model and their relevance to the atmospheric oxalate, sulfate, and iron cycles. *Geosci. Model Dev.*, 15: 3079–3120. DOI: https://doi.org/10.5194/gmd-15-3079-2022

Navarro-Barboza, H., Rovira, J., Obiso, V., Pozzer, A., Via, M., Alastuey, A., Querol, X., Perez, N., Savadkoohi, M., Chen, G., Yus-Díez, J., Ivancic, M., Rigler, M., Eleftheriadis, K., Vratolis, S., Zografou, O., Gini, M., Chazeau, B., Marchand, N., Prevot, A.S.H., Dallenbach, K., Ehn, M., Luoma, K., Petäjä, T., Tobler, A., Necki, J., Aurela, M., Timonen, H., Niemi, J., Favez, O., Petit, J.-E., Putaud, J.-P., Hueglin, C., Pascal, N., Chauvigné, A., Conil, S., Pandolfi, M. and **Jorba, O.** (2025) Characterization of brown carbon absorption in different European environments through source contribution analysis. *Atmospheric Chem. Phys.*, 25: 2667–2694. DOI: https://doi.org/10.5194/acp-25-2667-2025

Nenes, A., Pandis, S.N., Kanakidou, M., Russell, A.G., Song, S., Vasilakos, P. and **Weber, R.J.** (2021) Aerosol acidity and liquid water content regulate the dry deposition of inorganic reactive nitrogen. *Atmospheric Chem. Phys.*, 21: 6023–6033. DOI: https://doi.org/10.5194/acp-21-6023-2021

Neuberger, A., Decesari, S., Aktypis, A., Andersen, H., Baumgardner, D., Bianchi, F., Busetto, M., Cai, J., Cermak, J., Dipu, S., Ekman, A., Fuzzi, S., Gramlich, Y., Haslett, S.L., Heikkinen, L., Joutsensaari, J., Kaltsonoudis, C., Kangasluoma, J., Krejci, R., Lupi, A., Marinoni, A., Matrali, A., Mattsson, F., Mohr, C., Nenes, A., Paglione, M., Pandis, S.N., Patel, A., Riipinen, I., Rinaldi, M., Steimer, S.S., Stolzenburg, D., Sulo, J., Vasilakopoulou, C.N. and **Zieger, P.** (2025) From Molecules to Droplets: The Fog and Aerosol Interaction Research Italy (FAIRARI) 2021/22 Campaign. DOI: https://doi.org/10.1175/BAMS-D-23-0166.1

Neubauer, D., Ferrachat, S., Siegenthaler-Le Drian, C., Stier, P., Partridge, D.G., Tegen, I., Bey, I., Stanelle, T., Kokkola, H. and **Lohmann, U.** (2019) The global aerosol–climate model ECHAM6.3–HAM2.3 – Part 2: Cloud evaluation, aerosol radiative forcing, and climate sensitivity. *Geosci. Model Dev.*, 12: 3609–3639. DOI: https://doi.org/10.5194/gmd-12-3609-2019

Nieminen, T., Paasonen, P., Manninen, H.E., Sellegri, K., Kerminen, V.-M. and **Kulmala, M.** (2011) Parameterization of ion-induced nucleation rates based on ambient observations. *Atmospheric Chem. Phys.*, 11: 3393–3402. DOI: https://doi.org/10.5194/acp-11-3393-2011

Nordling, K., Keskinen, J.-P., Romakkaniemi, S., Kokkola, H., Räisänen, P., Lipponen, A., Partanen, A.-I., Ahola, J., Tonttila, J., Alper, M.E., Korhonen, H. and **Raatikainen, T.** (2024) Technical note: Emulation of a large-eddy simulator for stratocumulus clouds in a general circulation model. *Atmospheric Chem. Phys.*, 24: 869–890. DOI: https://doi.org/10.5194/acp-24-869-2024

Nordling, K., Korhonen, H., Räisänen, J., Partanen, A.-I., Samset, B.H. and **Merikanto, J.** (2021) Understanding the surface temperature response and its uncertainty to CO_2, CH_4, black carbon, and sulfate. *Atmospheric Chem. Phys.*, 21: 14941–14958. DOI: https://doi.org/10.5194/acp-21-14941-2021

Obiso, V., Gonçalves Ageitos, M., Pérez García-Pando, C., Perlwitz, J.P., Schuster, G.L., Bauer, S.E., Di Biagio, C., Formenti, P., Tsigaridis, K. and **Miller, R.L.** (2024) Observationally constrained regional variations of shortwave absorption by iron oxides emphasize the cooling effect of dust. *Atmospheric Chem. Phys.*, 24: 5337–5367. DOI: https://doi.org/10.5194/acp-24-5337-2024

Ohata, S., Moteki, N., Mori, T., Koike, M. and **Kondo, Y.** (2016) A key process controlling the wet removal of aerosols: new

observational evidence. *Sci. Rep.*, 6: 34113. DOI: https://doi.org/10.1038/srep34113

Oreopoulos, L., Cho, N. and **Lee, D.** (2020) A Global Survey of Apparent Aerosol-Cloud Interaction Signals. *J. Geophys. Res. Atmospheres*, 125: e2019JD031287. DOI: https://doi.org/10.1029/2019JD031287

O'Sullivan, D., Adams, M.P., Tarn, M.D., Harrison, A.D., Vergara-Temprado, J., Porter, G.C.E., Holden, M.A., Sanchez-Marroquin, A., Carotenuto, F., Whale, T.F., McQuaid, J.B., Walshaw, R., Hedges, D.H.P., Burke, I.T., Cui, Z. and **Murray, B.J.** (2018) Contributions of biogenic material to the atmospheric ice-nucleating particle population in North Western Europe. *Sci. Rep.*, 8: 13821. DOI: https://doi.org/10.1038/s41598-018-31981-7

Pai, S.J., Heald, C.L., Pierce, J.R., Farina, S.C., Marais, E.A., Jimenez, J.L., Campuzano-Jost, P., Nault, B.A., Middlebrook, A.M., Coe, H., Shilling, J.E., Bahreini, R., Dingle, J.H. and **Vu, K.** (2020) An evaluation of global organic aerosol schemes using airborne observations. *Atmospheric Chem. Phys.*, 20: 2637–2665. DOI: https://doi.org/10.5194/acp-20-2637-2020

Palmer, P.I., Marvin, M.R., Siddans, R., Kerridge, B.J. and **Moore, D.P.** (2022) Nocturnal survival of isoprene linked to formation of upper tropospheric organic aerosol. *Science*, 375(6580): 562–566. DOI: https://doi.org/10.1126/science.abg4506

Partridge, D.G., Vrugt, J.A., Tunved, P., Ekman, A.M.L., Struthers, H. and **Sorooshian, A.** (2012) Inverse modelling of cloud-aerosol interactions – Part 2: Sensitivity tests on liquid phase clouds using a Markov chain Monte Carlo based simulation approach. *Atmospheric Chem. Phys.*, 12: 2823–2847. DOI: https://doi.org/10.5194/acp-12-2823-2012

Pasquier, J.T., David, R.O., Freitas, G., Gierens, R., Gramlich, Y., Haslett, S., Li, G., Schäfer, B., Siegel, K., Wieder, J., Adachi, K., Belosi, F., Carlsen, T., Decesari, S., Ebell, K., Gilardoni, S., Gysel-Beer, M., Henneberger, J., Inoue, J., Kanji, Z.A., Koike, M., Kondo, Y., Krejci, R., Lohmann, U., Maturilli, M., Mazzolla, M., Modini, R., Mohr, C., Motos, G., Nenes, A., Nicosia, A., Ohata, S., Paglione, M., Park, S., Pileci, R.E., Ramelli, F., Rinaldi, M., Ritter, C., Sato, K., Storelvmo, T., Tobo, Y., Traversi, R., Viola, A. and **Zieger, P.** (2022b) The Ny-Ålesund Aerosol Cloud Experiment (NASCENT): Overview and First Results. *Bull. Am. Meteorol. Soc.*, 103: E2533–E2558. DOI: https://doi.org/10.1175/BAMS-D-21-0034.1

Pasquier, J.T., Henneberger, J., Korolev, A., Ramelli, F., Wieder, J., Lauber, A., Li, G., David, R.O., Carlsen, T., Gierens, R., Maturilli, M. and **Lohmann, U.** (2023) Understanding the History of Two Complex Ice Crystal Habits Deduced From a Holographic Imager. *Geophys. Res. Lett.*, 50: e2022GL100247. DOI: https://doi.org/10.1029/2022GL100247

Pasquier, J.T., Henneberger, J., Ramelli, F., Lauber, A., David, R.O., Wieder, J., Carlsen, T., Gierens, R., Maturilli, M. and **Lohmann, U.** (2022a) Conditions favorable for secondary ice production in Arctic mixed-phase clouds. *Atmospheric Chem. Phys.*, 22: 15579–15601. DOI: https://doi.org/10.5194/acp-22-15579-2022

Patoulias, D., Florou, K., Pandis, S.N. and **Nenes, A.** (2024) New Particle Formation Events Can Reduce Cloud Droplets in Boundary Layer Clouds at the Continental Scale. *Geophys. Res. Lett.*, 51: e2023GL106182. DOI: https://doi.org/10.1029/2023GL106182

Pelucchi, P., Neubauer, D. and **Lohmann, U.** (2021) Vertical grid refinement for stratocumulus clouds in the radiation scheme of the global climate model ECHAM6.3-HAM2.3-P3. *Geosci. Model Dev.*, 14: 5413–5434. DOI: https://doi.org/10.5194/gmd-14-5413-2021

Pereira Freitas, G., Adachi, K., Conen, F., Heslin-Rees, D., Krejci, R., Tobo, Y., Yttri, K.E. and **Zieger, P.** (2023) Regionally sourced bioaerosols drive high-temperature ice nucleating particles in the Arctic. *Nat. Commun.*, 14: 5997. DOI: https://doi.org/10.1038/s41467-023-41696-7

Pereira Freitas, G., Kopec, B., Adachi, K., Krejci, R., Heslin-Rees, D., Yttri, K.E., Hubbard, A., Welker, J.M. and **Zieger, P.** (2024) Contribution of fluorescent primary biological aerosol particles to low-level Arctic cloud residuals. *Atmospheric Chem. Phys.*, 24: 5479–5494. DOI: https://doi.org/10.5194/acp-24-5479-2024

Perlwitz, J.P., Pérez García-Pando, C. and **Miller, R.L.** (2015) Predicting the mineral composition of dust aerosols – Part 1: Representing key processes. *Atmospheric Chem. Phys.*, 15: 11593–11627. DOI: https://doi.org/10.5194/acp-15-11593-2015

Phillips, V.T.J., Yano, J.-I., Formenton, M., Ilotoviz, E., Kanawade, V., Kudzotsa, I., Sun, J., Bansemer, A., Detwiler, A.G., Khain, A. and **Tessendorf, S.A.** (2017) Ice Multiplication by Breakup in Ice–Ice Collisions. Part II: Numerical Simulations. *J. Atmospheric Sci.*, 74: 2789–2811. DOI: https://doi.org/10.1175/JAS-D-16-0223.1

Phillips, V.T.J., Yano, J.-I. and **Khain, A.** (2017) Ice Multiplication by Breakup in Ice–Ice Collisions. Part I: Theoretical Formulation. *J. Atmos. Sci.*, 74: 1705–1719. DOI: https://doi.org/10.1175/JAS-D-16-0224.1

Pöhlker, M.L., Pöhlker, C., Quaas, J., Mülmenstädt, J., Pozzer, A., Andreae, M.O., Artaxo, P., Block, K., Coe, H., Ervens, B., Gallimore, P., Gaston, C.J., Gunthe, S.S., Henning, S., Herrmann, H., Krüger, O.O., McFiggans, G., Poulain, L., Raj, S.S., Reyes-Villegas, E., Royer, H.M., Walter, D., Wang, Y. and **Pöschl, U.** (2023) Global organic and inorganic aerosol hygroscopicity and its effect on radiative forcing. *Nat. Commun.*, 14: 6139. DOI: https://doi.org/10.1038/s41467-023-41695-8

Possner, A., Eastman, R., Bender, F. and **Glassmeier, F.** (2020) Deconvolution of boundary layer depth and aerosol constraints on cloud water path in subtropical stratocumulus decks. *Atmospheric Chem. Phys.*, 20: 3609–3621. DOI: https://doi.org/10.5194/acp-20-3609-2020

Possner, A., Pfannkuch, K. and **Ramadoss, V.** (2024) Cloud-Resolving ICON Simulations of Secondary Ice Production in Arctic Mixed-Phase Stratocumuli Observed during

M-PACE. *J. Atmos. Sci.*, 81(2): 417–434. DOI: https://doi.org/10.1175/JAS-D-23-0069.1

Pozzer, A., Reifenberg, S.F., Kumar, V., Franco, B., Kohl, M., Taraborrelli, D., Gromov, S., Ehrhart, S., Jöckel, P., Sander, R., Fall, V., Rosanka, S., Karydis, V., Akritidis, D., Emmerichs, T., Crippa, M., Guizzardi, D., Kaiser, J.W., Clarisse, L., Kiendler-Scharr, A., Tost, H. and **Tsimpidi, A.** (2022) Simulation of organics in the atmosphere: evaluation of EMACv2.54 with the Mainz Organic Mechanism (MOM) coupled to the ORACLE (v1.0) submodel. *Geosci. Model Dev.*, 15: 2673–2710. DOI: https://doi.org/10.5194/gmd-15-2673-2022

Prank, M., Tonttila, J., Ahola, J., Kokkola, H., Kühn, T., Romakkaniemi, S. and **Raatikainen, T.** (2022) Impacts of marine organic emissions on low-level stratiform clouds – a large eddy simulator study. *Atmospheric Chem. Phys.*, 22: 10971–10992. DOI: https://doi.org/10.5194/acp-22-10971-2022

Prank, M., Tonttila, J., Shang, X., Romakkaniemi, S. and **Raatikainen, T.** (2025) Can pollen affect precipitation? *Atmospheric Chem. Phys.*, 25: 183–197. DOI: https://doi.org/10.5194/acp-25-183-2025

Pratt, K.A., DeMott, P.J., French, J.R., Wang, Z., Westphal, D.L., Heymsfield, A.J., Twohy, C.H., Prenni, A.J. and **Prather, K.A.** (2009) In situ detection of biological particles in cloud ice-crystals. *Nat. Geosci.*, 2: 398–401. DOI: https://doi.org/10.1038/ngeo521

Pringle, K.J., Tost, H., Message, S., Steil, B., Giannadaki, D., Nenes, A., Fountoukis, C., Stier, P., Vignati, E. and **Lelieveld, J.** (2010) Description and evaluation of GMXe: a new aerosol submodel for global simulations (v1). *Geosci. Model Dev.*, 3: 391–412. DOI: https://doi.org/10.5194/gmd-3-391-2010

Proske, U., Bessenbacher, V., Dedekind, Z., Lohmann, U. and **Neubauer, D.** (2021) How frequent is natural cloud seeding from ice cloud layers (< −35 °C) over Switzerland? *Atmospheric Chem. Phys.*, 21: 5195–5216. DOI: https://doi.org/10.5194/acp-21-5195-2021

Proske, U., Ferrachat, S., Klampt, S., Abeling, M. and **Lohmann, U.** (2023) Addressing Complexity in Global Aerosol Climate Model Cloud Microphysics. *J. Adv. Model. Earth Syst.*, 15: e2022MS003571. DOI: https://doi.org/10.1029/2022MS003571

Proske, U., Ferrachat, S. and **Lohmann, U.** (2024) Developing a climatological simplification of aerosols to enter the cloud microphysics of a global climate model. *Atmospheric Chem. Phys.*, 24: 5907–5933. DOI: https://doi.org/10.5194/acp-24-5907-2024

Proske, U., Ferrachat, S., Neubauer, D., Staab, M. and **Lohmann, U.** (2022) Assessing the potential for simplification in global climate model cloud microphysics. *Atmospheric Chem. Phys.*, 22: 4737–4762. DOI: https://doi.org/10.5194/acp-22-4737-2022

Quaas, J., Andrews, T., Bellouin, N., Block, K., Boucher, O., Ceppi, P., Dagan, G., Doktorowski, S., Eichholz, H.M., Forster, P., Goren, T., Gryspeerdt, E., Hodnebrog, Ø., Jia, H., Kramer, R., Lange, C., Maycock, A.C., Mülmenstädt, J., Myhre, G., O'Connor, F.M., Pincus, R., Samset, B.H., Senf, F., Shine, K.P., Smith, C., Stjern, C.W., Takemura, T., Toll, V. and **Wall, C.J.** (2024) Adjustments to Climate Perturbations—Mechanisms, Implications, Observational Constraints. *AGU Adv.*, 5: e2023AV001144. DOI: https://doi.org/10.1029/2023AV001144

Quaas, J., Arola, A., Cairns, B., Christensen, M., Deneke, H., Ekman, A.M.L., Feingold, G., Fridlind, A., Gryspeerdt, E., Hasekamp, O., Li, Z., Lipponen, A., Ma, P.-L., Mülmenstädt, J., Nenes, A., Penner, J.E., Rosenfeld, D., Schrödner, R., Sinclair, K., Sourdeval, O., Stier, P., Tesche, M., van Diedenhoven, B. and **Wendisch, M.** (2020) Constraining the Twomey effect from satellite observations: issues and perspectives. *Atmospheric Chem. Phys.*, 20: 15079–15099. DOI: https://doi.org/10.5194/acp-20-15079-2020

Quaas, J., Jia, H., Smith, C., Albright, A.L., Aas, W., Bellouin, N., Boucher, O., Doutriaux-Boucher, M., Forster, P.M., Grosvenor, D., Jenkins, S., Klimont, Z., Loeb, N.G., Ma, X., Naik, V., Paulot, F., Stier, P., Wild, M., Myhre, G. and **Schulz, M.** (2022) Robust evidence for reversal of the trend in aerosol effective climate forcing. *Atmospheric Chem. Phys.*, 22: 12221–12239. DOI: https://doi.org/10.5194/acp-22-12221-2022

Quaas, J., Ming, Y., Menon, S., Takemura, T., Wang, M., Penner, J.E., Gettelman, A., Lohmann, U., Bellouin, N., Boucher, O., Sayer, A.M., Thomas, G.E., McComiskey, A., Feingold, G., Hoose, C., Kristjánsson, J.E., Liu, X., Balkanski, Y., Donner, L.J., Ginoux, P.A., Stier, P., Grandey, B., Feichter, J., Sednev, I., Bauer, S.E., Koch, D., Grainger, R.G., Kirkev&aring, G, A., Iversen, T., Seland, Ø., Easter, R., Ghan, S.J., Rasch, P.J., Morrison, H., Lamarque, J.-F., Iacono, M.J., Kinne, S. and **Schulz, M.** (2009) Aerosol indirect effects – general circulation model intercomparison and evaluation with satellite data. *Atmospheric Chem. Phys.*, 9: 8697–8717. DOI: https://doi.org/10.5194/acp-9-8697-2009

Radke, L.F., Hobbs, P.V. and **Eltgroth, M.W.** (1980) Scavenging of Aerosol Particles by Precipitation. *J. App. Met.*, 19(6): 715–722. DOI: https://doi.org/10.1175/1520-0450(1980)019%3C0715:SOAPBP%3E2.0.CO;2

Regayre, L.A., Deaconu, L., Grosvenor, D.P., Sexton, D.M.H., Symonds, C., Langton, T., Watson-Paris, D., Mulcahy, J.P., Pringle, K.J., Richardson, M., Johnson, J.S., Rostron, J.W., Gordon, H., Lister, G., Stier, P. and **Carslaw, K.S.** (2023) Identifying climate model structural inconsistencies allows for tight constraint of aerosol radiative forcing. *Atmospheric Chem. Phys.*, 23: 8749–8768. DOI: https://doi.org/10.5194/acp-23-8749-2023

Regayre, L.A., Johnson, J.S., Yoshioka, M., Pringle, K.J., Sexton, D.M.H., Booth, B.B.B., Lee, L.A., Bellouin, N. and **Carslaw, K.S.** (2018) Aerosol and physical atmosphere model parameters are both important sources of uncertainty in aerosol ERF. *Atmospheric Chem. Phys.*, 18: 9975–10006. DOI: https://doi.org/10.5194/acp-18-9975-2018

Reutter, P., Su, H., Trentmann, J., Simmel, M., Rose, D., Gunthe, S.S., Wernli, H., Andreae, M.O. and **Pöschl, U.** (2009) Aerosol- and updraft-limited regimes of cloud droplet formation: influence of particle number, size and hygroscopicity on the activation of cloud condensation nuclei (CCN). *Atmospheric Chem. Phys.*, 9: 7067–7080. DOI: https://doi.org/10.5194/acp-9-7067-2009

Riccobono, F., Schobesberger, S., Scott, C.E., Baltensperger, U. *et al.* (2014) Oxidation Products of Biogenic Emissions Contribute to Nucleation of Atmospheric Particles. *Science*, 344: 717–721. DOI: https://doi.org/10.1126/science.1243527

Ridley, D.A., Heald, C.L., Kok, J.F. and **Zhao, C.** (2016) An observationally constrained estimate of global dust aerosol optical depth. *Atmospheric Chem. Phys.*, 16: 15097–15117. DOI: https://doi.org/10.5194/acp-16-15097-2016

Riipinen, I., Pierce, J.R., Yli-Juuti, T., Nieminen, T., Häkkinen, S., Ehn, M., Junninen, H., Lehtipalo, K., Petäjä, T., Slowik, J., Chang, R., Shantz, N.C., Abbatt, J., Leaitch, W.R., Kerminen, V.-M., Worsnop, D.R., Pandis, S.N., Donahue, N.M. and **Kulmala, M.** (2011) Organic condensation: a vital link connecting aerosol formation to cloud condensation nuclei (CCN) concentrations. *Atmospheric Chem. Phys.*, 11: 3865–3878. DOI: https://doi.org/10.5194/acp-11-3865-2011

Riipinen, I., Yli-Juuti, T., Pierce, J.R., Petäjä, T., Worsnop, D.R., Kulmala, M. and **Donahue, N.M.** (2012) The contribution of organics to atmospheric nanoparticle growth. *Nat. Geosci.*, 5: 453–458. DOI: https://doi.org/10.1038/ngeo1499

Robinson, A.L., Donahue, N.M., Shrivastava, M.K., Weitkamp, E.A., Sage, A.M., Grieshop, A.P., Lane, T.E., Pierce, J.R. and **Pandis, S.N.** (2007) Rethinking Organic Aerosols: Semivolatile Emissions and Photochemical Aging. *Science*, 315: 1259–1262. DOI: https://doi.org/10.1126/science.1133061

Roeckner, E., Brokopf, R., Esch, M., Giorgetta, M., Hagemann, S., Kornblueh, L., Manzini, E., Schlese, U. and **Schulzweida, U.** (2006) Sensitivity of Simulated Climate to Horizontal and Vertical Resolution in the ECHAM5 Atmosphere Model. *J. Clim.*, 19: 3771–3791. DOI: https://doi.org/10.1175/JCLI3824.1

Roelofs, G.-J. and **Lelieveld, J.** (1995) Distribution and budget of O3 in the troposphere calculated with a chemistry general circulation model. *J. Geophys. Res. Atmospheres*, 100: 20983–20998. DOI: https://doi.org/10.1029/95JD02326

Roelofs, G.J., Stier, P., Feichter, J., Vignati, E. and **Wilson, J.** (2006) Aerosol activation and cloud processing in the global aerosol-climate model ECHAM5-HAM. *Atmospheric Chem. Phys.*, 6: 2389–2399. DOI: https://doi.org/10.5194/acp-6-2389-2006

Roldin, P., Ehn, M., Kurtén, T., Olenius, T., Rissanen, M.P., Sarnela, N., Elm, J., Rantala, P., Hao, L., Hyttinen, N., Heikkinen, L., Worsnop, D.R., Pichelstorfer, L., Xavier, C., Clusius, P., Öström, E., Petäjä, T., Kulmala, M., Vehkamäki, H., Virtanen, A., Riipinen, I. and **Boy, M.** (2019) The role of highly oxygenated organic molecules in the Boreal aerosol-cloud-climate system. *Nat. Commun.*, 10: 4370. DOI: https://doi.org/10.1038/s41467-019-12338-8

Rönkkö, T., Saarikoski, S., Kuittinen, N., Karjalainen, P., Keskinen, H., Järvinen, A., Mylläri, F., Aakko-Saksa, P. and **Timonen, H.** (2023) Review of black carbon emission factors from different anthropogenic sources. *Environ. Res. Lett.*, 18: 033004. DOI: https://doi.org/10.1088/1748-9326/acbb1b

Ruuskanen, A., Romakkaniemi, S., Kokkola, H., Arola, A., Mikkonen, S., Portin, H., Virtanen, A., Lehtinen, K.E.J., Komppula, M. and **Leskinen, A.** (2021) Observations on aerosol optical properties and scavenging during cloud events. *Atmospheric Chem. Phys.*, 21: 1683–1695. DOI: https://doi.org/10.5194/acp-21-1683-2021

Saleh, R. (2020) From Measurements to Models: Toward Accurate Representation of Brown Carbon in Climate Calculations. *Curr. Pollut. Rep.*, 6: 90–104. DOI: https://doi.org/10.1007/s40726-020-00139-3

Saleh, R., Robinson, E.S., Tkacik, D.S., Ahern, A.T., Liu, S., Aiken, A.C., Sullivan, R.C., Presto, A.A., Dubey, M.K., Yokelson, R.J., Donahue, N.M. and **Robinson, A.L.** (2014) Brownness of organics in aerosols from biomass burning linked to their black carbon content. *Nat. Geosci.*, 7: 647–650. DOI: https://doi.org/10.1038/ngeo2220

Salvi, P., Ceppi, P. and **Gregory, J.M.** (2022) Interpreting Differences in Radiative Feedbacks From Aerosols Versus Greenhouse Gases. *Geophys. Res. Lett.*, 49: e2022GL097766. DOI: https://doi.org/10.1029/2022GL097766

Samset, B.H., Sand, M., Smith, C.J., Bauer, S.E., Forster, P.M., Fuglestvedt, J.S., Osprey, S. and **Schleussner, C.-F.** (2018) Climate Impacts From a Removal of Anthropogenic Aerosol Emissions. *Geophys. Res. Lett.*, 45: 1020–1029. DOI: https://doi.org/10.1002/2017GL076079

Sand, M., Samset, B.H., Myhre, G., Gliß, J., Bauer, S.E., Bian, H., Chin, M., Checa-Garcia, R., Ginoux, P., Kipling, Z., Kirkevåg, A., Kokkola, H., Le Sager, P., Lund, M.T., Matsui, H., van Noije, T., Olivié, D.J.L., Remy, S., Schulz, M., Stier, P., Stjern, C.W., Takemura, T., Tsigaridis, K., Tsyro, S.G. and **Watson-Parris, D.** (2021) Aerosol absorption in global models from AeroCom phase III. *Atmospheric Chem. Phys.*, 21: 15929–15947. DOI: https://doi.org/10.5194/acp-21-15929-2021

Saponaro, G., Sporre, M.K., Neubauer, D., Kokkola, H., Kolmonen, P., Sogacheva, L., Arola, A., de Leeuw, G., Karset, I.H.H., Laaksonen, A. and **Lohmann, U.** (2020) Evaluation of aerosol and cloud properties in three climate models using MODIS observations and its corresponding COSP simulator, as well as their application in aerosol–cloud interactions. *Atmospheric Chem. Phys.*, 20: 1607–1626. DOI: https://doi.org/10.5194/acp-20-1607-2020

Sato, Y., Goto, D., Michibata, T., Suzuki, K., Takemura, T., Tomita, H. and **Nakajima, T.** (2018) Aerosol effects on cloud water amounts were successfully simulated by a

global cloud-system resolving model. *Nat. Commun.*, 9: 985. DOI: https://doi.org/10.1038/s41467-018-03379-6

Schäfer, B., David, R.O., Georgakaki, P., Pasquier, J.T., Sotiropoulou, G. and **Storelvmo, T.** (2024) Simulations of primary and secondary ice production during an Arctic mixed-phase cloud case from the Ny-Ålesund Aerosol Cloud Experiment (NASCENT) campaign. *Atmospheric Chem. Phys.*, 24: 7179–7202. DOI: https://doi.org/10.5194/acp-24-7179-2024

Schnitzler, E.G., Gerrebos, N.G.A., Carter, T.S., Huang, Y., Heald, C.L., Bertram, A.K. and **Abbatt, J.P.D.** (2022) Rate of atmospheric brown carbon whitening governed by environmental conditions. *Proc. Natl. Acad. Sci.*, 119: e2205610119. DOI: https://doi.org/10.1073/pnas.2205610119

Schultz, M.G., Stadtler, S., Schröder, S., Taraborrelli, D., Franco, B., Krefting, J., Henrot, A., Ferrachat, S., Lohmann, U., Neubauer, D., Siegenthaler-Le Drian, C., Wahl, S., Kokkola, H., Kühn, T., Rast, S., Schmidt, H., Stier, P., Kinnison, D., Tyndall, G.S., Orlando, J.J. and **Wespes, C.** (2018) The chemistry–climate model ECHAM6.3-HAM2.3-MOZ1.0. *Geosci Model Dev.*, 11; 1695–1723. DOI: https://doi.org/10.5194/gmd-11-1695-2018

Schwarz, M., Savre, J., Sudhakar, D., Quaas, J. and **Ekman, A.M.L.** (2024) The Transition from Aerosol- to Updraft-Limited Susceptibility Regime in Large-Eddy Simulations with Bulk Microphysics. *Tellus B Chem. Phys. Meteorol.*, 76(1): 32–46. DOI: https://doi.org/10.16993/tellusb.94

Seidel, J.S., Kiselev, A.A., Keinert, A., Stratmann, F., Leisner, T. and **Hartmann, S.** (2024) Secondary ice production – no evidence of efficient rime-splintering mechanism. *Atmospheric Chem. Phys.*, 24: 5247–5263. DOI: https://doi.org/10.5194/acp-24-5247-2024

Seifert, A. and **Beheng, K.D.** (2006) A two-moment cloud microphysics parameterization for mixed-phase clouds. Part 1: Model description. *Meteorol. Atmospheric Phys.*, 92: 45–66. DOI: https://doi.org/10.1007/s00703-005-0112-4

Seinfeld, J.H., Bretherton, C., Carslaw, K.S., Coe, H., DeMott, P.J., Dunlea, E.J., Feingold, G., Ghan, S., Guenther, A.B., Kahn, R., Kraucunas, I., Kreidenweis, S.M., Molina, M.J., Nenes, A., Penner, J.E., Prather, K.A., Ramanathan, V., Ramaswamy, V., Rasch, P.J., Ravishankara, A.R., Rosenfeld, D., Stephens, G. and **Wood, R.** (2016) Improving our fundamental understanding of the role of aerosol–cloud interactions in the climate system. *Proc. Natl. Acad. Sci.*, 113: 5781–5790. DOI: https://doi.org/10.1073/pnas.1514043113

Seinfeld, J.H. and **Pandis, S.N.** (2016) *Atmospheric chemistry and physics: from air pollution to climate change*. Third edition. John Wiley & Sons, Inc., Hoboken, New Jersey.

Seland, Ø., Bentsen, M., Olivié, D., Toniazzo, T., Gjermundsen, A., Graff, L.S., Debernard, J.B., Gupta, A.K., He, Y.-C., Kirkevåg, A., Schwinger, J., Tjiputra, J., Aas, K.S., Bethke, I., Fan, Y., Griesfeller, J., Grini, A., Guo, C., Ilicak, M., Karset, I.H.H., Landgren, O., Liakka, J., Moseid, K.O., Nummelin, A., Spensberger, C., Tang, H., Zhang, Z., Heinze, C., Iversen, T. and **Schulz, M.** (2020) Overview of the Norwegian Earth System Model (NorESM2) and key climate response of CMIP6 DECK, historical, and scenario simulations. *Geosci. Model Dev.*, 13: 6165–6200. DOI: https://doi.org/10.5194/gmd-13-6165-2020

Shaw, T.A. and **Stevens, B.** (2025) The other climate crisis. *Nature*, 639: 877–887. DOI: https://doi.org/10.1038/s41586-025-08680-1

Shen, H., Vereecken, L., Kang, S., Pullinen, I., Fuchs, H., Zhao, D. and **Mentel, T.F.** (2022) Unexpected significance of a minor reaction pathway in daytime formation of biogenic highly oxygenated organic compounds. *Sci. Adv.*, 8: eabp8702. DOI: https://doi.org/10.1126/sciadv.abp8702

Shen, J., Russell, D.M., DeVivo, J., He, X.-C. *et al.* (2024) New particle formation from isoprene under upper-tropospheric conditions. *Nature*, 636: 115–123. DOI: https://doi.org/10.1038/s41586-024-08196-0

Shen, X., Liu, Q., Sun, J., Kong, W., Ma, Q., Qi, B., Han, L., Zhang, Y., Liang, L., Liu, L., Liu, S., Hu, X., Lu, J., Yu, A., Che, H. and **Zhang, X.** (2025) Measurement report: The influence of particle number size distribution and hygroscopicity on the microphysical properties of cloud droplets at a mountain site. *Atmospheric Chem. Phys.*, 25: 5711–5725. DOI: https://doi.org/10.5194/acp-25-5711-2025

Shinozuka, Y., Clarke, A.D., Nenes, A., Jefferson, A., Wood, R., McNaughton, C.S., Ström, J., Tunved, P., Redemann, J., Thornhill, K.L., Moore, R.H., Lathem, T.L., Lin, J.J. and **Yoon, Y.J.** (2015) The relationship between cloud condensation nuclei (CCN) concentration and light extinction of dried particles: indications of underlying aerosol processes and implications for satellite-based CCN estimates. *Atmospheric Chem. Phys.*, 15: 7585–7604. DOI: https://doi.org/10.5194/acp-15-7585-2015

Shipway, B.J. and **Hill, A.A.** (2012) Diagnosis of systematic differences between multiple parametrizations of warm rain microphysics using a kinematic framework. *Q. J. R. Meteorol. Soc.*, 138(669): 2196–2211. DOI: https://doi.org/10.1002/qj.1913

Shiraiwa, M., Li, Y., Tsimpidi, A.P., Karydis, V.A., Berkemeier, T., Pandis, S.N., Lelieveld, J., Koop, T. and **Pöschl, U.** (2017) Global distribution of particle phase state in atmospheric secondary organic aerosols. *Nat. Commun.*, 8: 15002. DOI: https://doi.org/10.1038/ncomms15002

Shrivastava, M., Cappa, C.D., Fan, J., Goldstein, A.H., Guenther, A.B., Jimenez, J.L., Kuang, C., Laskin, A., Martin, S.T., Ng, N.L., Petaja, T., Pierce, J.R., Rasch, P.J., Roldin, P., Seinfeld, J.H., Shilling, J., Smith, J.N., Thornton, J.A., Volkamer, R., Wang, J., Worsnop, D.R., Zaveri, R.A., Zelenyuk, A. and **Zhang, Q.** (2017) Recent advances in understanding secondary organic aerosol: Implications for global climate forcing. *Rev. Geophys.*, 55(2): 509–559. DOI: https://doi.org/10.1002/2016RG000540

Siegel, K., Gramlich, Y., Haslett, S.L., Freitas, G., Krejci, R., Zieger, P. and **Mohr, C.** (2023) Arctic observations of hydroperoxymethyl thioformate (HPMTF) – seasonal

behavior and relationship to other oxidation products of dimethyl sulfide at the Zeppelin Observatory, Svalbard. *Atmospheric Chem. Phys.*, 23: 7569–7587. DOI: https://doi.org/10.5194/acp-23-7569-2023

Sihto, S.-L., Kulmala, M., Kerminen, V.-M., Dal Maso, M., Petäjä, T., Riipinen, I., Korhonen, H., Arnold, F., Janson, R., Boy, M., Laaksonen, A. and **Lehtinen, K.E.J.** (2006) Atmospheric sulphuric acid and aerosol formation: implications from atmospheric measurements for nucleation and early growth mechanisms. *Atmospheric Chem. Phys.*, 6: 4079–4091. DOI: https://doi.org/10.5194/acp-6-4079-2006

Sihto, S.-L., Mikkilä, J., Vanhanen, J., Ehn, M., Liao, L., Lehtipalo, K., Aalto, P.P., Duplissy, J., Petäjä, T., Kerminen, V.-M., Boy, M. and **Kulmala, M.** (2011) Seasonal variation of CCN concentrations and aerosol activation properties in boreal forest. *Atmospheric Chem. Phys.*, 11: 13269–13285. DOI: https://doi.org/10.5194/acp-11-13269-2011

Simon, M., Dada, L., Heinritzi, M., Curtius, J. *et al.* (2020) Molecular understanding of new-particle formation from α-pinene between −50 and +25°C. *Atmospheric Chem. Phys.*, 20: 9183–9207. DOI: https://doi.org/10.5194/acp-20-9183-2020

Simpson, D., Fagerli, H., Colette, A., Denier van der Gon, H., Dore, C., Hallquist, M., Hansson, H.-C., Maas, R., Rouil, L., Allemand, N., Bergstrom, R., Bessagnet, B., Couvidat, F., El Haddad, I., Safont, J.G., Goile, F., Grieshop, A.P., Fraboulet, I., Hallquist, Å., Hamilton, J., Juhrich, K., Klimont, Z., Kregar, Z., Mawdsely, I., Megaritis, A., Ntziachristos, L., Pandis, S., Prevot, A.S.H., Schindlbacher, S., Seljeskog, M., Sirina-Leboine, N., Sommers, J. and **Ånström, S.** (2020) How should condensables be included in PM emission inventories reported to EMEP/CLRTAP? Tech. Rep. MSC-W 42020.

Simpson, E., Connolly, P. and **McFiggans, G.** (2014) An investigation into the performance of four cloud droplet activation parameterisations. *Geosci. Model Dev.*, 7: 1535–1542. DOI: https://doi.org/10.5194/gmd-7-1535-2014

Skamarock, C., Klemp, B., Dudhia, J., Gill, O., Liu, Z., Berner, J., Wang, W., Powers, G., Duda, G., Barker, D. and **Huang, X.** (2021) A Description of the Advanced Research WRF Model Version 4.3, National Center for Atmospheric Research. DOI: https://doi.org/10.5065/1dfh-6p97

Skyllakou, K., Korras-Carraca, M.-B., Matsoukas, C., Hatzianastassiou, N., Pandis, S.N. and **Nenes, A.** (2024) Predicted Concentrations and Optical Properties of Brown Carbon from Biomass Burning over Europe. *ACS EST Air*, 1: 897–908. DOI: https://doi.org/10.1021/acsestair.4c00032

Song, Q., Ginoux, P., Gonçalves Ageitos, M., Miller, R.L., Obiso, V. and **Pérez García-Pando, C.** (2024) Modeling impacts of dust mineralogy on fast climate response. *Atmospheric Chem. Phys.*, 24: 7421–7446. DOI: https://doi.org/10.5194/acp-24-7421-2024

Sotiropoulou, G., Lewinschal, A., Georgakaki, P., Phillips, V.T.J., Patade, S., Ekman, A.M.L. and **Nenes, A.** (2024) Sensitivity of Arctic Clouds to Ice Microphysical Processes in the NorESM2 Climate Model. *J. Climate*, 37: 4275–4290. DOI: https://doi.org/10.1175/JCLI-D-22-0458.1

Sotiropoulou, G., Vignon, É., Young, G., Morrison, H., O'Shea, S.J., Lachlan-Cope, T., Berne, A. and **Nenes, A.** (2021) Secondary ice production in summer clouds over the Antarctic coast: an underappreciated process in atmospheric models. *Atmospheric Chem. Phys.*, 21: 755–771. DOI: https://doi.org/10.5194/acp-21-755-2021

Soussé Villa, R., Jorba, O., Gonçalves Ageitos, M., Bowdalo, D., Guevara, M. and **Pérez García-Pando, C.** (2025) A comprehensive global modeling assessment of nitrate heterogeneous formation on desert dust. *Atmospheric Chem. Phys.*, 25: 4719–4753. DOI: https://doi.org/10.5194/acp-25-4719-2025

Sporre, M.K., Blichner, S.M., Schrödner, R., Karset, I.H.H., Berntsen, T.K., van Noije, T., Bergman, T., O'Donnell, D. and **Makkonen, R.** (2020) Large difference in aerosol radiative effects from BVOC-SOA treatment in three Earth system models. *Atmospheric Chem. Phys.*, 20: 8953–8973. DOI: https://doi.org/10.5194/acp-20-8953-2020

Spracklen, D.V. and **Heald, C.L.** (2014) The contribution of fungal spores and bacteria to regional and global aerosol number and ice nucleation immersion freezing rates. *Atmospheric Chem. Phys.*, 14: 9051–9059. DOI: https://doi.org/10.5194/acp-14-9051-2014

Srivastava, R.C. (1991) Growth of Cloud Drops by Condensation: Effect of Surface Tension on the Dispersion of Drop Sizes. DOI: https://doi.org/10.1175/1520-0469(1991)048<1596:GOCDBC>2.0.CO;2

Stevens, B., Giorgetta, M., Esch, M., Mauritsen, T., Crueger, T., Rast, S., Salzmann, M., Schmidt, H., Bader, J., Block, K., Brokopf, R., Fast, I., Kinne, S., Kornblueh, L., Lohmann, U., Pincus, R., Reichler, T. and **Roeckner, E.** (2013) Atmospheric component of the MPI-M Earth System Model: ECHAM6. *J. Adv. Model. Earth Syst.*, 5: 146–172. DOI: https://doi.org/10.1002/jame.20015

Stevens, B., Sherwood, S.C., Bony, S. and **Webb, M.J.** (2016) Prospects for narrowing bounds on Earth's equilibrium climate sensitivity. *Earths Future*, 4(11): 512–522. DOI: https://doi.org/10.1002/2016EF000376

Stevens, B., Vali, G., Comstock, K., Wood, R., Zanten, M.C., van Austin, P.H., Bretherton, C.S. and **Lenschow, D.H.** (2005) Pockets of open cells and drizzle in marine stratocumulus. *Bull. Amer. Meteor. Soc.*, 86: 51–58. DOI: https://doi.org/10.1175/BAMS-86-1-51

Stier, P. (2016) Limitations of passive remote sensing to constrain global cloud condensation nuclei. *Atmospheric Chem. Phys.*, 16: 6595–6607. DOI: https://doi.org/10.5194/acp-16-6595-2016

Stier, P., Feichter, J., Kinne, S., Kloster, S., Vignati, E., Wilson, J., Ganzeveld, L., Tegen, I., Werner, M., Balkanski, Y., Schulz, M., Boucher, O., Minikin, A. and **Petzold, A.** (2005) The aerosol-climate model ECHAM5-HAM. *Atmospheric Chem. Phys.*, 5: 1125–1156. DOI: https://doi.org/10.5194/acp-5-1125-2005

Stier, P., Seinfeld, J.H., Kinne, S. and **Boucher, O.** (2007) Aerosol absorption and radiative forcing. *Atmospheric Chem. Phys.*, 7: 5237–5261. DOI: https://doi.org/10.5194/acp-7-5237-2007

Stolzenburg, D., Cai, R., Blichner, S.M., Kontkanen, J., Zhou, P., Makkonen, R., Kerminen, V.-M., Kulmala, M., Riipinen, I. and **Kangasluoma, J.** (2023) Atmospheric nanoparticle growth. *Rev. Mod. Phys.*, 95: 045002. DOI: https://doi.org/10.1103/RevModPhys.95.045002

Stolzenburg, D., Fischer, L., Vogel, A.L., Winkler, P.M. *et al.* (2018) Rapid growth of organic aerosol nanoparticles over a wide tropospheric temperature range. *Proc. Natl. Acad. Sci.*, 115: 9122–9127. DOI: https://doi.org/10.1073/pnas.1807604115

Sundqvist, H. (1978) A parameterization scheme for non-convective condensation including prediction of cloud water content. *Q. J. R. Meteorol. Soc.*, 104: 677–690. DOI: https://doi.org/10.1002/qj.49710444110

Surratt, J.D., Chan, A.W.H., Eddingsaas, N.C., Chan, M., Loza, C.L., Kwan, A.J., Hersey, S.P., Flagan, R.C., Wennberg, P.O. and **Seinfeld, J.H.** (2010) Reactive intermediates revealed in secondary organic aerosol formation from isoprene. *Proc. Natl. Acad. Sci.*, 107: 6640–6645. DOI: https://doi.org/10.1073/pnas.0911114107

Suzuki, K., Stephens, G., Bodas-Salcedo, A., Wang, M., Golaz, J.-C., Yokohata, T. and **Koshiro, T.** (2015) Evaluation of the Warm Rain Formation Process in Global Models with Satellite Observations. *J. Atmospheric Sci.*, 72: 3996–4014. DOI: https://doi.org/10.1175/JAS-D-14-0265.1

Szopa, S., Naik, V., Adhikary, B., Artaxo, P., Berntsen, T., Collins, W.D., Fuzzi, S., Gallardo, L., Kiendler-Scharr, A., Klimont, Z., Liao, H., Unger, N. and **Zanis, P.** (2021) Short-Lived Climate Forcers. In: Masson-Delmotte, V., Zhai, P., Pirani, A., Connors, S.L., Péan, C., Berger, S., Caud, N., Chen, Y., Goldfarb, L., Gomis, M.I., Huang, M., Leitzell, K., Lonnoy, E., Matthews, J.B.R., Maycock, T.K., Waterfield, T., Yelekçi, O., Yu, R. and Zhou, B. (eds.) *Climate Change 2021: The Physical Science Basis*. Cambridge, United Kingdom and New York, NY, USA: Cambridge University Press. pp. 817–922. DOI: https://doi.org/10.1017/9781009157896.008

Takahashi, T., Nagao, Y. and **Kushiyama, Y.** (1995) Possible High Ice Particle Production during Graupel–Graupel Collisions. *J. Atmospheric Sci.*, 52: 4523–4527. DOI: https://doi.org/10.1175/1520-0469(1995)052<4523:PHIPPD>2.0.CO;2

Talvinen, S., Kim, P., Tovazzi, E., Holopainen, E., Cremer, R., Kühn, T., Kokkola, H., Kipling, Z., Neubauer, D., Teixeira, J.C., Sellar, A., Watson-Parris, D., Yang, Y., Zhu, J., Krishnan, S., Virtanen, A. and **Partridge, D.G.** (2025) Towards an improved understanding of the impact of clouds and precipitation on the representation of aerosols over the Boreal Forest in GCMs. *EGUsphere*, 1–49. DOI: https://doi.org/10.5194/egusphere-2025-721

Tapiador, F.J., Roca, R., Genio, A.D., Dewitte, B., Petersen, W. and **Zhang, F.** (2019) Is Precipitation a Good Metric for Model Performance? *Bull. Am. Meteorol. Soc.*, 100(2): 223–233. DOI: https://doi.org/10.1175/BAMS-D-17-0218.1

Tasoglou, A., Louvaris, E., Florou, K., Liangou, A., Karnezi, E., Kaltsonoudis, C., Wang, N. and **Pandis, S.N.** (2020) Aerosol light absorption and the role of extremely low volatility organic compounds. *Atmospheric Chem. Phys.*, 20: 11625–11637. DOI: https://doi.org/10.5194/acp-20-11625-2020

Tegen, I., Neubauer, D., Ferrachat, S., Siegenthaler-Le Drian, C., Bey, I., Schutgens, N., Stier, P., Watson-Parris, D., Stanelle, T., Schmidt, H., Rast, S., Kokkola, H., Schultz, M., Schroeder, S., Daskalakis, N., Barthel, S., Heinold, B. and **Lohmann, U.** (2019) The global aerosol–climate model ECHAM6.3–HAM2.3 – Part 1: Aerosol evaluation. *Geosci Model Dev*, 12: 1643–1677. DOI: https://doi.org/10.5194/gmd-12-1643-2019

Thomas, M.A., Wyser, K., Wang, S., Chatziparaschos, M., Georgakaki, P., Costa-Surós, M., Gonçalves Ageitos, M., Kanakidou, M., García-Pando, C.P., Nenes, A., van Noije, T., Le Sager, P. and **Devasthale, A.** (2024) Recent improvements and maximum covariance analysis of aerosol and cloud properties in the EC-Earth3-AerChem model. *Geosci. Model Dev.*, 17: 6903–6927. DOI: https://doi.org/10.5194/gmd-17-6903-2024

Thompson, D.R., Green, R.O., Bradley, C., Zandbergen, S. *et al.* (2024) On-orbit calibration and performance of the EMIT imaging spectrometer. *Remote Sens. Environ.*, 303: 113986. DOI: https://doi.org/10.1016/j.rse.2023.113986

Thornhill, G., Collins, W., Olivié, D., Skeie, R.B., Archibald, A., Bauer, S., Checa-Garcia, R., Fiedler, S., Folberth, G., Gjermundsen, A., Horowitz, L., Lamarque, J.-F., Michou, M., Mulcahy, J., Nabat, P., Naik, V., O'Connor, F.M., Paulot, F., Schulz, M., Scott, C.E., Séférian, R., Smith, C., Takemura, T., Tilmes, S., Tsigaridis, K. and **Weber, J.** (2021) Climate-driven chemistry and aerosol feedbacks in CMIP6 Earth system models. *Atmospheric Chem. Phys.*, 21: 1105–1126. DOI: https://doi.org/10.5194/acp-21-1105-2021

Tiitta, P., Leskinen, A., Kaikkonen, V.A., Molkoselkä, E.O., Mäkynen, A.J., Joutsensaari, J., Calderon, S., Romakkaniemi, S. and **Komppula, M.** (2022) Intercomparison of holographic imaging and single-particle forward light scattering in situ measurements of liquid clouds in changing atmospheric conditions. *Atmospheric Meas. Tech.*, 15: 2993–3009. DOI: https://doi.org/10.5194/amt-15-2993-2022

Tobo, Y., Prenni, A.J., DeMott, P.J., Huffman, J.A., McCluskey, C.S., Tian, G., Pöhlker, C., Pöschl, U. and **Kreidenweis, S.M.** (2013) Biological aerosol particles as a key determinant of ice nuclei populations in a forest ecosystem. *J. Geophys. Res. Atmospheres*, 118(17): 10,100–10,110. DOI: https://doi.org/10.1002/jgrd.50801

Toll, V., Christensen, M., Quaas, J. and **Bellouin, N.** (2019) Weak average liquid-cloud-water response to anthropogenic aerosols. *Nature*, 572: 51–55. DOI: https://doi.org/10.1038/s41586-019-1423-9

Tröstl, J., Chuang, W.K., Gordon, H., Baltensperger, U. *et al.* (2016) The role of low-volatility organic compounds in

initial particle growth in the atmosphere. *Nature*, 533: 527–531. DOI: https://doi.org/10.1038/nature18271

Trump, E.R., Fountoukis, C., Donahue, N.M. and **Pandis, S.N.** (2015) Improvement of simulation of fine inorganic PM levels through better descriptions of coarse particle chemistry. *Atmos. Environ.*, 102: 274–281. DOI: https://doi.org/10.1016/j.atmosenv.2014.11.059

Tsigaridis, K., Daskalakis, N., Kanakidou, M., Zhang, X. *et al.* (2014) The AeroCom evaluation and intercomparison of organic aerosol in global models. *Atmospheric Chem. Phys.*, 14: 10845–10895. DOI: https://doi.org/10.5194/acp-14-10845-2014

Tsigaridis, K. and **Kanakidou, M.** (2018) The Present and Future of Secondary Organic Aerosol Direct Forcing on Climate. *Curr. Clim. Change Rep.*, 4: 84–98. DOI: https://doi.org/10.1007/s40641-018-0092-3

Tsimpidi, A.P., Karydis, V.A., Pandis, S.N. and **Lelieveld, J.** (2016) Global combustion sources of organic aerosols: model comparison with 84 AMS factor-analysis data sets. *Atmospheric Chem. Phys.*, 16: 8939–8962. DOI: https://doi.org/10.5194/acp-16-8939-2016

Tsimpidi, A.P., Karydis, V.A., Pandis, S.N. and **Lelieveld, J.** (2017) Global-scale combustion sources of organic aerosols: sensitivity to formation and removal mechanisms. *Atmospheric Chem. Phys.*, 17: 7345–7364. DOI: https://doi.org/10.5194/acp-17-7345-2017

Tsimpidi, A.P., Karydis, V.A., Pozzer, A., Pandis, S.N. and **Lelieveld, J.** (2014) ORACLE (v1.0): module to simulate the organic aerosol composition and evolution in the atmosphere. *Geosci. Model Dev.*, 7: 3153–3172. DOI: https://doi.org/10.5194/gmd-7-3153-2014

Tsimpidi, A.P., Karydis, V.A., Pozzer, A., Pandis, S.N. and **Lelieveld, J.** (2018) ORACLE 2-D (v2.0): an efficient module to compute the volatility and oxygen content of organic aerosol with a global chemistry–climate model. *Geosci. Model Dev.*, 11: 3369–3389. DOI: https://doi.org/10.5194/gmd-11-3369-2018

Tsimpidi, A.P., Karydis, V.A., Zavala, M., Lei, W., Molina, L., Ulbrich, I.M., Jimenez, J.L. and **Pandis, S.N.** (2010) Evaluation of the volatility basis-set approach for the simulation of organic aerosol formation in the Mexico City metropolitan area. *Atmospheric Chem. Phys.*, 10: 525–546. DOI: https://doi.org/10.5194/acp-10-525-2010

Tsimpidi, A.P., Scholz, S.M.C., Milousis, A., Mihalopoulos, N. and **Karydis, V.A.** (2025) Aerosol composition trends during 2000–2020: in-depth insights from model predictions and multiple worldwide near-surface observation datasets. *Atmospheric Chem. Phys.*, 25: 10183–10213. DOI: https://doi.org/10.5194/acp-25-10183-2025

Tunved, P., Cremer, R.S., Zieger, P. and **Ström, J.** (2021) Using correlations between observed equivalent black carbon and aerosol size distribution to derive size resolved BC mass concentration: a method applied on long-term observations performed at Zeppelin station, Ny-Ålesund, Svalbard. *Tellus B Chem. Phys. Meteorol.*, 73. DOI: https://doi.org/10.1080/16000889.2021.1933775

Tunved, P., Ström, J. and **Krejci, R.** (2013) Arctic aerosol life cycle: linking aerosol size distributions observed between 2000 and 2010 with air mass transport and precipitation at Zeppelin station, Ny-Ålesund, Svalbard. *Atmospheric Chem. Phys.*, 13: 3643–3660. DOI: https://doi.org/10.5194/acp-13-3643-2013

Twomey, S. (1959) The nuclei of natural cloud formation part II: The supersaturation in natural clouds and the variation of cloud droplet concentration. *Geofis. Pura E Appl.*, 43: 243–249. DOI: https://doi.org/10.1007/BF01993560

Twomey, S. (1974) Pollution and the planetary albedo. *Atmospheric Environ.* 1967, 8: 1251–1256. DOI: https://doi.org/10.1016/0004-6981(74)90004-3

Usher, C.R., Michel, A.E., Stec, D. and **Grassian, V.H.** (2003) Laboratory studies of ozone uptake on processed mineral dust. *Atmos. Environ.*, 37: 5337–5347. DOI: https://doi.org/10.1016/j.atmosenv.2003.09.014

van Noije, T., Bergman, T., Le Sager, P., O'Donnell, D., Makkonen, R., Gonçalves-Ageitos, M., Döscher, R., Fladrich, U., von Hardenberg, J., Keskinen, J.-P., Korhonen, H., Laakso, A., Myriokefalitakis, S., Ollinaho, P., Pérez García-Pando, C., Reerink, T., Schrödner, R., Wyser, K. and **Yang, S.** (2021) EC-Earth3-AerChem: a global climate model with interactive aerosols and atmospheric chemistry participating in CMIP6. *Geosci. Model Dev.*, 14: 5637–5668. DOI: https://doi.org/10.5194/gmd-14-5637-2021

van Vuuren, D.P., Edmonds, J., Kainuma, M., Riahi, K., Thomson, A., Hibbard, K., Hurtt, G.C., Kram, T., Krey, V., Lamarque, J.-F., Masui, T., Meinshausen, M., Nakicenovic, N., Smith, S.J. and **Rose, S.K.** (2011) The representative concentration pathways: an overview. *Clim. Change*, 109: 5. DOI: https://doi.org/10.1007/s10584-011-0148-z

Vassel, M., Ickes, L., Maturilli, M. and **Hoose, C.** (2019) Classification of Arctic multilayer clouds using radiosonde and radar data in Svalbard. *Atmospheric Chem. Phys.*, 19: 5111–5126. DOI: https://doi.org/10.5194/acp-19-5111-2019

Vehkamäki, H., Kulmala, M., Napari, I., Lehtinen, K.E.J., Timmreck, C., Noppel, M. and **Laaksonen, A.** (2002) An improved parameterization for sulfuric acid–water nucleation rates for tropospheric and stratospheric conditions. *J. Geophys. Res. Atmospheres*, 107: AAC 3-1–AAC 3-10. DOI: https://doi.org/10.1029/2002JD002184

Vergara-Temprado, J., Miltenberger, A.K., Furtado, K., Grosvenor, D.P., Shipway, B.J., Hill, A.A., Wilkinson, J.M., Field, P.R., Murray, B.J. and **Carslaw, K.S.** (2018) Strong control of Southern Ocean cloud reflectivity by ice-nucleating particles. *Proc. Natl. Acad. Sci.*, 115: 2687–2692. DOI: https://doi.org/10.1073/pnas.1721627115

Vignati, E., Wilson, J. and **Stier, P.** (2004) M7: An efficient size-resolved aerosol microphysics module for large-scale aerosol transport models. *J. Geophys. Res. Atmospheres*, 109. DOI: https://doi.org/10.1029/2003JD004485

Virtanen, A., Joutsensaari, J., Kokkola, H., Partridge, D.G., Blichner, S., Seland, Ø., Holopainen, E., Tovazzi, E.,

Lipponen, A., Mikkonen, S., Leskinen, A., Hyvärinen, A.-P., Zieger, P., Krejci, R., Ekman, A.M.L., Riipinen, I., Quaas, J. and **Romakkaniemi, S.** (2025) High sensitivity of cloud formation to aerosol changes. *Nat. Geosci.*, 18: 289–295. DOI: https://doi.org/10.1038/s41561-025-01662-y

Voliotis, A., Du, M., Wang, Y., Shao, Y., Alfarra, M.R., Bannan, T.J., Hu, D., Pereira, K.L., Hamilton, J.F., Hallquist, M., Mentel, T.F. and **McFiggans, G.** (2022) Chamber investigation of the formation and transformation of secondary organic aerosol in mixtures of biogenic and anthropogenic volatile organic compounds. *Atmospheric Chem. Phys.*, 22: 14147–14175. DOI: https://doi.org/10.5194/acp-22-14147-2022

Wang, C. and **Crutzen, P.J.** (1995) Impact of a simulated severe local storm on the redistribution of sulfur dioxide. *J. Geophys. Res.*, 100: 11357–11367. DOI: https://doi.org/10.1029/95JD00697

Wang, K., Zhang, Y., Tong, H., Han, J., Fu, P., Huang, R.-J., Zhang, H. and **Hoffmann, T.** (2024) Molecular-Level Insights into the Relationship between Volatility of Organic Aerosol Constituents and PM2.5 Air Pollution Levels: A Study with Ultrahigh-Resolution Mass Spectrometry. *Environ. Sci. Technol.*, 58: 7947–7957. DOI: https://doi.org/10.1021/acs.est.3c10662

Wang, M., Kong, W., Marten, R., Donahue, N.M. *et al.* (2020) Rapid growth of new atmospheric particles by nitric acid and ammonia condensation. *Nature*, 581: 184–189. DOI: https://doi.org/10.1038/s41586-020-2270-4

Wang, M., Xiao, M., Bertozzi, B., Donahue, N.M. *et al.* (2022) Synergistic HNO3–H2SO4–NH3 upper tropospheric particle formation. *Nature*, 605: 483–489. DOI: https://doi.org/10.1038/s41586-022-04605-4

Wang, X., Gordon, H., Grosvenor, D.P., Andreae, M.O. and **Carslaw, K.S.** (2023) Contribution of regional aerosol nucleation to low-level CCN in an Amazonian deep convective environment: results from a regionally nested global model. *Atmospheric Chem. Phys.*, 23: 4431–4461. DOI: https://doi.org/10.5194/acp-23-4431-2023

Wang, X., Heald, C.L., Liu, J., Weber, R.J., Campuzano-Jost, P., Jimenez, J.L., Schwarz, J.P. and **Perring, A.E.** (2018) Exploring the observational constraints on the simulation of brown carbon. *Atmospheric Chem. Phys.*, 18: 635–653. DOI: https://doi.org/10.5194/acp-18-635-2018

Wang, X., Zhang, L. and **Moran, M.D.** (2010) Uncertainty assessment of current size-resolved parameterizations for below-cloud particle scavenging by rain. *Atmospheric Chem. Phys.*, 10: 5685–5705. DOI: https://doi.org/10.5194/acp-10-5685-2010

Wang, Y., Liu, X., Hoose, C. and **Wang, B.** (2014) Different contact angle distributions for heterogeneous ice nucleation in the Community Atmospheric Model version 5. *Atmospheric Chem. Phys.*, 14: 10411–10430. DOI: https://doi.org/10.5194/acp-14-10411-2014

Wang, Y., Xia, W. and **Zhang, G.J.** (2021) What rainfall rates are most important to wet removal of different aerosol types? *Atmospheric Chem. Phys.*, 21: 16797–16816. DOI: https://doi.org/10.5194/acp-21-16797-2021

Watson-Parris, D., Christensen, M.W., Laurenson, A., Clewley, D., Gryspeerdt, E. and **Stier, P.** (2022) Shipping regulations lead to large reduction in cloud perturbations. *Proc. Natl. Acad. Sci.*, 119: e2206885119. DOI: https://doi.org/10.1073/pnas.2206885119

Weigel, R., Borrmann, S., Kazil, J., Minikin, A., Stohl, A., Wilson, J.C., Reeves, J.M., Kunkel, D., de Reus, M., Frey, W., Lovejoy, E.R., Volk, C.M., Viciani, S., D'Amato, F., Schiller, C., Peter, T., Schlager, H., Cairo, F., Law, K.S., Shur, G.N., Belyaev, G.V. and **Curtius, J.** (2011) In situ observations of new particle formation in the tropical upper troposphere: the role of clouds and the nucleation mechanism. *Atmospheric Chem. Phys.*, 11: 9983–10010. DOI: https://doi.org/10.5194/acp-11-9983-2011

Westervelt, D.M., Pierce, J.R. and **Adams, P.J.** (2014) Analysis of feedbacks between nucleation rate, survival probability and cloud condensation nuclei formation. *Atmospheric Chem. Phys.*, 14: 5577–5597. DOI: https://doi.org/10.5194/acp-14-5577-2014

Wex, H., Huang, L., Sheesley, R., Bossi, R. and **Traversi, R.** (2019) Annual concentrations of ice nucleating particles at different Arctic stations. *PANGAEA*. DOI: https://doi.org/10.5194/acp-19-5293-2019

Wieder, J., Ihn, N., Mignani, C., Haarig, M., Bühl, J., Seifert, P., Engelmann, R., Ramelli, F., Kanji, Z.A., Lohmann, U. and **Henneberger, J.** (2022) Retrieving ice-nucleating particle concentration and ice multiplication factors using active remote sensing validated by in situ observations. *Atmospheric Chem. Phys.*, 22: 9767–9797. DOI: https://doi.org/10.5194/acp-22-9767-2022

Wildt, J., Mentel, T.F., Kiendler-Scharr, A., Hoffmann, T., Andres, S., Ehn, M., Kleist, E., Müsgen, P., Rohrer, F., Rudich, Y., Springer, M., Tillmann, R. and **Wahner, A.** (2014) Suppression of new particle formation from monoterpene oxidation by NO_x. *Atmospheric Chem. Phys.*, 14: 2789–2804. DOI: https://doi.org/10.5194/acp-14-2789-2014

Williamson, C.J., Kupc, A., Axisa, D., Bilsback, K.R., Bui, T., Campuzano-Jost, P., Dollner, M., Froyd, K.D., Hodshire, A.L., Jimenez, J.L., Kodros, J.K., Luo, G., Murphy, D.M., Nault, B.A., Ray, E.A., Weinzierl, B., Wilson, J.C., Yu, F., Yu, P., Pierce, J.R. and **Brock, C.A.** (2019) A large source of cloud condensation nuclei from new particle formation in the tropics. *Nature*, 574: 399–403. DOI: https://doi.org/10.1038/s41586-019-1638-9

Willis, M.D., Burkart, J., Thomas, J.L., Köllner, F., Schneider, J., Bozem, H., Hoor, P.M., Aliabadi, A.A., Schulz, H., Herber, A.B., Leaitch, W.R. and **Abbatt, J.P.D.** (2016) Growth of nucleation mode particles in the summertime Arctic: a case study. *Atmospheric Chem. Phys.*, 16: 7663–7679. DOI: https://doi.org/10.5194/acp-16-7663-2016

Wilson, T.W., Ladino, L.A., Alpert, P.A., Breckels, M.N., Brooks, I.M., Browse, J., Burrows, S.M., Carslaw, K.S., Huffman, J.A., Judd, C., Kilthau, W.P., Mason, R.H., McFiggans, G., Miller, L.A., Nájera, J.J., Polishchuk, E., Rae, S., Schiller,

C.L., Si, M., Temprado, J.V., Whale, T.F., Wong, J.P.S., Wurl, O., Yakobi-Hancock, J.D., Abbatt, J.P.D., Aller, J.Y., Bertram, A.K., Knopf, D.A. and **Murray, B.J.** (2015) A marine biogenic source of atmospheric ice-nucleating particles. *Nature*, 525: 234–238. DOI: https://doi.org/10.1038/nature14986

Wong, J.P.S., Tsagkaraki, M., Tsiodra, I., Mihalopoulos, N., Violaki, K., Kanakidou, M., Sciare, J., Nenes, A. and **Weber, R.J.** (2019) Atmospheric evolution of molecular-weight-separated brown carbon from biomass burning. *Atmospheric Chem. Phys.*, 19: 7319–7334. DOI: https://doi.org/10.5194/acp-19-7319-2019

Wood, R. (2012) Stratocumulus Clouds. *Mon. Wea. Rev.*, 140: 2373–2423. DOI: https://doi.org/10.1175/MWR-D-11-00121.1

Wu, R., Vereecken, L., Tsiligiannis, E., Kang, S., Albrecht, S.R., Hantschke, L., Zhao, D., Novelli, A., Fuchs, H., Tillmann, R., Hohaus, T., Carlsson, P.T.M., Shenolikar, J., Bernard, F., Crowley, J.N., Fry, J.L., Brownwood, B., Thornton, J.A., Brown, S.S., Kiendler-Scharr, A., Wahner, A., Hallquist, M. and **Mentel, T.F.** (2021) Molecular composition and volatility of multi-generation products formed from isoprene oxidation by nitrate radical. *Atmospheric Chem. Phys.*, 21: 10799–10824. DOI: https://doi.org/10.5194/acp-21-10799-2021

Xiao, M., Hoyle, C.R., Dada, L., Dommen, J. *et al.* (2021) The driving factors of new particle formation and growth in the polluted boundary layer. *Atmospheric Chem. Phys.*, 21: 14275–14291. DOI: https://doi.org/10.5194/acp-21-14275-2021

Xiong, R., Li, J., Zhang, Y., Zhang, L., Jiang, K., Zheng, H., Kong, S., Shen, H., Cheng, H., Shen, G. and **Tao, S.** (2022) Global brown carbon emissions from combustion sources. *Environ. Sci. Ecotechnology*, 12: 100201. DOI: https://doi.org/10.1016/j.ese.2022.100201

Xu, H., Ren, Y., Zhang, W., Meng, W., Yun, X., Yu, X., Li, J., Zhang, Y., Shen, G., Ma, J., Li, B., Cheng, H., Wang, X., Wan, Y. and **Tao, S.** (2021a) Updated Global Black Carbon Emissions from 1960 to 2017: Improvements, Trends, and Drivers. *Environ. Sci. Technol.*, 55: 7869–7879. DOI: https://doi.org/10.1021/acs.est.1c03117

Xu, L. and **Penner, J.E.** (2012) Global simulations of nitrate and ammonium aerosols and their radiative effects. *Atmospheric Chem. Phys.*, 12: 9479–9504. DOI: https://doi.org/10.5194/acp-12-9479-2012

Xu, W., Fossum, K.N., Ovadnevaite, J., Lin, C., Huang, R.-J., O'Dowd, C. and **Ceburnis, D.** (2021b) The impact of aerosol size-dependent hygroscopicity and mixing state on the cloud condensation nuclei potential over the north-east Atlantic. *Atmospheric Chem. Phys.*, 21: 8655–8675. DOI: https://doi.org/10.5194/acp-21-8655-2021

Yan, C., Nie, W., Vogel, A.L., Worsnop, D.R. *et al.* (2020) Size-dependent influence of NOx on the growth rates of organic aerosol particles. *Sci. Adv.*, 6: eaay4945. DOI https://doi.org/10.1126/sciadv.aay4945

Yan, C., Yin, R., Lu, Y., Bianchi, F. *et al.* (2021) The Synergistic Role of Sulfuric Acid, Bases, and Oxidized Organics Governing New-Particle Formation in Beijing. *Geophys. Res. Lett.*, 48: e2020GL091944. DOI: https://doi.org/10.1029/2020GL091944

Yli-Juuti, T., Mielonen, T., Heikkinen, L., Arola, A., Ehn, M., Isokääntä, S., Keskinen, H.-M., Kulmala, M., Laakso, A., Lipponen, A., Luoma, K., Mikkonen, S., Nieminen, T., Paasonen, P., Petäjä, T., Romakkaniemi, S., Tonttila, J., Kokkola, H. and **Virtanen, A.** (2021) Significance of the organic aerosol driven climate feedback in the boreal area. *Nat. Commun.*, 12: 5637. DOI: https://doi.org/10.1038/s41467-021-25850-7

Young, G., Lachlan-Cope, T., O'Shea, S.J., Dearden, C., Listowski, C., Bower, K.N., Choularton, T.W. and **Gallagher, M.W.** (2019) Radiative Effects of Secondary Ice Enhancement in Coastal Antarctic Clouds. *Geophys. Res. Lett.*, 46: 2312–2321. DOI: https://doi.org/10.1029/2018GL080551

Zaveri, R.A., Easter, R.C., Shilling, J.E. and **Seinfeld, J.H.** (2014) Modeling kinetic partitioning of secondary organic aerosol and size distribution dynamics: representing effects of volatility, phase state, and particle-phase reaction. *Atmospheric Chem. Phys.*, 14: 5153–5181. DOI: https://doi.org/10.5194/acp-14-5153-2014

Zhang, A., Wang, Y., Zhang, Y., Weber, R.J., Song, Y., Ke, Z. and **Zou, Y.** (2020) Modeling the global radiative effect of brown carbon: a potentially larger heating source in the tropical free troposphere than black carbon. *Atmospheric Chem. Phys.*, 20: 1901–1920. DOI: https://doi.org/10.5194/acp-20-1901-2020

Zhang, C., Hai, S., Gao, Y., Wang, Y., Zhang, S., Sheng, L., Zhao, B., Wang, S., Jiang, J., Huang, X., Shen, X., Sun, J., Lupascu, A., Shrivastava, M., Fast, J.D., Cheng, W., Guo, X., Chu, M., Ma, N., Hong, J., Wang, Q., Yao, X. and **Gao, H.** (2023) Substantially positive contributions of new particle formation to cloud condensation nuclei under low supersaturation in China based on numerical model improvements. *Atmospheric Chem. Phys.*, 23: 10713–10730. DOI: https://doi.org/10.5194/acp-23-10713-2023

Zhao, B., Donahue, N.M., Zhang, K., Mao, L., Shrivastava, M., Ma, P.-L., Shen, J., Wang, S., Sun, J., Gordon, H., Tang, S., Fast, J., Wang, M., Gao, Y., Yan, C., Singh, B., Li, Z., Huang, L., Lou, S., Lin, G., Wang, H., Jiang, J., Ding, A., Nie, W., Qi, X., Chi, X. and **Wang, L.** (2024) Global variability in atmospheric new particle formation mechanisms. *Nature*, 631: 98–105. DOI: https://doi.org/10.1038/s41586-024-07547-1

Zhao, B., Shrivastava, M., Donahue, N.M., Gordon, H., Schervish, M., Shilling, J.E., Zaveri, R.A., Wang, J., Andreae, M.O., Zhao, C., Gaudet, B., Liu, Y., Fan, J. and **Fast, J.D.** (2020) High concentration of ultrafine particles in the Amazon free troposphere produced by organic new particle formation. *Proc. Natl. Acad. Sci. U SA*, 117: 25344–25351. DOI: https://doi.org/10.1073/pnas.2006716117

Zhao, X. and **Liu, X.** (2021) Global Importance of Secondary Ice Production. *Geophys. Res. Lett*., 48: e2021GL092581. DOI: https://doi.org/10.1029/2021GL092581

Zhao, X. and **Liu, X.** (2022) Primary and secondary ice production: interactions and their relative importance. *Atmospheric Chem. Phys*., 22: 2585–2600. DOI: https://doi.org/10.5194/acp-22-2585-2022

Zheng, G., Kuang, C., Uin, J., Watson, T. and **Wang, J.** (2020a) Large contribution of organics to condensational growth and formation of cloud condensation nuclei (CCN) in the remote marine boundary layer. *Atmospheric Chem. Phys*., 20: 12515–12525. DOI: https://doi.org/10.5194/acp-20-12515-2020

Zheng, Y., Thornton, J.A., Ng, N.L., Cao, H., Henze, D.K., McDuffie, E.E., Hu, W., Jimenez, J.L., Marais, E.A., Edgerton, E. and **Mao, J.** (2020b) Long-term observational constraints of organic aerosol dependence on inorganic species in the southeast US. *Atmospheric Chem. Phys*., 20: 13091–13107. DOI: https://doi.org/10.5194/acp-20-13091-2020

Zhong, Q., Schutgens, N., van der Werf, G.R., Takemura, T., van Noije, T., Mielonen, T., Checa-Garcia, R., Lohmann, U., Kirkevåg, A., Olivié, D.J.L., Kokkola, H., Matsui, H., Kipling, Z., Ginoux, P., Le Sager, P., Rémy, S., Bian, H., Chin, M., Zhang, K., Bauer, S.E. and **Tsigaridis, K.** (2023) Threefold reduction of modeled uncertainty in direct radiative effects over biomass burning regions by constraining absorbing aerosols. *Sci. Adv*., 9: eadi3568. DOI: https://doi.org/10.1126/sciadv.adi3568

Zhou, C. and **Penner, J.E.** (2017) Why do general circulation models overestimate the aerosol cloud lifetime effect? A case study comparing CAM5 and a CRM. *Atmospheric Chem. Phys*., 17: 21–29. DOI: https://doi.org/10.5194/acp-17-21-2017

Zhu, H., Martin, R.V., Croft, B., Zhai, S., Li, C., Bindle, L., Pierce, J.R., Chang, R.Y.-W., Anderson, B.E., Ziemba, L.D., Hair, J.W., Ferrare, R.A., Hostetler, C.A., Singh, I., Chatterjee, D., Jimenez, J.L., Campuzano-Jost, P., Nault, B.A., Dibb, J.E., Schwarz, J.S. and **Weinheimer, A.** (2023) Parameterization of size of organic and secondary inorganic aerosol for efficient representation of global aerosol optical properties. *Atmospheric Chem. Phys*., 23: 5023–5042. DOI: https://doi.org/10.5194/acp-23-5023-2023

Zimmermann, F., Weinbruch, S., Schütz, L., Hofmann, H., Ebert, M., Kandler, K. and **Worringen, A.** (2008) Ice nucleation properties of the most abundant mineral dust phases. *J. Geophys. Res. Atmospheres*, 113. DOI: https://doi.org/10.1029/2008JD010655

Zipfel, L., Andersen, H. and **Cermak, J.** (2022) Machine-Learning Based Analysis of Liquid Water Path Adjustments to Aerosol Perturbations in Marine Boundary Layer Clouds Using Satellite Observations. *Atmosphere*, 13: 586. DOI: https://doi.org/10.3390/atmos13040586

Zipfel, L., Andersen, H., Grosvenor, D.P. and **Cermak, J.** (2024) How Cloud Droplet Number Concentration Impacts Liquid Water Path and Precipitation in Marine Stratocumulus Clouds—A Satellite-Based Analysis Using Explainable Machine Learning. *Atmosphere*, 15: 596. DOI: https://doi.org/10.3390/atmos15050596

TO CITE THIS ARTICLE:
Riipinen, I., Talvinen, S., Chassaing, A., Georgakaki, P., Li, X., García-Pando, C.P., Bergman, T., Kommula, S.M., Proske, U., Gkouvousis, A., Tsimpidi, A.P., Chatziparaschos, M., Neuberger, A., Karydis, V.A., Calderón, S.M., Romakkaniemi, S., Partridge, D.G., Khadir, T., Dada, L., van Noije, T., Decesari, S., Seland, Ø., Zieger, P., Bender, F., Carslaw, K., Cermak, J., Costa-Surós, M., (JIŰ<⇳Q@N!"B@⓪JN^ .], Gramlich, :]^!Haugvaldstad, O.W., Holopainen, E., Hoose, C., Jorba, O., Kakavas, S., Kanakidou, M., Kokkola, H., Krejci, R., Kühn, T., Kulmala, M., Le Sager, P., Makkonen, R., Manavi, S.E.I., Mentel, T.F., Milousis, A., Myriokefalitakis, S., Nenes, A., Nieminen, T., Pandis, S.N., Patoulias, D., Petäjä, T., Quaas, J., Regayre, L., Scholz, S.M.C., Schulz, M., Skyllakou, K., Sousse, R., Stier, P., Thomas, M.A., Villinger, J.T., Virtanen, A., Wyser, K. and Ekman, A.M.L. 2026. Treatment of Key Aerosol and Cloud Processes in Earth System Models – Recommendations from the FORCeS Project. *Tellus B: Chemical and Physical Meteorology*, 78(1): 1–66. DOI: https://doi.org/10.16993/tellusb.1883

Submitted: 24 April 2025 **Accepted:** 03 November 2025 **Published:** 08 January 2026